Republic of Iraq
Ministry of Higher Education
And Scientific Research
University of Babylon
College of Materials Engineering
Department of Metallurgical Engineering

Corrosion Erosion of low carbon steel used in high Concentrated Sulphuric Acid

A Thesis

Submitted to the council of the College of Materials Engineering/ University of Babylon in Partial Fulfillment of the Requirements for the Master Degree in Materials Engineering/Metallurgical

By

Nadheer Razzaq Ali Salih

(B.Sc. Materials Engineering)

(2001)

Supervised by

Prof. Haydar A.H. Al- juboori (Ph.D.)

Prof. Ekbal M.S. Salih (Ph.D.)

2022A.D 1443A.H

بِسۡمِ ٱللَّهِ ٱلرَّحۡمَٰنِ ٱلرَّحِيمِ

(نَرۡفَعُ دَرَجَٰتٖ مَّن نَّشَآءُۗ وَفَوۡقَ كُلِّ ذِي عِلۡمٍ عَلِيم)

صدق الله العلي العظيم

(سُورَةُ يُوسُفَ)

الآية(76)

Examining Committee Certification

We certify that we have read this thesis entitled (**Corrosion Erosion of low carbon steel used in high Concentrated sulphuric acid**) and as an examining committee, we have examined the student (**Nadheer Razzaq Ali Salih**) in contents and that is related to it, and that in our opinion it meets the standard of a thesis for the Master degree in Materials Engineering.

Signature

Prof. Dr.Haydar Al-Ethari

Committee Chair

Date: / / 2022

Signature

Prof. Dr.Abdul Raheem K. Abid Ali

Committee Member

Date: / / 2022

Signature

Assist. Prof. Dr.Iman Adnan Annon

Committee Member

Date: / / 2022

Signature

Prof.Dr.Ekbal M.S.Salih

Supervisor

Date: / / 2022

Signature

Prof.Dr.Haydar A.H. Al –juboori

Supervisor

Date: / / 2022

Approval of the Department of Metallurgical Engineering

Head of Metallurgy Engineering Department

Approval of the College of Materials Engineering

Dean of the College of Materials Engineering

Signature

Prof. Dr.Saad Hameed Al-Shafaie

Date: / / 2022

Signature

Prof. Dr.Imad Ali Disher

Date: / / 2022

Supervisors Certificate

We certify that this thesis entitled **"Corrosion Erosion of low carbon steel used in high concentrated Sulphuric acid "** is prepared by

(Nadheer Razzaq Ali Salih)

Under our supervision at the Department of Metallurgical Engineering/ College of Materials Engineering/ University of Babylon in partial fulfillment of the requirements for the Degree of Master in Material's Engineering/Metallurgical

Signature:	**Signature:**
Name of Supervisor:	Name of Supervisor:
Prof.Dr. Haydar A.H. Al- juboori	**Prof. Dr. Ekbal M.S. Salih**
Date: / / 2021	Date: / / 2021

Dedication

To my uncle* (Bashir) *(may God have mercy on him); this is your last request from me

Nadheer

2022

"Acknowledgement"

Praise is to **Allah**, Lord of the Worlds, and prayers and peace be upon the most honorable prophets and messengers, our master **Muhammad**, and upon his pure family.

I thank **Allah** Almighty for His bounty, as He made it possible for me to complete this work by His grace, to Him be praised first and foremost.

I thank my supervisors, **Prof. Dr. Haydar Abed Hassan Al-Jubouri** and Dr. **Ekbal Muhammad Saeed Salih**, for their guidance and follow-up with me in all aspects of the research.

Thanks and appreciation to **Prof. Dr.Abdul-Raheem Kadhim**, **Dr. Naba star**, **M.SC. Bashar Said Khanjar** and all the professors of the College of Materials Engineering, especially the Department of Metallurgical Engineering at University of Babylon.

Thanks and appreciation to Al-Furat General Company for Chemical Industries and Pesticides, represented by the Director General, Engineer **Ali Qassem Al-Shammry**, and all its affiliates and all departments for their support and assistance in completing the research.

Thanks and appreciation to the Research and Development Department, represented by **Mr. Eng. Safa Nayef Abdel-Jabber**, the center's sulfuric acid factory department, represented by **Mr. Engineer Haydar Yassin**, and the Central Workshop Department, represented by **Mr. Eng.Ali Kadhim and Mr. Mohammad Shanan**, for support, advice and assistance in conducting practical tests at the center's sulfuric acid factory site.

Abstract

Metallic and composite coatings are one of the techniques for surface modification of the surfaces of metals and alloys for the purpose of giving them new properties in addition to their original properties or improving their original properties.

The research problem is the low corrosion resistance of the carbon steel used in the manufacture of pipes for transporting concentrated sulphuric acid (98%) in the concentrated acid factory in the Al-Furat State Company.

Chromium electroplating and Chromium composite plating with silicon carbide particles on the base metal (carbon steel) were used for improving corrosion resistance.

Electroplating of carbon steel was carried out with chromium metal at constant current density(20A/dm^2),voltage(4.5),distance between electrodes(5)cm, stirrer speed(300)rpm PH(2), and optimum chrome plating was extracted based on Taguchi design (gray method) and by using Minitab program.Electroplating process included nine experiments with temperature range (40, 50, 60) degrees Celsius and the electroplating process time (1, 1.5, 2) hour, conducting tests for the chromium plating layer included (Vickers hardness, thickness, roughness), calculating the highest value of the gray relational grade.

Electrodeposition of composite coatings of silicon carbide microparticles embedded in chromium on carbon steel was carried out based on the optimum chromium plating factors and three weights of silicon carbide microparticles were added to the chrome plating solution (10, 20, and 30) grams.

Energy-dispersive X-ray Spectroscopy (EDS) and X-Ray Diffraction (XRD)tests were performed to confirm the elements and phases constituting the base metal (carbon steel), an optimum metal chromium plating sample, and three samples of composite coatings for silicon carbide microparticles (10, 20, and 30) g/l embedded in chromium metal, as well as Scanning Electron Microscope(SEM) and Atomic Force Microscope (AFM) examinations.

The optimum Chromium plating properties assay values were as follows: hardness (740) kg/mm^2, thickness (20.91) µm and surface roughness (0.098) µm.

Two types of corrosion rate tests were carried out by a weight loss method. The first test is a simple immersion test in static acid, and the second test is the (Corrosion-Erosion) test, The percentage of improvement that occurred on carbon steel protected with chromium metal plating and chromium silicon carbide composite coatings compared with the rate of corrosion of unprotected carbon steel in the simple immersion test as follows: chromium plating (56.73%),Cr-10g/l (67.3%),Cr-20g/l (76.95%),Cr-30g\l (53.2%). The percentage of improvement that occurred on carbon steel protected with chromium metal plating and chromium silicon carbide composite coatings compared with the rate of corrosion of unprotected carbon steel in the (Erosion-Corrosion) test was as follows: chrome plating (24.53%), Cr-10g/l (72.56%), Cr-20g/l (80.26%), Cr-30g/l (59.86%).

The polarization test was carried out for samples in concentrated sulfuric acid (98%), and the improvement rate in corrosion resistance that occurred on carbon steel protected with chromium metal plating and chromium silicon carbide composite coatings as follows: chromium plating (97.8%), chromium

plating-10g/l (98.4%), chromium plating-20g/l (99.5%), chromium plating-30g/l (88.5%).

The composite coatings with (chromium-20g/l silicon carbide) resist corrosion in conditions of concentrated acid flow (98%), where the corrosion rate is reduced by five times compared to the corrosion of carbon steel without a protective layer in (Erosion-Corrosion) test.

List of Contents

List of Figures

List of Tables

List of Symbols

Symbol	Meaning	Unit
A	Acid-exposed surface area	Cm^2
Ce	Total corrosion component in the presence of erosion	
Co	Rate of corrosion in the absence of erosion	
ΔCe	Change in corrosion rate due to erosion	
E^o	Electrode Potential	Volt
E_{corr}	Corrosion potential	Volt
Ec	Total erosion component in the presence of corrosion	
Eo	Rate of erosion in the absence of corrosion	
ΔEc	Change in erosion rate due to corrosion	
F	Fisher ratio	
$FeSO_4$	Ferrous sulfate	
H_2SO_4 (98%)	Concentrated Sulfuric Acid	
I_{corr}	Corrosion current density	$\mu A/cm^2$
Δ0i(k)	Deviation sequence	
M	Metal	
M^{n+}	Metal ion	
P	Value of Probability	
R^2	Coefficient of determination	
R^2adj	Adjusted Coefficient of Determination	
S	Synergistic component	
SV	Stirrer velocity	Revolution per minute
SS	Sum of squares	
To	material's total mass loss rate	Gram
W0	Origin weight	Gram
W1	Weight after immersion in Acid	Gram
xi (k)	Original sequence	
Xi*(k)	Normalized value of xi (k)	

List of Greek Symbols

Symbol	Meaning	Unit
β	Coefficient of differentiation or identification	
δi	Grey relational grade(GRG)	
§i (k)	Grey relational coefficient	
ρ	Density	g/cm^3 or Kg/m^3

List of Abbreviation

Symbol	Meaning	Unit
ANOVA	Analysis of variance	
AFM	Atomic Force Microscope	
ASTM	American Society for Testing and Materials	
EDS	Energy-dispersive X-ray Spectroscopy	
C.R.	Corrosion Rate	$g/cm^2.day$
C.R.(b)	Corrosion rate for (carbon steel as base metal)	$g/cm^2.day$
C.R.(c)	Corrosion rate for coated carbon steel	$g/cm^2.day$
DF	Degree of freedom	
CVD	Chemical vapor deposition	
GRA	Grey relational analysis	
HV	Vickers Hardness	Kg/mm^2
IP%	The improvement percent	
MS	Mean of squares	
PED	Pulse electrodeposition	
PVD	Physical vapor deposition	
Red	Reducing agent	
RH	Relative humidity	
SS	Sum of squares	
SEM	Scanning Electron Microscope	
Vol %	Volume percent	
Wt.%	Weight percent	
XRD	X-Ray Diffraction	
XRF	X-ray Fluorescence	

Chapter One

Introduction

Chapter One

Introduction

1.1 General Review

Corrosion in metals and alloys is one of the most damaging processes that affects equipment and industrial construction and causes various types of economic damage. This problem led most researchers in this field to study the phenomenon of corrosion and methods of protection or reducing it. Among the many engineering materials, carbon steel is considered one of the most important of these materials and the most used in various applications due to its high mechanical properties compared to its low cost when compared with the types of stainless steel. However, the problem of carbon steel's poor corrosion resistance limited its use in many applications especially that related to human health, such as the food and pharmaceutical industries.Surface modification technology has become an important way to achieve the required properties. As in the case of carbon steel, corrosion resistance is improved by surface modification in addition to other properties that are already present in steel as a base metal, such as strength and hardness. Surface modification includes surface treatment and coatings, which result in a new surface layer in terms of microstructure and composition. It is done in several ways, such as plasma spraying, electrodeposition, ion implantation, or sputter deposition [1, 2].

Corrosion is a natural process that leads to damage the materials as a result of their interaction with the surrounding medium. This process is not limited to metals, but includes all materials, but with a mechanism different from metals. Corrosion is an extractive metallurgy in reverse. For instance,

iron is made from hematite by heating with carbon. Iron corrodes and reverts to rust, thus completing its life cycle. The hematite and rust have the same composition as shown in Figure (1.1) [3].

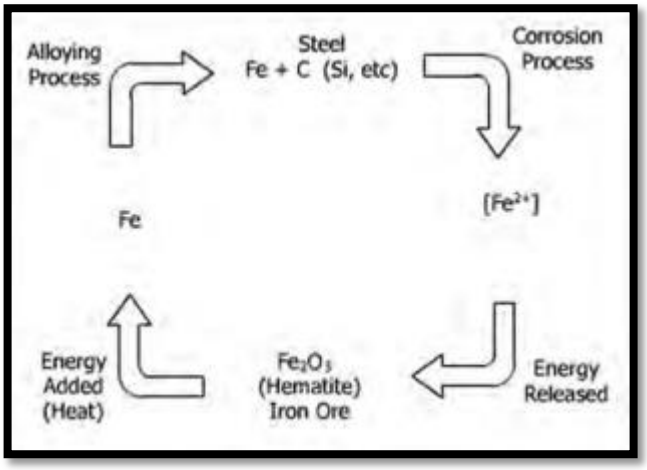

Figure (1.1): Refining-corrosion cycle [3]

Corrosion is a destructive attack on a metal that occurs as a result of the metal's chemical or electrochemical reaction with the environment. Another type of damage to the metal surface is the result of mechanical action known as erosion. In some cases, damage to the metal may occur as a result of a chemical action accompanied by a physical action, and then it is known as corrosion-erosion or corrosion-wear [4].

Corrosion is one of the major factors that limits or restricts the use of steel in the chemical and petrochemical industries. If steel is utilized, it becomes a source of loss, as material losses can amount to millions of dollars per year due to corrosion. Despite the development of new materials such as polymers and composites, their resistance, hardness, durability, and high temperature resistance do not compensate for the important properties found in metal composition [5].

Chromium is added to carbon steel to improve corrosion resistance. Due to the creation of a protective layer of oxide, chromium oxide has a high

corrosion resistance (Cr_2O_3), which considerably improves corrosion resistance. This layer is known as the passive layer [6].The protective layer of chromium oxide is dense and has high tenacity, and its thickness increases as the chromium content in the steel increases [7].

Composite coatings are the combination of two or more substances deposited on the base metal whose main goal is to improve the surface properties, such as corrosion and wear resistance, and high temperature resistance. They consist of metal coatings such as (nickel, chromium, molybdenum, cobalt, zinc and gold) added to them by weight ratios of non-metallic compounds such as metal oxides (Al_2O_3, TiO_2) or carbides (WC, SiC, TiC) so that these particles are implanted into the metal coatings to produce a layer with high surface hardness properties as a result of the particles and high corrosive properties due to the metal coatings deposited [8].

Electrodeposition is an electrochemical technique for depositing solid materials on the surface of conductive materials, as shown in figure (1.2). It's a commercially important method that's the foundation for a variety of industrial applications, including electro-winning, processing, and metal plating. Metal plating is the method with the most direct interaction with most people's daily lives, since we are constantly surrounded by items with a protective or decorative coating, such as watches, buttons, belt buckles, doorknobs, handlebars, etc. [9].

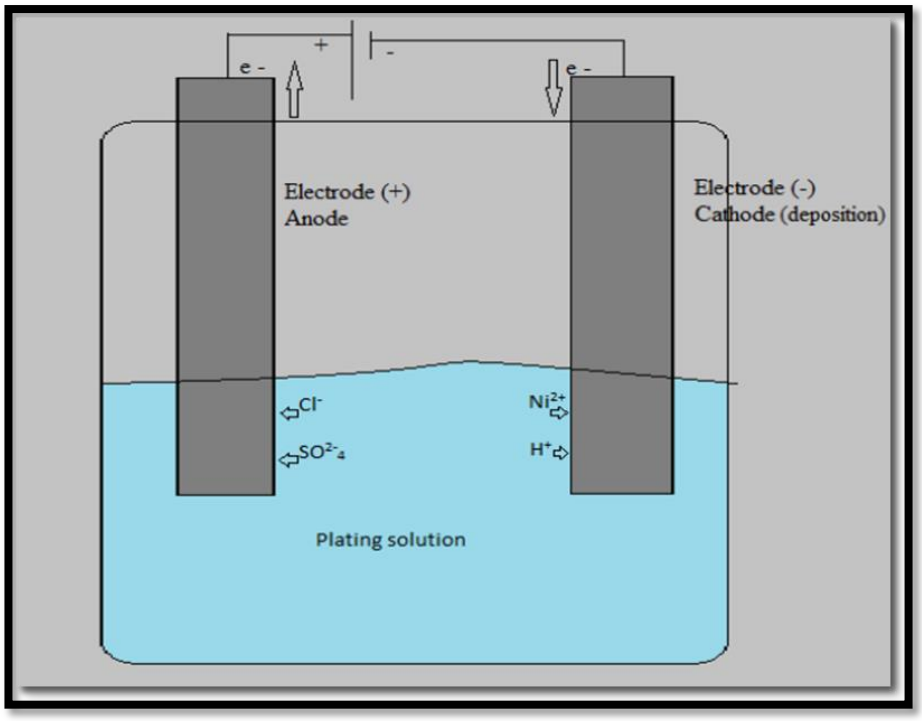

Figure (1.2): The electroplating process's schematic ion movement [9]

1.2 Statement of the problem

The objective of this research is to reduce the rates of corrosion and oxidation of equipment in the concentrated sulfuric acid factory (98%), one of the factories of the Al-Furat State Company for Chemical Industries and Pesticides/Ministry of Industry and Minerals.The process of producing Concentrated Sulphuric Acid (98%) is shown in figure (1.3) with working conditions for each stage.

From what was presented, and according to the progress of the production process, the equipment is exposed to different corrosive conditions, such as Sulfur, Sulfur dioxide, Sulfur trioxide, and concentrated Sulfuric acid.

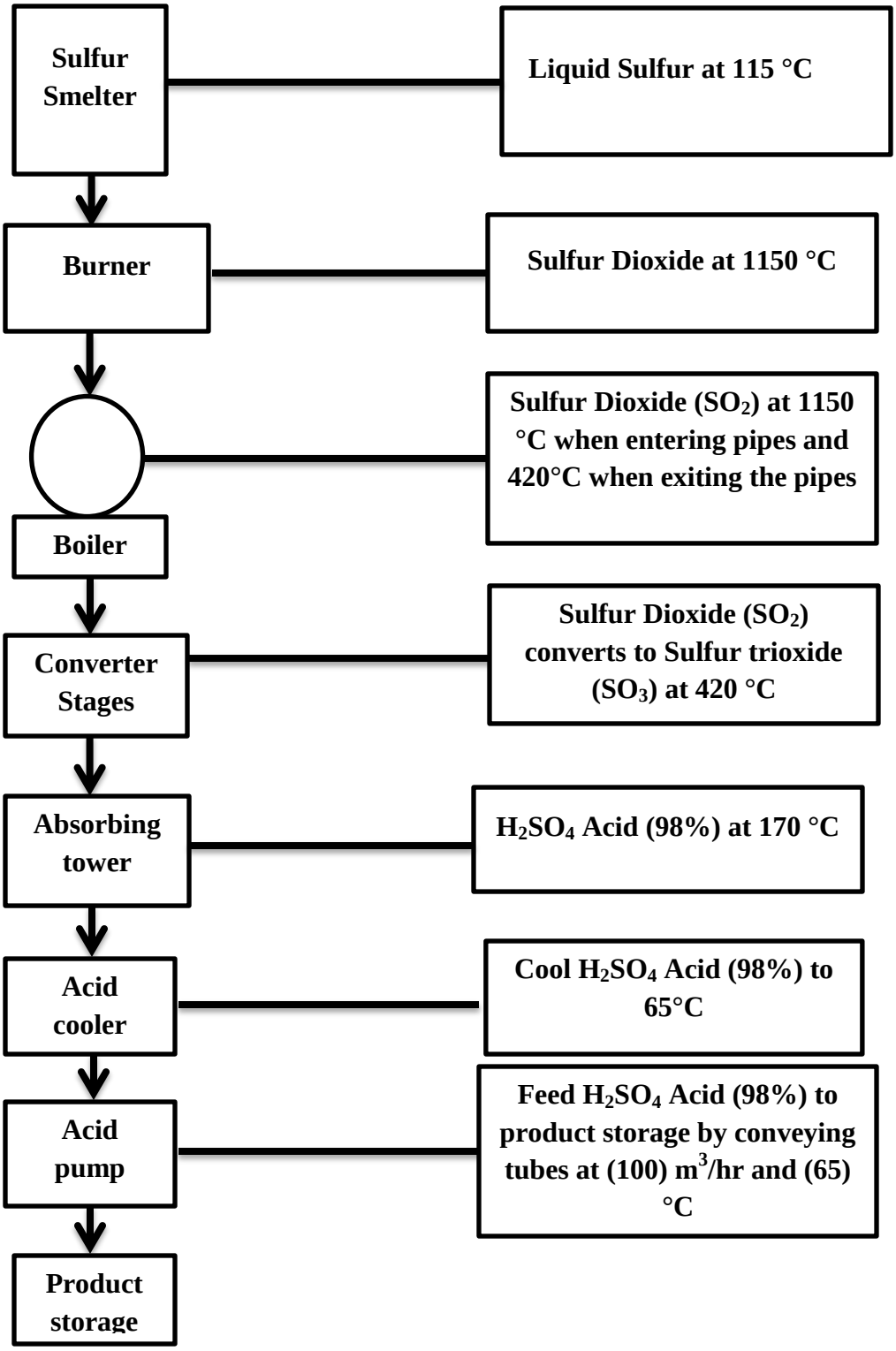

Figure(1.3): Diagram showing the stages of producing concentrated sulfuric acid (98%) with its working conditions

These conditions pose several problems as a result of corrosion, as they cause damage to parts, which leads to high costs as a result of replacement of parts and maintenance costs, in addition to the problem of stops for the factory, especially sudden stops, as they cause losses as a result of stopping marketing, especially in the absence of sufficient storage for acid to meet market requirements. In addition, a very important issue that concerns the life and safety of workers, as damage to equipment containing acid under pressure may cause a sudden explosion of the tube, which causes burns and loss of parts of the human body.

1.3 Problem solving methodology

The technique that was followed in addressing the problem of corrosion in the factory includes electroplating of carbon steel with chromium metal (Cr-coating) and chromium metal adding to its different concentrations of silicon carbide particles to form composite coatings (Cr-SiC) and comparison between composite coatings of Chromium metal and silicon carbide particles and coatings of chromium metal with the base metal (carbon steel).

The operating conditions of pipes carrying concentrated sulfuric acid (98%)were considered as a case for the purpose of studying it in this search and applying special tests for corrosion rate based on the technology of surface modification as one of solutions and treatments to protect against corrosion and reduce its rate, and if successful, it is generalized to the rest of factory parts as shown in figure (1.4), which shows the stage of pumping concentrated sulfuric acid (98%) to the production tank by pipes and a tube that has failed as a result of acid flowing at high speed and this is the stage that was studied in this research.

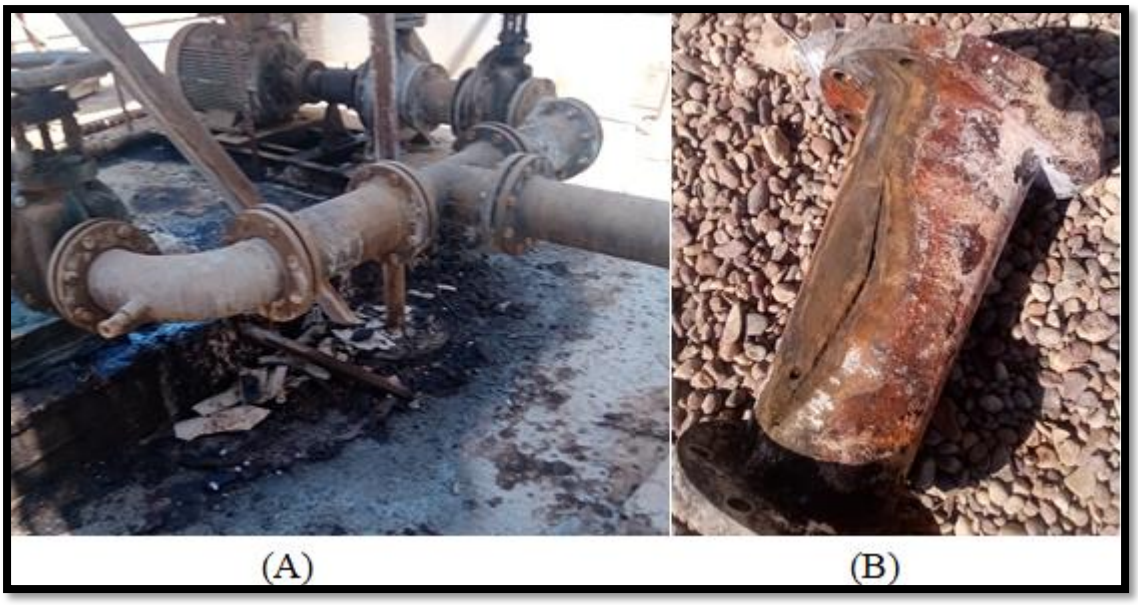

Figure (1.4): (A): The stage of transfer of concentrated sulfuric acid (98%) through the tubes, (B): Failed tube due to corrosion

The examination was carried out in the factory to ensure that the same corrosive conditions were obtained by subjecting the samples to two types of examination: First, a simple immersion in sulfuric acid at ambient temperature and without movement of the acid, and second with a flow rate of the acid similar to the speed of flow in the conveying pipes in the factory and at a temperature of (65)°C to determine the rate of corrosion in both types of examination and draw a relationship between corrosion rate and time for a period of (30) days during which the corrosion rate is carried out every (3) days for all samples.

Chapter Two

Theoretical Part and Literature Review

Chapter Two
Theoretical Part and Literature Review

2.1 Introduction

This chapter includes an explanation about the concept of corrosion, the mechanism of its occurrence and methods of protection from it. Explanation of the corrosion mechanism of carbon steel in concentrated sulfuric acid (98%). The use of metallic coatings and composite coatings as a method of protection against corrosion. Explained of the statistical method used in the research, and previous studies similar to the method used in the research.

2.2 Corrosion

2.2.1 Corrosion definition

Corrosion is the deterioration of the properties of metals and alloys as a result of their interaction with the environment, so that the rate of performance decreases over time and thus leads to their complete collapse. The decrease in a system's Gibbs energy is the underlying cause or driving force for all corrosion. Almost all metals need energy to be produced from it is ores. The metals has a powerful driving force to return to its original, low-energy oxide state as a result of this uphill thermodynamic struggle [10].

Pure metals and alloys react chemically or electrochemically with corrosive media, leading to the formation of corrosion products, which are in the form of a metal compound as a result of corrosion in the metal in order to reach the most stable state. Corrosion involves the transfer of metal ions into the solution at active areas (anode), the transit of electrons from the metal to a receiver at less active areas (cathode). The presence of an electron acceptor,

such as oxygen or oxidizing agents, or hydrogen ions, is required for the cathodic process. Corrosion can be reduced by employing appropriate techniques that restrict, delay, or entirely stop anodic or cathodic reactions, or both [11].

The corrosion process includes oxidation reaction whereby the metal is oxidized (M) by losing electrons and turning into a metal ion (M+). This process is undesirable for two basic reasons: the environment and working conditions. Corrosion is divided into two categories: both externally and internally. Internal corrosion is the type of corrosion that happens inside tanks, pipes, boilers, and other similar structures. The flow and storage of fluids and hydrocarbons inside tanks and pressure vessels causes internal corrosion. Interior corrosion is accelerated by any corrosive component found in fluids and hydrocarbons. Any corrosive material subjected to the outside environment, such as seawater, temperature, humidity, rain, bacteria, and external pressures that can injure the surface, is referred to as external corrosion [12].

2.2.2 Corrosion cell

Corrosion is dependent on the development of electrochemical cells, and these cells must be produced in order for corrosion to proceed. There are five requirements, or characteristics, as shown in figure (2.1), that must be satisfied, as below: [13]

1. The metal or the spot on the metal where oxidation occurs is called an anode (loss of electrons). Because it has a smaller negative voltage than the cathode, the anode has a lower noble value.

2. The metal or the region on the metal where reduction occurs is known as the cathode (gain of electrons). The cathode is nobler than the anode because it has a higher positive potential.
3. The anode and cathode are both in an electrically conductive substance called the electrolyte.
4. The anode and cathode must be electrically connected.
5. There must be a voltage difference between the anode and the cathode for creating the corrosion cells according to the galvanic series as shown in figure (2.2).

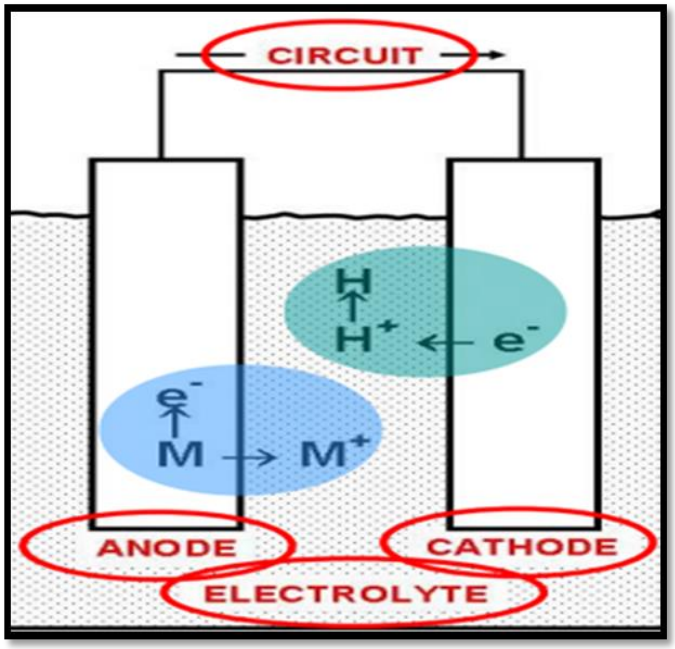

Figure (2.1): Schematic of the corrosion cell [13]

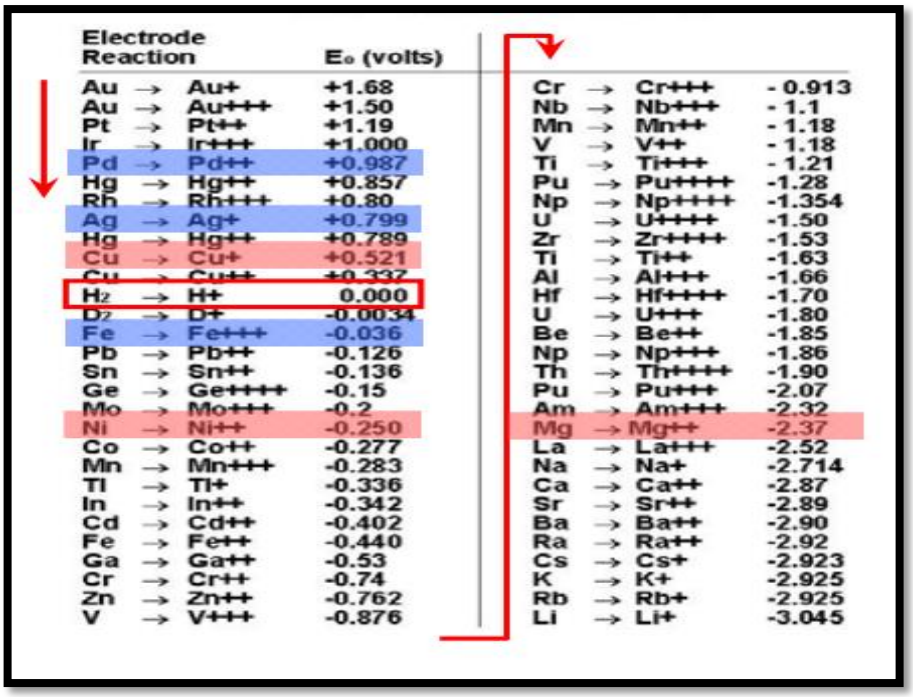

Figure (2.2): The galvanic series of metals [13]

2.2.3 Corrosion and the environment

Under natural conditions such as room temperature and open air, some metals are chemically stable, while other metals corrode quickly upon exposure to air, as the metal loses electrons and resorts to forming stable compounds at low energy levels. The reason for this behavior is due to the difference in the electrode potentials (E°) of the metals, as shown in table (2.1), where the positive voltage metals are stable so that it is difficult to form compounds of the metal while the negative voltage metals do it spontaneously [14].

Table (2.1): Electrode Potentials of common metals [14]

Metal (symbol)	(E° (v))
Gold (Au)	+1.50
Mercury (Hg)	+0.857
Silver (Ag)	+0.80
Copper (Cu)	+0.337
Antimony (Sb)	+0.10
Lead(pb)	-0.126

Tin (Sn)	-0.136
Iron (Fe)	-0.44
Zinc (Zn)	-0.762

The flash corrosion of the surface, as seen in the manufacturing of iron objects, is caused by the iron's relatively high negative electrode potential. This oxide layer on the metal's surface prevents further corrosion in an indoor setting. At room temperature and a relative humidity (RH) of 65% or less, this layer is usually stable. When the RH rises above 65%, a layer of active corrosion emerges quickly, which is bright orange, friable, and called active Lepdiocrosite, is the most common corrosion product [14].

2.3 Forms of corrosion

2.3.1 Uniform corrosion

This type of corrosion occurs when the rate of corrosion is evenly distributed on the surface of the metal so that the reduction in the thickness of the metal is uniform, as shown in figure (2.3).This type of corrosion is one of the most common and is not considered dangerous because the rate of decrease in the thickness of the metal can be easily determined with simple tests, allowing the amount of corrosion tolerances to be added during the design while taking into account the required resistance and service life, as well as providing an effective protection method such as cathodic protection and coating [15].

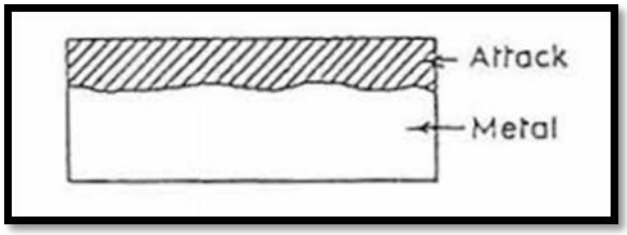

Figure (2.3): Uniform corrosion in metals [16]

2.3.2 Pitting corrosion

Pitting corrosion is corrosion that occurs in certain places on the surface of the metal that leads to the formation of deep and directed pits inside the metal, as shown in figure (2.4) as in steel tubes buried in the soil. It occurs in the protective layers and noble metals, where these pits form and grow in the event of any scratching or breaking of the protective layers or the metal oxide layer. The depth of the pits is large compared to their diameter. This type of corrosion is extremely dangerous because it can occur just below the metal oxide layer and cause a reduction in thickness in specific areas of the surface, resulting in metal failure. The effect of pitting corrosion can be reduced by reducing the content of chlorine ions in the conductive solution, reducing the level of oxygen gas, decreasing the acidity of the solution, avoiding stagnation of solutions in the tubes and tanks, and the appropriate design that causes better fluid drainage [17].

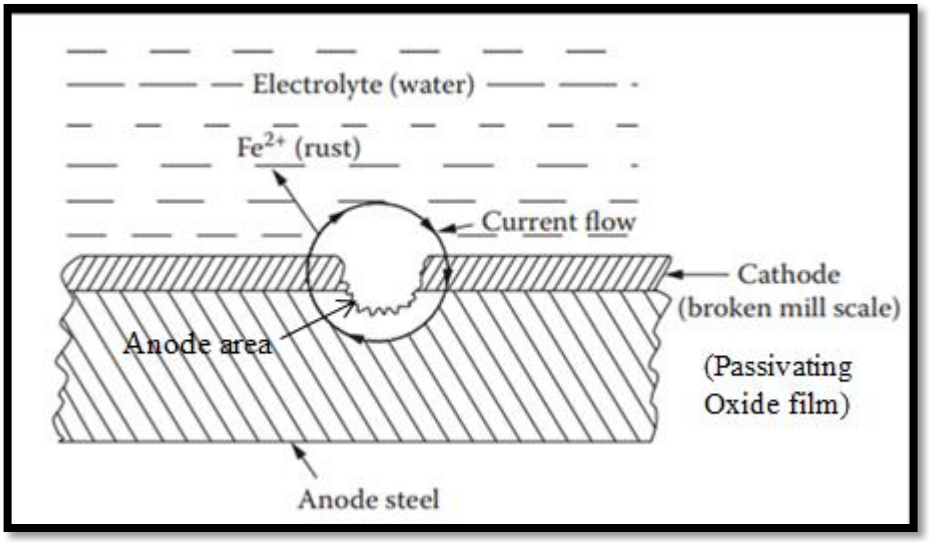

Figure (2.4): Pitting corrosion in metals [18]

2.3.3 Galvanic Corrosion

Galvanic corrosion results from the contact between two different metals in the presence of a medium for the conduction between them, so that the most effective metal is the anode, in which the corrosion rate is high, and the most noble metal is the cathode electrode, where the corrosion is small. The difference in potential between the component metals or alloys is the driving factor for galvanic corrosion. It is preferable to avoid a design that leads to contact between different metals, and if we are obliged to do so, the ratio between the area of the most effective metal (the anode) and the area of the less effective metal (the cathode) must be large as it results in a slight corrosion rate because polarization occurs in less reactive (more noble) materials. An example of this type of corrosion is corrugated iron sheet rusting, which occurs when the protective zinc coating is broken and the underlying steel is exposed [19].

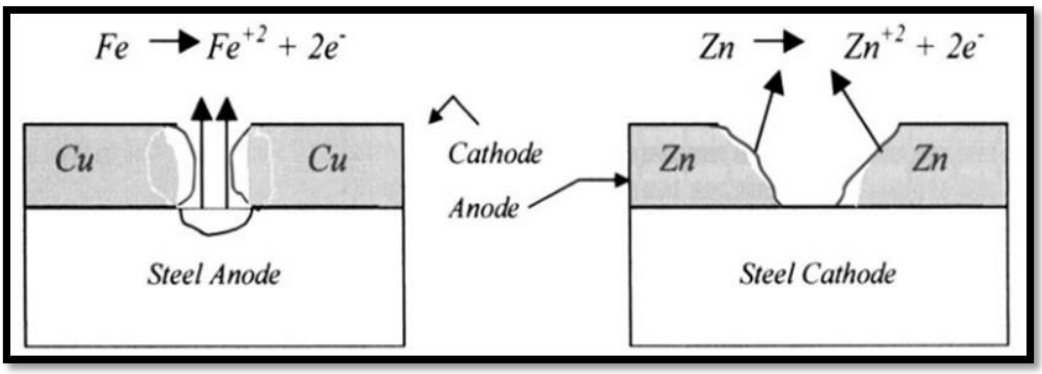

Figure (2.5): Explains the difference between the behavior of copper plating layer and zinc plating on steel [20]

Figure (2.5) shows two cases of galvanic influence in the case of steel coated with copper and zinc. So the steel is an anode relative to copper and the steel is subjected to corrosion due to the low ratio of the area between the anode and the cathode, and thus the coating loses its function in protecting

against corrosion. On the other hand, steel is a cathode relative to zinc, and there is no effect on steel, and zinc is a sacrificial anode to achieve protection for steel from corrosion [20].

2.3.4 Stress corrosion

Stress corrosion occurs when the surface is subjected to mechanical load combined with a corrosive environment, resulting in fast fracture propagation from the surface into the metal substrate. For example, aluminum alloys fracture in chloride-containing solutions, mild steel fractures in alkali-and nitrate-containing solutions, and copper alloys crack in ammoniac solutions (season cracking). Another type of corrosive process, known as corrosion fatigue, occurs when oscillating mechanical forces mix with a corrosive environment to cause cracks to develop and spread quickly, as shown in the figure(2.6) [16].

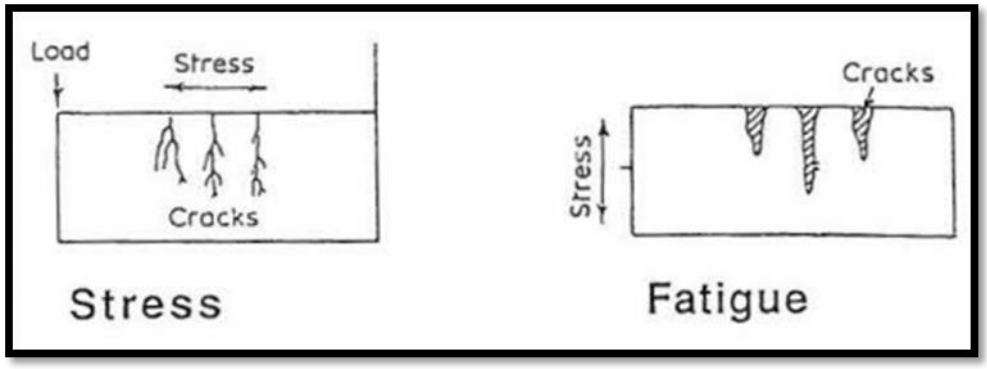

Figure (2.6): Stress and fatigue failure in a corrosive environment [16]

2.3.5 Intergranular corrosion

It is local corrosion that occurs in the grain boundary region due to the formation of chromium carbide, so that the chromium content decreases in the regions adjacent to the grain boundary and these regions become anodic relative to the rest of the regions and corrode, as in stainless steel alloys [21].

2.3.6 Erosion-Corrosion

It is a type of metal damage caused by a combination of chemical and mechanical action caused by the speed of the flow of any corrosive fluid unstable on the metal surface, which causes surface erosion by the corrosive medium's flow. When compared to the quantity of individual erosion and corrosion impacts, this combined effect is relatively large. This is due to the fact that erosion is enhanced by corrosion, and corrosion is enhanced by erosion. Because of the flow velocity, the impact energy will wipe out the passive film covering, exposing the surface to assault and resulting in material loss. The consequent mass loss will be more than the rate of erosion in inert environments, and the rate of corrosion will be greater than in erosion-free environments, as illustrated in the figure (2.7) [22].

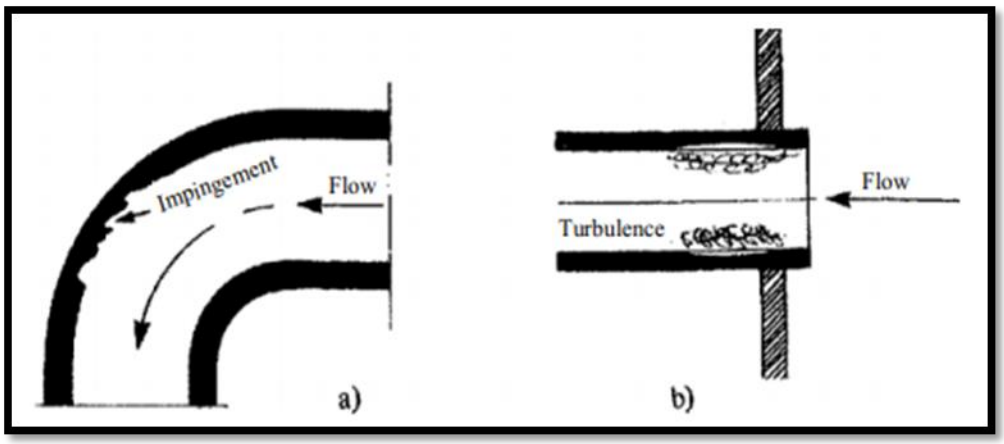

Figure (2.7): a) Impingement, b) turbulence corrosion. [15]

Erosion is defined as the exposure of a metal surface to damage resulting from fluid flow due to the speed of the flow or when the liquid contains solid impurities such as sand particles, which results in the gradual removal of parts of the metal surface until failure, which led parts to be useless for the purpose intended, in addition to economic and serious losses [23].

Figure (2.8): Effect of corrosion-erosion in-service failure: (a) AISI 304L and (b) Tantalum on the metal surface [22]

In some industrial and production applications, such as oil and gas transmission pipelines, electric power stations and chemical plants, another effect of erosion emerges, represented by the fact that liquids and gases that flow on metal surfaces or inside pipes are corrosive as shown in figure (2.8). Thus, metal surfaces are subject to damage as a result of the combined effect resulting from the chemical effect of the medium with the mechanical result of the movement of the fluid at a specific speed, especially when the flow is under the influence of pump pressure, meaning at a relatively high speed. This behavior of chemical and mechanical influence is known as the (synergy effect), which is defined as a metal's extra degradation rate as a result of the combined action of (erosion–corrosion) environments. There have been several attempts to describe the interaction regimes of (erosion–corrosion) of materials in aquatic settings. These patterns reveal whether erosion or corrosion is the dominant waste mechanism. Intermediate regimes in which corrosion and erosion interact with one another, on the other hand, may result in waste that is substantially more than the sum of the processes acting individually. This problem arises in a number of industrial parts, such as

transmission pipes, valves, heat exchangers, pressure vessels, and rotating parts such as compressors, turbines and pumps [23, 24].

Figure (2.9) depicts the mechanism by which this sort of damage is created on the surface of fluid transporting pipes; after the soldering was completed, a solder drop was left within the pipeline, as shown in the figure. The direction of fluid flow in a pipe, fluid flow comes into contact with a drop. The soldering drop causes turbulence inside the pipe, and the abrasive particles in the fluid begin to wear away the pipe's surface, exposing it to corrosion drivers. Inside the pipe, the corrosive fluid begins to corrode and degrade the material. Using a material with a high degree of hardness isn't always the ideal choice. The material's resistance to erosion corrosion is not guaranteed, making the fluid more laminar, the velocity of the fluid should be reduced. Increases in pipe diameter are also desirable in order to extend the part's lifetime when it gets corroded. Another suggestion is to create a portion with no rough surfaces, since this will reduce the impingement angle of solid particles, which will speed up the erosion of the surface. [12].

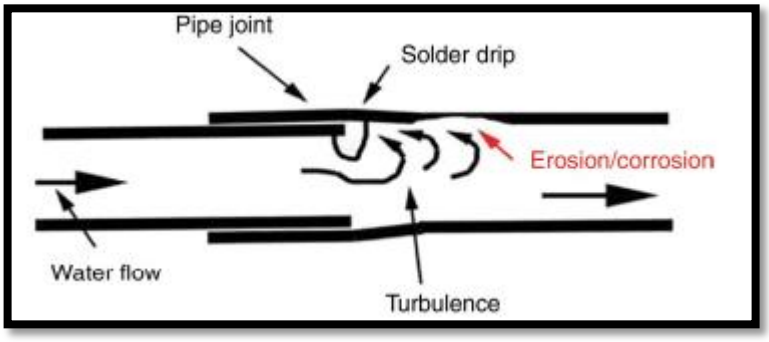

Figure (2.9): Mechanism of erosion corrosion inside a pipe [12]

The recurrence of accidents involving transmission pipes due to (erosion-corrosion) damage has elevated this issue to one of the industry's main concerns because overall weight loss from the metal surface due to (corrosion-erosive) surpasses total weight loss due to pure chemical corrosion and pure

mechanical erosion. Erosion–corrosion is a type of localized corrosion that poses a serious threat. The weakest part of a pipeline's gathering and transferring system is the elbow. Despite the significant consequences of the synergistic impact of erosion–corrosion, the elbow's erosion–corrosion mechanism, as impacted by velocity, is still poorly understood due to its complexity [25].The overall material loss during the erosion-corrosion process is calculated as follows: [26]

$$To=Eo+Co+S \quad \ldots (2.1)$$

Where To is the material's total mass loss rate, Eo is the rate of erosion in the absence of corrosion, Co is the rate of corrosion in the absence of erosion, and S is the synergistic component, which is defined as,

$$S=\Delta Ce+\Delta Ec \quad \ldots (2.2)$$

Where,

$$\Delta Ce=Ce-Co \quad \ldots (2.3)$$

$$\Delta Ec=Ec-Eo \quad \ldots (2.4)$$

Where ΔCe is the change in corrosion rate due to erosion and ΔEc is the change in erosion rate due to corrosion. Ec is the total erosion component in the presence of corrosion and Ce is the total corrosion component in the presence of erosion.

2.4 Carbon steel

It's an iron-carbon alloy with a maximum carbon content of (1.5 to 2.0) % as shown in figure (2.10), (Iron-Iron Carbide Phase Diagram). Steel's hardness and strength are improved by the presence of carbon in the form of iron carbide. Silicon, Phosphorus, Sulphur, and Manganese are also present in various proportions to produce a variety of desired qualities. Plain carbon steel or carbon steel is the most common steel made recently. Carbon steel is defined as steel with qualities principally derived from its carbon content and

containing no more than (0.5%) silicon and (1.5%) manganese. Carbon content is usually used to classify plain steels as table (2.2) [27].

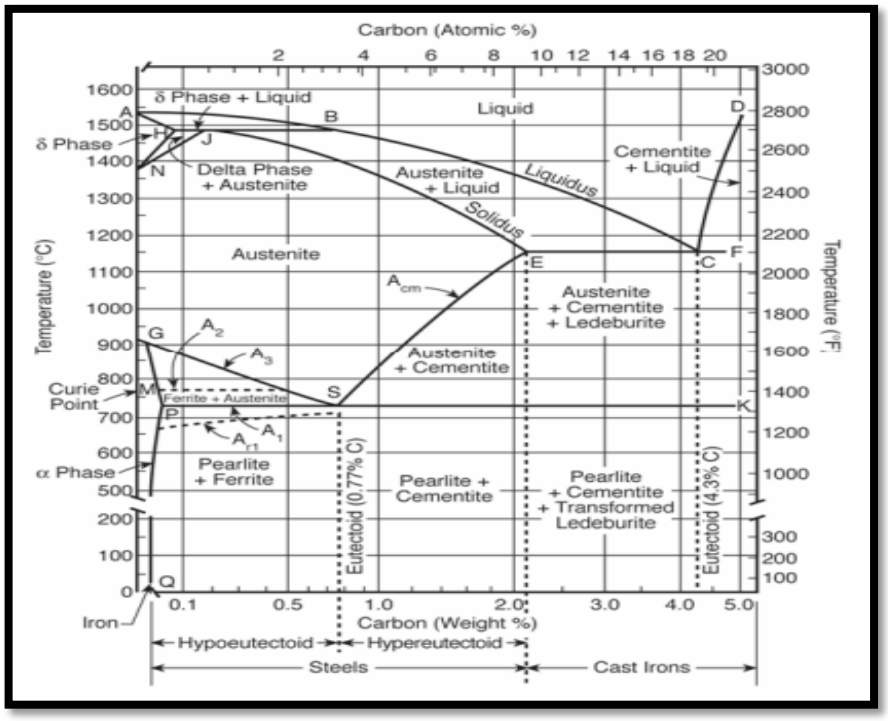

Figure (2.10): Iron-Iron Carbide Phase Diagram [28]

Table (2.2): Applications of carbon steels [27]

Carbon %	Applications
Low carbon steel (0.05-0.25)%C	Wire, rod, and solid drawn tubes are all thin sheets.
Medium carbon steel(0.3-0.5)%C	Boiler plates, bridge building, structural pieces, drop forgings, and other common workshop requirements are all available.
High carbon steel(0.6-1.0)%C	Axes, high-tensile tubes, and wire agricultural equipment are among the things provided.
Ultra high carbon steel (1.25 – 2)%	Metal-cutting machines, hand files, drills, gauges

Carbon is the primary alloying ingredient in these iron-based materials. Since carbon is such a powerful alloying factor in steel, even small variations

in carbon levels in the composition can result in significant differences in strength, hardness, and ductility. Other critical factors, such as material fabrication, heat treatment, component fabrication, and fabrication processes, can alter the properties of carbon steel components significantly [28]. All steels contain carbon, which is the main element in the steel surface straightening process. The mechanical properties of steel also increase with an increase in the carbon content, such as tensile strength, hardness, and wear resistance, in exchange for a reduction in ductility, durability, and workability [28]. To enhance the characteristics of carbon steels , small quantities of elements such as silicon, tungsten, aluminum, nickel, molybdenum, chromium, manganese, and vanadium are added during the production process, as shown in table (2.3) below [29].

Table (2.3): The effect of alloying elements on carbon steel [30]

Element	Primary Effect	Secondary Effect
Silicon	Mechanical properties improvement Strengthens the steel	improve corrosion resistance
Chromium	Corrosion resistance increases Increases resistance to oxidation	Enhances high-temperature resistance Abrasion resistance is improved.
Molybdenum	Hardenability is improved. Enhances high-temperature resistance	Softening resistance. In the presence of chromium, it improves corrosion resistance.
Nickel	Toughness is increased. Hardenability is increased	Localized corrosion can be aided.
Manganese	Hardenability is increased.	Free sulfur and FeS aren't formed when MnS is present. MnS could be a potential pit formation site.
Tungsten	Increases strength	Aids in the hardenability

	Increases resistance to softening	
Columbium and Vanadium	The hardenability of the material is improved. Strengthens the body's resilience to softness.	Improves resistance to high temperatures
Titanium	The matrix is strengthened. Resistance to corrosion improves.	Deoxidizer

Carbon steel is the most widely used conventional structural material in building, transportation, environmental protection, and energy power infrastructure. Carbon steel is invariably exposed to the atmosphere during its service life, resulting in atmospheric corrosion, which accounts for 50% of overall corrosion loss [31].

Despite the good mechanical properties of carbon steel that give it industrial applications, its low corrosion resistance is one of the determinants that make the use of this material ineffective, especially in harsh corrosive conditions. Therefore, adding alloying elements such as chromium is an appropriate solution to improve the corrosion resistance of carbon steels [32]. Chromium is added to carbon steel at a rate of (0.5-18) %, and when this addition exceeds 12% that lead to form stainless steel alloys, which mean that amount of improvement in corrosion resistance has reached excellent limits, because of the creation of a layer of chromium oxide that insulates the metal from the environment, reducing corrosion and increasing the metal's lifetime performance in applications [33].

2.5 Corrosion of carbon steel in concentrated sulfuric acid

The carbon steel tubes used to transport concentrated sulfuric acid (H_2SO_4) (98%) in the concentrated sulfuric acid plant are subjected to corrosion. But the effect of corrosion on carbon steel is depend on the kinetic state of the acid, meaning the stagnation state as in acid storage tanks; the other case is the flow state of the acid, as in acid transport tubes. If the concentrated sulfuric acid (H_2SO_4) is under stagnation conditions, carbon steel or low-alloy steel is subjected to slight corrosion at ambient temperature so that the corrosion rate does not exceed 0.5 mm/year[34,35]. The reason for this is due to the reaction of concentrated sulfuric acid with iron forming a stable layer of ferrous sulfate as shown in figure (2.11). This layer is a product of corrosion, but it forms a protective layer for carbon steel against continued corrosion due to acid. If the acid flows at a speed exceeding the critical speed, the protective layer ($FeSO_4$) will be damaged as a result of the acid flowing quickly and the steel surface will be exposed and corrode, this is known as the effect of (erosion-corrosion) due to the flow of concentrated sulfuric acid as shown in figure (2.12) [34,35].

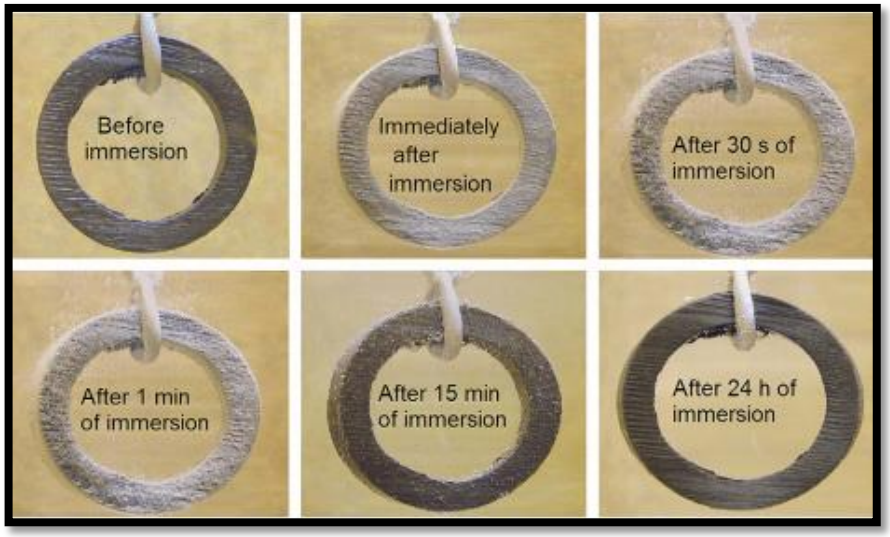

Figure (2.11): Carbon steel ring in H_2SO_4 (96%) under static conditions at 25ºC [36]

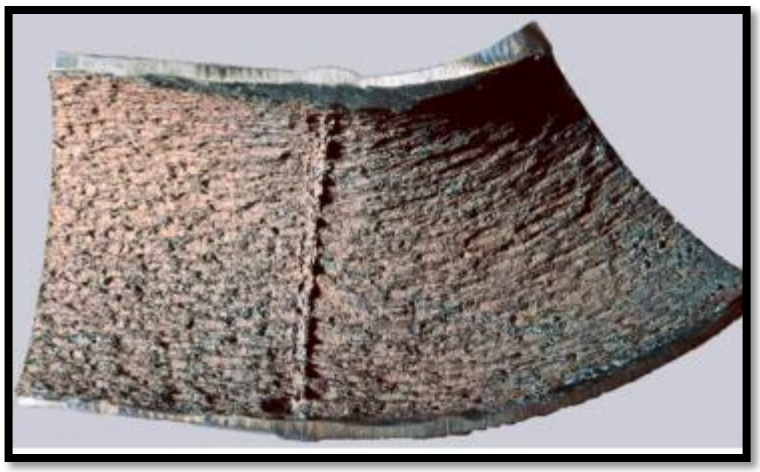

Figure (2.12): Erosion-Corrosion of steel pipe at high velocity Sulphuric acid [34]

Increasing the temperature of the concentrated acid more than (40ºC) with the acid flow rate exceeding (> 0.6 m/s) relative to the surface of the metal is one of the most important factors that causes the breakdown of the ferrous sulfate layer and, thus, the rate of corrosion of carbon steel increases as shown in table (2.4) [36].

Table (2.4): Estimated corrosion rates (mm /year) for carbon steel [36]

Temperature (C)	Acid velocity (m/s)								
	0	1	2	3	4.5	6.5	8.5	11.5	12
	Corrosion rate (mm/year)								
6	0.13	0.18	0.23	0.3	1.14	1.52	1.9	2.4	2.
15	0.3	0.38	0.43	0.51	1.65	2.16	2.8	3.5	4.3
33	1.27	1.4	1.52	1.78	6.86	9.14	11.4	14.7	18.3
50	2.54	3.81	5.08	7.62	25.37	25.3	25.4	25.3	25.3

In Sulfuric acid conditions, hydrogen gas can be an issue for carbon steel because it can essentially cause mechanically weak of the iron sulphate layer that protects the steel from attack. During normal flow, the gas bubbles are small and distributed equally, and they are swiftly moved downstream with the acid, without causing any damage to the pipe wall, as in equation (2.5).

When the acid flow stopped, the gas bubbles in the upper part of the pipe gathered along the pipe wall. When the flow is restored, the hydrogen gas bubbles become dislodged and climb to the top of the pipe, scraping the protective film away in the process. The surface deteriorated quickly when the film was removed from the top of the pipe, until the iron sulphate film was reformed. Repeating this case results in a pattern of curved grooves in the pipe's upper half, all radiating toward a center longitudinal groove at the very top, as shown in figures (2.13) and (2.14). [37,39]

$Fe+H_2SO_4 \rightarrow FeSO_4 + H_2$ ……. (2.5)

Figure (2.13): A close-up of the pipe's interior surface before cleaning [38]

Figure (2.14): A close-up of the pipe's interior surface after cleaning [38]

2.6 Corrosion protection methods

Corrosion protection encompasses all strategies and techniques aimed at preventing or reducing corrosion damage to the bare minimum [40]. Corrosion can be prevented or reduced in a variety of ways, as below: [41]

- Changes in the environment: By reducing aeration, eliminating moisture, pumping an inert gas, decreasing turbulence, and/or lowering the temperature, this strategy decreases corrosion.
- Adding inhibitors: In general, inhibitors are administered at a concentration of less than 0.1% by weight to a system. As a result, the inhibitors either adsorb onto the metal surface and form a protective coating, or they remove the corrosive agent from the surface.
- Cathodic protection uses galvanic activity to transform a metal surface into the cathode of an electrochemical cell. Metal protection can be accomplished by using a sacrificial metal as an anode or by employing impressed electromotive force (emf) techniques.
- Anodic protection is an extremely new technique in comparison to cathodic protection. An anodic current applied from the outside keeps an active-passive metal or alloy in the passive state, preventing corrosion. It has a number of advantages over cathodic protection, including the following: (i) low current requirements, (ii) significant corrosion rate reduction, and (iii) application to some very corrosive acids and other media.
- Appropriate material selection and equipment design: By designing a system with perfect liquid drainage, preventing cracks, avoiding direct contact between two distinct metals, especially if their

electrochemical activity differs greatly, and making the equipment easy to clean, examine, and maintain, corrosion can be prevented.

- Lining and coating: cladding, electroplating and organic coating are only a few of the methods for applying a coat or line on top of the surface or inside pipes.

2.6.1 Protective coating

Protective coatings are a common approach to corrosion prevention because they give the shielded portion a long operational life. If the objective is to defend against corrosion, these coatings do not add mechanical qualities to the base metal, but they may invest in boosting strength in other applications. Protective coatings are primarily used to separate the corrosion-prone sections of corrosive media; they make up a very tiny portion of the protected system's overall size. Scratching or damage that removes even a small portion of the coating causes damage and corrosion to the substrate's metal, which is one of the most important things to keep these coatings functional. Figure (2.15) depicts a cross section of an insulating pipe [42].

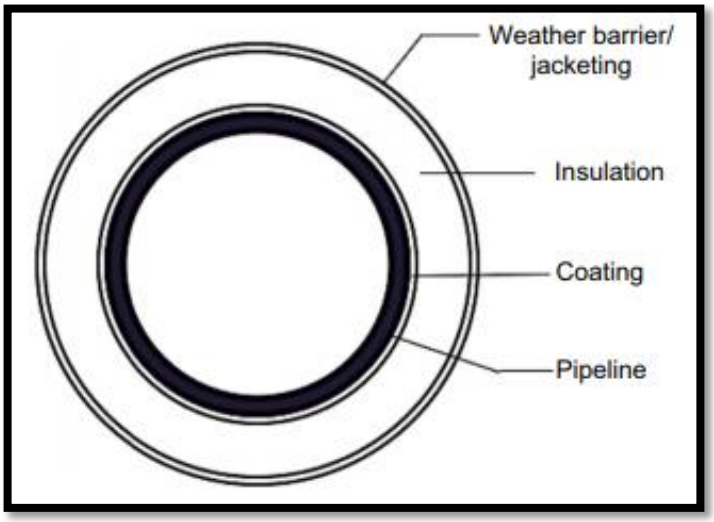

Figure (2.15): Typical cross section of an insulated pipe [43]

Protective coating includes:

- **Organic coating**

In comparison to other methods of metal protection, organic coatings are thought to be the most suitable in terms of weight. These coatings, which include paint, resins, and varnishes, create a physical barrier between the metal and the medium and may contain corrosion inhibitors or other additives that slow down the corrosion process [43].

- **Inorganic coating**

Enamels, glass linings, and conversion coatings are examples of inorganic coatings. Porcelain enamel coatings are water-resistant and resistant to a variety of weather conditions. Glass-lined metals are employed in process industries where product contamination or corrosion is a concern. Conversion coatings are made by deliberately corroding metal surfaces in a controlled manner. This is done to create a corrosion product that adheres to the metal and protects it from additional corrosion. One of the most prevalent aluminum conversion coating processes is anodization, which creates a protective aluminum oxide covering on the metal [44].

2.6.2 Metallic coating

Metallic coatings are considered to have high costs relative to organic coatings, so this type is resorted to when we want a longer operating life for the protected part. This layer is a metal barrier between the substrate and the environment, or by corroding more quickly in relation to the substrate. Metallic coatings are applied to the base metal by several techniques, such as electrodepositing, spraying, hot dipping, chemical vapor deposition (CVD), physical vapor deposition (PVD), welding, cladding, and bonding [45].

Metal coatings protect structural metals against corrosion in corrosive environments. There are two types of metal coatings: those that are more reactive than the base metal, and those that are nobler. The first group of coatings for steel protection includes zinc, aluminum, and, to a lesser extent, cadmium. These coatings work as sacrificial anodes, providing cathodic protection for the metal. The coating thickness, which affects the amount of sacrificial material, is frequently linked to the longevity of a coated structure. The second group of coatings includes the more noble metals of the substrate, such as chromium, nickel and copper, and the protective nature of these coatings depends on their continuity. Despite the hazards, these coatings are employed in a variety of applications because they provide unique features such as shine, hardness, and electrical conductivity [46].

In relation to the base metal, metallic coatings might be cathodic or anodized. The primary distinction between cathodic and anodic coatings is how they behave in the presence of a fault. In the event that the coatings are cathodic, which is represented by the figure (2.16a), the base metal is subjected to severe corrosion. The reason for this is the galvanic effect, where the ratio between the cathodic and anodic areas is high, which increases the rate of corrosion. In the second case, which is illustrated in figure (2.16b), a cathodic reaction occurs on the surface of the base metal while the coating layer is exposed to the galvanic effect, but it is simple because it occurs in a large area that represents the anode relative to the base metal (the cathode). In order to keep the substrate safe, for a cathodic coating, minimal porosity, great mechanical strength, and continuous adherence are significantly more important than for an anodic coating [47].

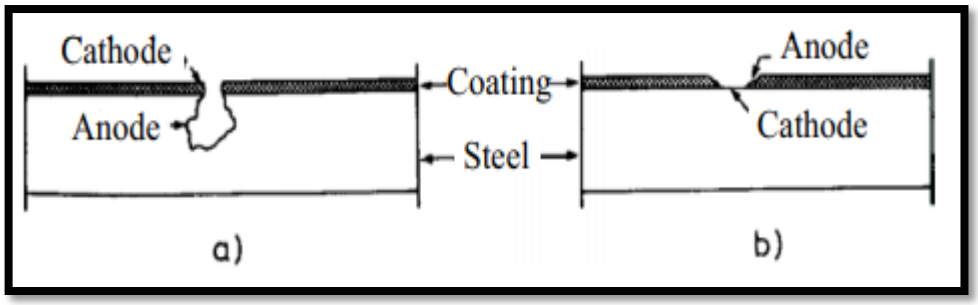

Figure (2.16): localization of corrosion at a defect in a metal coating on steel a) Cathodic coating. b) Anodic coating [48]

2.6.3 Electrochemical deposition

Electrochemical deposition represents the possibility of generating metal by reduction of the metal ion in aqueous and organic solutions, as well as salt electrolytes, which is represented by the equation (2.6) that shows the reduction of the metal ion (M^{n+}) which results in the metal (M) [51].

$M^{n+} + ne \rightarrow M$ ……. (2.6)

In this technique, there are two ways to obtain the metal from the solution; the first is by using electrical power (source of n electrons) to reduce the metal ion, which is known as (electrodeposition). The second method depends on the fact that reducing agent in the solution is the source of the electrons required to accomplish the reduction process, which is known as (electroless deposition), which does not require an electrical power source [48].

Electroless plating is a technique for depositing thin layers of metals, salts, oxides, and other compounds that can be employed in a variety of industrial and technological applications. This method uses the reducing agent as a source of electrons required to reduce the metal ions. It involves obtaining the metal from the reaction of the reducing agent with the salt containing the metal ion, depositing the metal on the surface to be protected without the need for an electrical power source. The reactions were as follows: [49].

Metal ion +Red → Metal Deposit +Oxidized product ……. (2.7)

Electroless plating consists of two reactions:

Metal deposition: $M^{+}+e \rightarrow M$ …… (2.8)

Oxidation: $Red+ H_2O \rightarrow Ox +H^{+}+e$ …… (2.9)

Where, M: Metal, e: electron, Red: Reducing agent, Ox: Oxidized product

As illustrated in Figure (2.17), the process is both electrolytic and electroless.

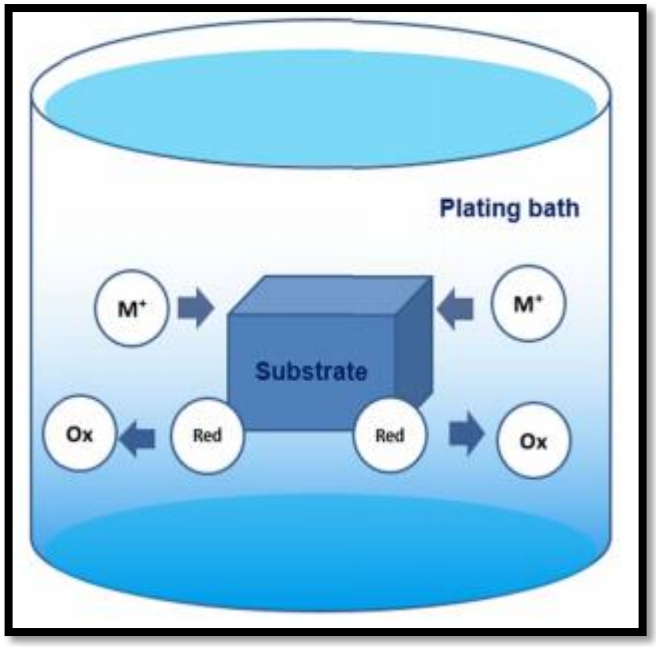

Figure (2.17): Schematic representation of electroless metal deposition [49]

The process of electrodeposition in general involves the dissolution of the metal to the positive electrode in an electrolytic solution containing ions of the same dissolved metal, where there is a constant electric current passes from the positive electrode to the electrolyte solution, then the electric charge is discharged at the electrode of the other metal complementing the electric cycle, which is the cathode. The process current results from the application of an external voltage difference between the two electrodes, where the charge of the anode is positive and the cathode electrode is negative. As a result, positive metal ions in the solution gravitate toward the negative electrode (the

cathode) and negative metal ions gravitate toward the positive electrode (the anode), resulting in an electric current [50].

The main objective of the electrodeposition process is to create a layer on the surface of the substrate metal so that this layer adds new properties that are not present in the substrate metal or are low, such as electrical properties, corrosion resistance, wear resistance, and improved thermal properties. This purpose is achieved by immersion of two electrodes of conductive metal in a solution (electrolyte) containing the metal ion used for the purpose of coating. One is connected to the negative electrode of the electrical power supply (cathode) and the other represents the anode electrode. For the purpose of depositing the coating metal on the cathode electrode (the substrate), the metal solution will electrolytically decompose, forming positive ions (the metal ions) and negative ions (the negative group from the decomposition of the metal solution) as shown in equation (2.10) [51, 52].

$MA\ (aq) \rightarrow M^{n+}\ (aq) + A^{n-}(aq)$ ……. (2.10)

The anode electrode can be soluble and is usually in solutions consisting of chloride as shown in equation (2.11) where the oxidation process of the metal occurs, or it can be insoluble and the process of water oxidation occurs as shown in equation (2.12), (2.13). As a result, the anode metal must be an excellent conductor and unaffected by the bath, whether or not current is flowing.

The reaction for soluble anode is: [51, 52]

$M(s) \rightarrow M^{n+} + ne^-$ …… (2.11)

Depending on the pH of the solution, there are two reactions for insoluble anodes: [51, 52]

$2H_2O \rightarrow O_2 + 2H^+ + 4e^-$ (acid solutions) …… (2.12)

$4OH^- \rightarrow O_2 + 2H_2O + 4e^-$ (basic solutions) …… (2.13)

Metal ions are reduced and deposited as metal atoms at the cathode, as in equation (2.14).

$M^{n+} + ne^- \rightarrow M(s)$ …….. (2.14)

2.6.4 Factors Effecting Electrodeposition process:

2.6.4.1 Effect of Current Density and Distribution

The current density and its distributing parameters are crucial in defining the uniformity of the resulting deposit coating. The current density across a cathode will change from spot to spot throughout the electro deposition process. With respect to bath composition and temperature, the cathode current density must be kept within the appropriate interval during the electro deposition process. Weak coating will occur from inadequate current for a particular specimen. Reduced current densities are associated with increased impurity levels in deposits because hydrogen ions are discharged; the pH level at the cathode rises, leading metal hydroxide ions to be included in the deposit layer. Finally, the salt content, operating parameters, and plating technique decide the best current density range for a certain plating bath. Another key plating parameter that must be carefully regulated is anode current density. Adjusting the overall anode area and the fraction of it formed of the metal to be deposited can achieve this [53, 54].

2.6.4.2 Effect of temperature

The size of the crystals grows as the bath temperature rises. The rise in bath temperature improves solubility and, as a result, the transport number, which raises the solution's conductivity. It also reduces the viscosity of the solution, allowing the double layer to be replenished more quickly. The high bath temperature prevents hydrogen from adsorbing on the deposits, minimizing stress and cracking risk. The grain size of the deposit somewhat decreased when the bath temperature was increased from 45°C to 55°C for

Chromium electroplating, but additional increases in bath temperature had the opposite effect[53, 54].

2.6.4.3 Effect of time

The thickness of the plating rises in direct proportion to the plating period and current. The quantity of charge flow (Q)(Coulomb) in a solution is proportional to the current flow (I)(Ampere) and the flow time (T)(second), according to Faraday's Laws as shown in the following equation (2.15): [53, 54].

$$Q = I \times T \qquad \text{……………………………………… (2.15)}$$

2.6.4.4 Effect of bath concentration

Generally, bath concentration has a significant impact on plating performance in the electro deposition process. In standard plating parameters, increase the concentration of metal ions in solution is due to increase the bath concentration .As a result, the plating process' deposition rate will rise[53, 54].

2.6.4.5 Effect of agitation

The metal salt is sufficiently mixed by agitation, allowing the chemical reagents to become intimate and react with one another. The thickness of the diffusion layer is reduced by agitating the plating solution, which replenishes metal salts or ions at the cathode. It reduces the number of gas bubbles, which could otherwise result in pits. Agitation aids in the increase in operational current density, allowing for a larger operating current density. These parameters influence the deposit metal ion structure as well as the concentration of the metal, because they compensate for metal ion loss by discharging more quickly at the cathode. Agitation in the plating process may result in coarse-grained deposits owing to the mechanical inclusion of sludge and other impurities floating in the electrode, but it also allows for depositing at high current densities. While all other parameters stay constant, the level of agitation should vary proportionally with the current density. Agitation is

frequently combined with filtration electroplating to eliminate coarse-grained defects caused by contaminants in the electrolyte. Filtration electroplating is frequently used in conjunction with agitation. Agitation promotes noble metal deposition on the cathode. In summary, by ensuring that the metal salt is thoroughly mixed, an agitation device can significantly improve plating efficiency [53, 54].

2.6.4.6 Influence of pH

The chemistry of the solution determines the acidity of the solution (pH). pH can affect the balance of numerous processes in a complicated bath. At the anode, oxygen evolution occurs when the anode is insoluble. The formation of hydroxide ion is accompanied by hydrogen evolution at the cathode: If the current efficiency at the anode is higher than at the cathode in a balance bath, the bath becomes alkaline. The pH of the bath gives stability if the electrode efficiencies are similar. As a result, the pH of a plating bath can be used to determine electrode efficiencies. Metal hydroxides may precipitate locally inside the cathodic double layer under some conditions, co-depositing with the plated metal and causing a faulty deposit while raising the pH owing to hydrogen evolution. As a result, buffers are required to keep pH fluctuations to a minimum [53, 54].

2.6.4.7 Effect of distance between electrodes

The distance or gap between the electrodes of the electroplating (anode and cathode) has an inverse effect on the thickness of the coating, i.e., with a decrease in the distance, the thickness of the coating increases because the decrease in the distance causes an increase in the strength of the electric field and a decrease in the resistance of the electrolyte between the electrolyte electrodes [53,54].

2.6.5 Applications of Electroplating

Electroplating is utilized in a variety of industrial settings. These applications can be divided into four categories: [55]

1. Decoration: To improve the aesthetics of a base metal, it may be coated with a more expensive metal. This is suitable for jewelry, furniture fittings, and other objects of a similar nature.
2. Protection: The coating is applied to a base material in order to protect it from corrosion, oxidation, and wear. Chromium coating, cadmium coating, and zinc coating are examples of corrosion resistance coatings.
3. Electroforming: Molds, dies, screens, and record stampers are all made using this technique.
4. Enhancement: Improved electrical and thermal conductivity, reflectivity, and solder ability.

2.6.6 Chromium Electroplating

Chromium and its alloys are one of the most important and commonly used coatings in the industry for improving corrosion resistance (particularly at high temperatures), hardness, abrasion and wear resistance, lubricity, and aesthetic features, including surface roughness and brightness. Electrochemical deposition is commonly used to apply chromium coating to various metallic substrates. There are two types of Cr coatings: one is decorative with a thickness of (<1.5 μm) and is frequently put over another under-layer coating such as copper or nickel. The other is a hard coating with a thickness of (2.5-500) μm or larger and a hardness of (850-1200 HV), which is commonly applied directly to the base metal [56].

The corrosion resistance of chromium is due to the formation of a thin oxide layer that protects the metal from further oxidation. Because of its passive oxide film, chromium, while being a non-noble metal, has great resistance to attack by

many oxidizing and reducing agents. Chemical attacks, such as those caused by hydrochloric acid and moderately concentrated sulphuric and nitric acids, usually originate in the deposit's fissures. The limited wetability of chromium deposits also prevents corrosive fluids from reaching the narrow gaps in them [57].

Hexavalent chromium bath is used to deposit chromium because it has higher throwing power, a brighter surface finish, less porous deposition, better corrosion resistance, and is easier to apply. The coating solution is prepared from hexa-chromium oxide (CrO_3) according to the following steps: (i) As a deposition bath, an aqueous solution containing CrO_3 and H_2SO_4 in a weight ratio of 100:1 (typically 250 and 2.5 $g.dm^{-3}$, respectively) is used.(ii) An operating temperature of around 50ºC. (III) 0.200 to 0.400 $A.cm^{-2}$ current density, these solution conditions for low carbon steel as a substrate[58]. Despite the fact that electrochemical deposition can be done at constant current, voltage control is preferable due to the difficulty of precisely measuring the area of complex shaped components. Because most of the current is lost in hydrogen gas reduction reactions, the efficiency of the current in the electrodeposition process does not exceed 18%. CrO_3 compounds should not be used since they are poisonous, carcinogenic, and can induce lasting genetic alterations. Also, CrO_3 oxidizing tendency makes it hazardous for the environment. One option to avoid these problems is to deposit chromium coatings into trivalent chromium salt solutions, which do not pose the same health and environmental risks. [58, 59].

2.6.6.1 Hard Chromium electroplating

Hard plating involves depositing a relatively thick coating of chromium directly on the base metal (typically steel) to create a surface with wear resistance, low coefficient of friction hardness, and corrosion resistance, or to

repair surfaces that have been degraded by use. Hydraulic cylinders and rods, industrial rolls, zinc die castings, plastic molds, engine components, and nautical hardware are all hard plated. The procedure is typically referred to as hard chromium plating, or functional chromium plating, when chromium is applied for any other reason or when aesthetics is a secondary consideration. The thickness of hard chromium plating normally ranges from 0.1 to 10 mils. Hydraulic cylinders and rods, crankshafts, printing plates/rolls, pistons for internal combustion engines, molds for plastic and fiberglass parts manufacturing, and cutting tools are all examples of functional plating uses. For rebuilding worn parts like rolls, molding dies, cylinder liners, and crankshafts, functional chromium is typically specified [60].

2.6.6.2 Hard Chromium electroplating operation

Chrome Chemical Bath, Anode, Cathode Potentials, Parts to be Coated, Heaters, Rectifiers, and Electrical Control Systems are all used in the coating process. The bath must first be heated to the desired temperature. The cathode electrode must be linked to the deposited piece, and the anode electrode must be connected to the positive potential. Before beginning the operation, the object should be completely cleaned and free of any surface blemishes or imperfections. Then, despite the passing of current to the part to be deposited, the deposition of the hard chromium deposit begins with the separation of ions from the chemical bath. Depending on the size of the component, the quantity of current flow and the length of the procedure will vary. In most cases, 30-40 amps are applied per square decimeter. For the current flow described above, the deposition rate will range between 25 and 30 microns per hour. The process is powered by a DC source [60].

2.6.7 Metal matrix composite coating

Composite coatings are formed as a result of combining two phases of materials to form a homogeneous one phase structure called the matrix, which can be metallic, polymeric, or ceramic. The reinforcing material is particulate, laminar, or fibrous in shape and can be metallic, ceramic, or polymeric. Metal matrix coatings may have better wear resistance, low friction coefficient, and toughness, as well as improved resistance to high temperatures, corrosion, and electromagnetic and optical interference. Metal matrix coatings are commonly employed as coatings for metallic components as well as bulk materials. It is a very inexpensive approach for improving the mechanical, thermomechanical, tribological, and corrosion properties of metallic components in order to increase their resistance to severe working conditions and component service life. Composite coatings consist of inert particles that are embedded in coatings of metals or alloys, this particals may be oxides (TiO_2, Al_2O_3, Cr_2O_3, etc.), carbide (TiC, WC, SiC, etc.) [60, 61].

The kind and structure of the metallic matrix, as well as the type and size of the built-in particles, determine the attributes of composite coatings. There are ultramicro-composite, micro-composite, and macro-composites, depending on the size of the embedded particles, as shown in figure (2.18). Composite coatings are a form of material made up of a crystalline or amorphous matrix in which another phase's material has been dispergated. A combination of qualities distinct from the attributes of the initial materials is produced as a result of the matrix's engagement with the components. The multiphase structure of these materials is a distinguishing feature [62].

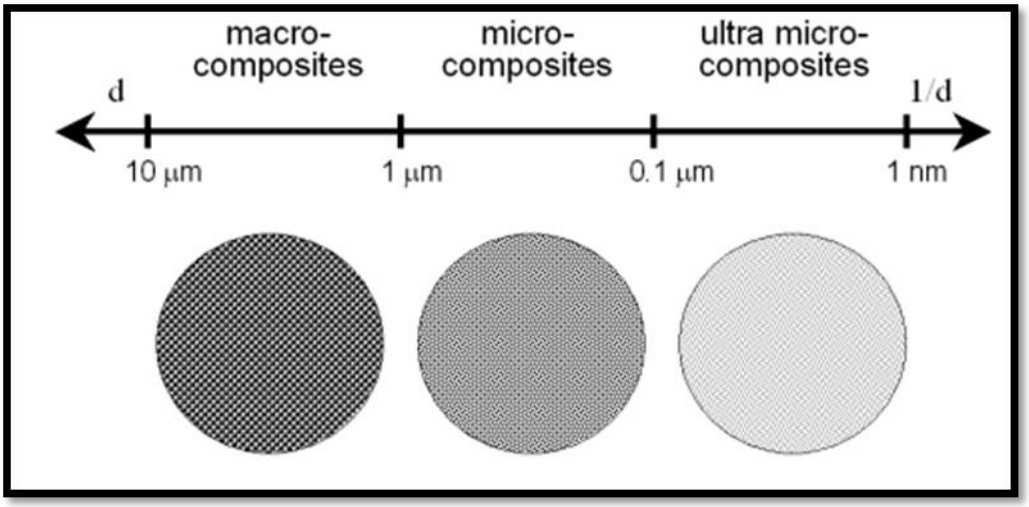

Figure (2.18): The size of the built-in particles influences the scale of composite materials [62]

2.6.7.1 Composite coating electrodeposition

Electrolytic codeposition is a technique for creating composite coatings by embedding particles, which are put into the plating solution purposely.The presence of particles scattered in the bulk, as well as the microstructural alterations made to the metal matrix and/or the exposed particles, which are only partially incorporated into the coating surface, give composite coatings their functional features. There are two basic techniques in which inert particles can be placed in the metal matrix: (a) by mechanically stirring them in the plating bath to keep them suspended. As the metallic ions around the particles are reduced, the particles are transported to the cathode and incorporated into the metallic matrix. (b) During electrodeposition, the particles that were initially suspended in the plating bath are allowed to settle on the cathodic surface (located at the bottom of the cell) and become embedded in the metal matrix, which means the particle content of the composite coating is usually higher [62,63].

2.6.7.2 The mechanism of particle deposition into a metal deposit

Two common processes involved in the incorporation of particles into metallic coatings can be recognized, namely physical dispersion of particles in the electrolyte and electrophoretic migration of particles. Investigations into micron-sized particles led to the development of codeposition processes for the dispersion of inert particles into metallic coatings. The particle transmission mechanism involves movement towards the cathode electrode due to electrophoresis, mechanical entrapment, adsorption, and convective-diffusion [63, 64].

As seen in Figure (2.19), the mechanism comprises of five steps. A particle must pass through several stages on its path from the bulk of the electrolyte to the site of inclusion at the cathode surface. As below: [64, 65].

1. Ionic species absorption on its surface.
2. Forced convection transport of the particles to the hydrodynamic boundary layer.
3. Particle diffusion through the diffusion layer.
4. Absorption of the particles at the cathode surface, which is surrounded by an ionic cloud.
5. Some ionic species are reduced, causing the particle to become irreversibly embedded in the metal matrix.

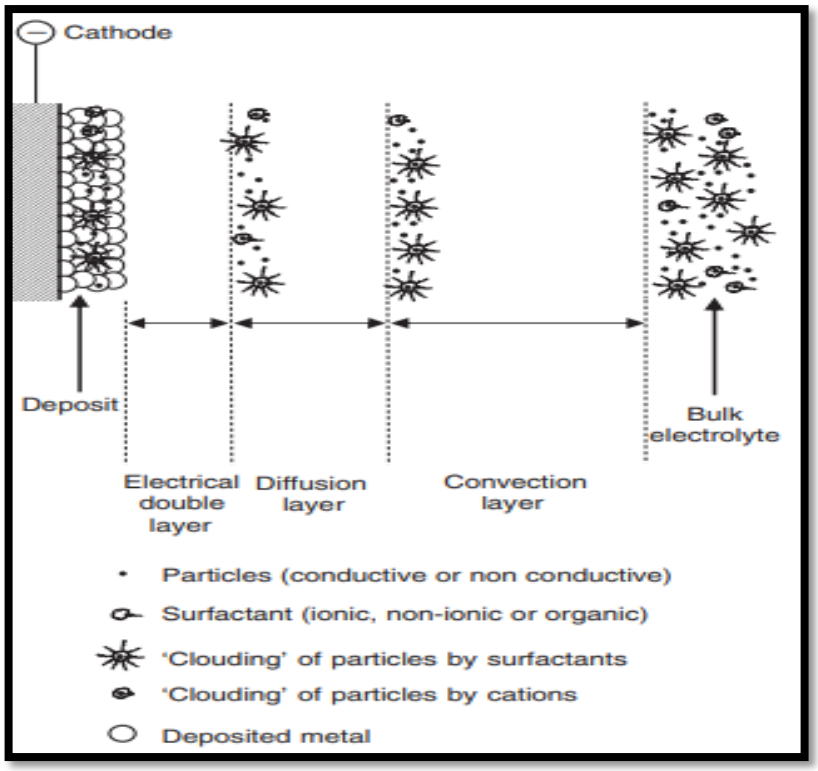

Figure (2.19): Particle codeposition mechanisms in a metal deposit [65]

In figure (2.19) the regions are as follows: (bulk electrolyte, normal length in cm); (convection layer, typical length 1 cm) Ionic clouds form surrounding particles. Diffusion via a concentration boundary layer (diffusion layer, generally hundreds of meters long); convection toward the cathode An electrical double layer (average dimensions of nm) follows adsorption and particle entrapment [65].

2.7 Optimization and Mathematical modeling

It is described as the quest for the best solution to a problem with the least amount of time and money spent in exchange for the best productivity and effectiveness. As a result, it is valued highly in practice and applications, and in order to meet this objective, the elements influencing the discovery of optimal solutions must be explored and analyzed using mathematical rules and equations known as models. A mathematical model is a mathematical

description of the behavior of real equipment and objects. It uses formulas to explain things and events so that we can better comprehend them. Mathematical modeling is a step-by-step procedure [66].

2.7.1 Grey system theory

Grey systems theory, developed by Julong Deng in 1982, is a method of problem solving that focuses on tiny sample sizes and limited knowledge. It deals with unknown systems with incomplete information by generating, excavating, and extracting useful information from the available data. As a result, the operational actions of systems and their laws of evolution can be accurately defined and monitored. Uncertain processes with small samples and limited knowledge are normal in nature. This fact defines the grey systems theory's broad spectrum of applicability [67]. The term "grey" in the theory's name refers to a characteristic that exists somewhere between black and white. "Black" indicates that required information is not exactly accessible, but "white" indicates that required information is precisely available. The proposed "grey" scheme establishes a link between black and white [68].

2.7.2 Grey relational analysis (GRA)

One of the most common methods for analyzing relationships between distinct data sets is Grey Relational Analysis. It is also used in multi-attribute situations to make decisions. The main benefits of Grey Relational Analysis are that it is based on original data, it is simple to calculate, and it is one of the best tools for making decisions in a business setting. Grey Relational Analysis uses information from the Grey System to compare variables quantitatively in a complex way. This method establishes relationships between variables based on their degree of similarity and variability [69].

The GRA strategy is to convert the output of all alternatives into a series of comparability, which is referred to as grey relational generating. A reference sequence (ideal target sequence) is defined based on these sequences. Then, for all comparability sequences and the reference sequence, the grey relational coefficient is computed. Finally, the grey relational grade between the reference sequence and each comparability sequence is determined using these grey relational coefficients. The best option is a comparability sequence translated from an alternative that has the highest grey relational grade between the reference sequence and itself. The procedures for grey relational analysis are shown in figure (2.20) [70].

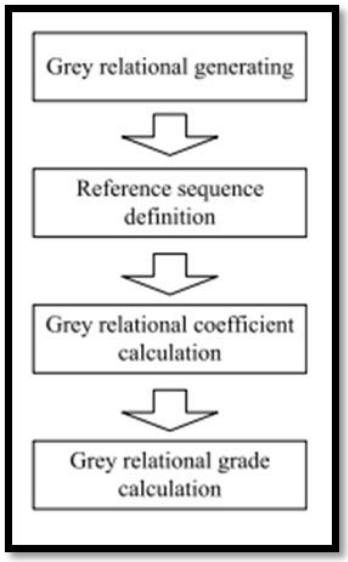

Figure (2.20): Procedure of grey relational analysis [70]

Grey relational analysis, unlike the Taguchi technique, which is designed to maximize a single response, can optimize many, often conflicting responses. Because the range and unit of one response will differ from those of the others, the output parameters should be normalized to a range of zero to one [71].

The following are the steps in Grey Relation Analysis: [72]

- Quality characteristics, also known as problems and response variables, must be defined.
- The process of acquiring data.
- Data should be normalized so that the lower the number, the better the quality characteristics, and the higher the number, the better the quality characteristics.
- Find the grey relationship coefficient for normalized data.
- Determine a grey reference's grade.
- Based on the grade value, select the best standard.

For a greater, higher-quality feature, the normalized value (Xi* (k)) is given by equation (2.16).

$$Xi^*(k) = \frac{Xi(k) - \min Xi\,(k)}{\max Xi(k) - \min Xi\,(k)} \qquad \ldots\ldots\ldots\ldots\ldots\ldots\ldots\ldots\ (2.16)$$

For the smaller the better quality characteristic, the normalized value (Xi* (k) is given by equation (2.17).

$$Xi^*(k) = \frac{\max Xi\,(k) - Xi(k)}{\max Xi\,(k) - \min Xi\,(k)} \qquad \ldots\ldots\ldots\ldots\ldots\ldots\ldots\ldots\ (2.17)$$

In which xi (k) is the original sequence; Xi* (k) is the normalized value of xi (k); min xi (k) is the smallest value of xi (k) for the (k^{th}) response, and max Xi (k) is the largest value of Xi (k) for the (k^{th}) response; k=1, 2,..., n.

It is important to create a relationship between ideal and actual normalized experimental values when processing data. It's achieved by calculating the grey relational coefficient, which can be found using the formula below: [73].

$$\S i\,(k) = \frac{\Delta \min + \beta\, \Delta \max}{\Delta 0i(k) + \beta\, \Delta \max} \qquad \ldots\ldots\ldots\ldots\ldots\ldots\ldots\ldots\ldots\ (2.18)$$

$$\Delta 0i\,(k) = |\, X0^*(k) - Xi^*(k)\,| \qquad \ldots\ldots\ldots\ldots\ldots\ldots\ldots\ldots\ldots\ (2.19)$$

Where Δ0i (k) is the deviation sequence of the reference sequence X0* (k) and the comparability sequence Xi* (k).

Δ min is the smallest divergence; Δ max is the highest standard deviation.

β is the coefficient of differentiation or identification. If all of the parameters are prioritized equally, it is taken as (0.5).

The grey relational grade is calculated by combining the grey relational coefficients for each output characteristic into the equation (2.20) [77].

$$\delta i = \frac{1}{n} \sum_{k}^{n} \S i(k) \quad \ldots\ldots\ldots\ldots\ldots\ldots\ldots\ldots\ldots\ldots\ldots\ldots \quad (2.20)$$

Where i = 1, 2, 3,... 9 (the L_9 orthogonal array is chosen), §i (k) is the Grey relational coefficient of (k^{th}) response in the (i^{th}) experiment, and(δi) the grey relational grade for the(i^{th}) experiment, and (n) is the number of performance characteristics.

2.7.3 Analysis of variance (ANOVA)

The analysis of variance (ANOVA) is used to determine which process parameters have a major influence on the quality characteristics. ANOVA is recommended for distinguishing significant factors by using the Grey relational grade value. Aside from degree of freedom (DF), mean of squares (MS), sum of squares (SS), F-ratio, p-value and contribution (C) were displayed alongside it. The greater the percentage contribution, the more significant the factor in influencing output characteristics [74].

Variance analysis includes a set of elements that determine the extent to which factors influence the outputs of operations, as shown below: [75,76]

- Degree of Freedom (DF): It shows how many independent variables are required to calculate the response data's sum of squares.
- Sum of square (SS): The deviation is the distance between any point in a set of data and the data's mean. The sum of all such squared variances is the sum of squares. The overall variation in the data is SS_{Total}. The portion of the variation explained by the model is called $SS_{Regression}$.

SS_{Error}, on the other hand, is the fraction of the data that is not explained by the model and is assigned to error.

$$SS_{Total} = \sum_{i=1}^{n} \sum_{j=1}^{h} (yij - \bar{y})^2 \quad \ldots\ldots (2.21)$$

$$SS_{Error} = \sum_{i=1}^{n} \sum_{j=1}^{h} (yij - \hat{y}i)^2 \quad \ldots\ldots (2.22)$$

$$SS_{regression} = SS_{Total} - SS_{Error} \quad \ldots\ldots (2.23)$$

yij= ith observed response of jth replicate, ŷi = ith fitted response, h = set of replicate, ȳ =mean of all (n*r) observation.

- Mean square (MS): The expression Mean Square refers to a variance estimate based on the variability among a group of variables in an ANOVA. The mean square of the model terms is calculated as follows:

$$MS_{Term} = \frac{\text{Adj SS (Term)}}{\text{DF (Term)}} \quad \ldots\ldots (2.24)$$

- Fisher's Test (F-ratio): The F-value is a metric for determining the distance between individual distributions. The F test is used to see if the interaction and the main effect are both significant. The model term formula is as follows:

$$F = \frac{\text{MS (Term)}}{\text{MS (Error)}} \quad \ldots\ldots (2.25)$$

The high value of the Fisher ratio gives an indication of the greater influence of the factor on the outputs of the system.

- Value of Probability (P-value): The P-value is used to evaluate whether a null hypothesis should be accepted or rejected in hypothesis testing. The p-value is the chance of receiving a test statistic at least as severe as

the actual calculated value if the null hypothesis is true. A common cut–off number for the p-value is (0.05).

- Coefficient of determination (R^2): The model's ability to explain how much variation in the response is measured. The R^2 value indicates how well the model fits your data. The formula is as follows:

$$R^2 = 1 - \frac{SS\ (Error)}{SS\ (Total)} \qquad \ldots\ldots\ldots\ldots\ldots\ldots\ldots\ldots\ (2.26)$$

- Adjusted Coefficient of Determination (R^2adj): The number of components in the model is taken into consideration by adjusted R^2, which is represented by the formula below:

$$R^2_{adj} = 1 - \frac{MS\ (Error)\ .\ DF\ (Total)}{SS\ (Total)} \qquad \ldots\ldots\ldots\ldots\ldots\ldots\ (2.27)$$

2.8 Literature Review for electrodeposition

In **1996, Ning et al** [77] in this study, composite coating of particles was performed (Al_2O_3) in hexa-chromium solution. effect of coating variables on the amount of (Al_2O_3) content in the composite coating The value of the coating hardness is about (1300) HV when the content is (0.7-1.0) wt% (Al_2O_3). The wear resistance of the coating is improved by two to six times when compared to the chromium coating. The maximum co-deposition was observed at 20 A dm-2, temperature 40 °C, rare earth content of 2.0 g l^{-1}, and bath loading of Al203 greater than 400 g l^{-1}.

In **(2005), Surviliene et al** [78] in this study, silicon carbide powder were used in a chromium bath (VI) to form (SiC) coatings for the purpose of studying the changes that occur in composite coatings (SiC) as a result of exposure to sulfate solutions. The electrochemical examination was used to achieve this

purpose. After capturing impedance spectra at various periods of exposure to the sulphate solution, the data was analyzed using different equivalent circuit models. The results showed an improvement in the corrosion resistance of the chrome plating when adding silicon carbide particles according to the properties of the formed composite coatings, these results are consistent with the current research in terms of a decrease in the corrosion rate due to the addition of silicon carbide powder to the triple chromium plating solution, although the research used a hexagonal chromium solution., such as the size and number of pores.

In **(2011), Gao and Suo** [79] Cr–Al_2O_3/SiC composite coatings were coated in Cr (VI) baths including Al_2O_3-coated SiC powders to improve the SiC content in Cr-based coatings. The Al_2O_3-coated SiC composite particles were made by calcining a heterogeneous deposition precursor. The nano-SiC particles were bundled with alumina, according to transmission electron microscopy examination of the particles. The particles retrieved from the bath had a zeta potential of up to +23 mV, which was beneficial for particle-chromium co-deposition. During the electrodeposition, pulse current was employed.The coating was compact and blended nicely with the substrate, according to scanning electron microscopy (SEM). The concentration of SiC in Cr–Al_2O_3/SiC coatings was found to be around 2.5 wt. % using energy dispersive X-ray analysis. Potentiodynamic polarization and electrochemical impedance spectroscopy techniques were used to examine the corrosion behavior of the composite coating. The results showed that the Al_2O_3/SiC particles considerably improved the composite coating's corrosion resistance in a 0.05 M HCl solution.

In **(2013), Juneghani et al** [80] two types of coatings have been studied on carbon steel (substrate). The first is using metallic chromium coatings and the second is using chromium with silicon carbide nanoparticles. Constant current was used to complete the coating process. During the coating process, the effects of carbide particle content, mixing speed, and current density were studied. The result of the study of practical variables is the electrodeposition of It was found that through current density (32 A/dm^2) and mixing speed of the solution (200 rpm), you get the most amount of precipitation of silicon carbide particles in the chromium layer and the highest amount (1.13%) when its added concentration to the solution is (20g/l). Exceeding the content of carbide particles by an amount (20g/l) leads to the formation of clumps of these particles in the solution. The morphology of the Cr-SiC nanocomposite coating is finer, more regular, and denser than that of pure Cr coating. The SiC nanoparticles co-deposited in the Cr matrix are uniformly dispersed, enhancing the coating's corrosion and wear resistance. As the Sic particles of the coating increase, the corrosion current density decreases, and the corrosion potential shifts to a more positive potential, the micro-hardness of the coating increases. Cr-SiC Nanocomposite coatings offer the lowest friction coefficient and higher wear resistance than pure Cr coatings. By comparing our current research with the research (JUNEGHANI (2013), in which the researcher used a solution (0.05 mol/l HCL) with Hexavalent-chromium oxide, silicon carbide nanoparticles While in our research (Trivalent-Chromium oxide) was used with silicon carbide microparticles in concentrated sulphuric acid (98%) as a medium for corrosion, the results were consistent in terms of a decrease in the corrosion rate with an increase in the concentration of silicon carbide particles to (20g/l), but when the percentage was higher than (20g/l), a higher percentage occurred. In the corrosion rate in both studies, the reason for this

increase in the corrosion rate is the lack of high mixing speed to raise the silicon carbide particles to the surface of the cathode, taking into account the avoidance of turbulent movement of the particles.

In **(2016), Lakra et al** [81] Chromium-zirconia composite coatings were fabricated on low carbon steel substrates using direct current (DC) and pulse electrodeposition (PED) aim is to increase mechanical characteristics. To improve the matrix and increase the ZrO_2 content of the coating, greater pulse frequencies and pulsing were determined. Hardness and wear characteristics, as well as fine structure and dispersion, are all affected by the crystallographic orientation of the Cr matrix. The wear mechanism was discovered to be largely abrasive in DC deposition, with little sticky propensity.

In **(2016), Liao et al** [82] studied Cr-C/Si_3N_4 composite coatings are made by electroplating trivalent chromium plating baths with suspended Si_3N_4 nanoparticles under DC conditions. The effects of plating parameters such as the concentration of Si_3N_4 in the plating bath and the current density on the coating composition, deposition rate, morphology, surface roughness, micro-hardness, and wear conductivity of electrodeposited Cr-C/Si_3N_4 composite coatings were evaluated and compared to electrodeposited Cr-C coatings. The Si_3N_4 particles can be successfully co-deposited and uniformly distributed in the electrodeposited Cr-C matrix, according to the results. The highest degree of Si_3N_4 particle assimilation, around (17.22) vol %, is found at a bath loading of 5 g/l and a current density of 20 A/dm^2. Due to the improved dispersion strengthening effect, the addition of Si_3N_4 particles promotes the microhardness of the coatings and greatly increases their wear resistance.

In **(2018), Sheu et al** [83] in this study, the composite coating was carried out from chromium solution (III) to form two types of coatings (Cr-C) and (Cr-

C/Al_2O_3) and the aim is to study the mechanical and corrosion properties of the coatings. Although the Cr-C/Al_2O_3 composite coating has the highest corrosion protection (icorr = 2.84 $10^{-7}A/dm^2$), the corrosion resistance decreases as the heating temperature rises, caused by the formation of defects within Cr-C/Al_2O_3 composite coatings. Heat treatment effects on the mechanical characteristics and tribological performance of Cr-C and Cr-C/Al_2O_3 composite coatings are being studied. As per the findings, heat treatment improved the hardness of Cr-C coatings and Cr-C/Al_2O_3 composite coatings, mainly because of the precipitation of chromium carbide and chromium oxide. The micro-hardness of the Cr-C/Al_2O_3 composite coating is dramatically improved as Al_2O_3 particles are integrated into the Cr-C matrix, and the wear rate is significantly reduced when relative to the Cr-C coating. The maximum micro-hardness (22.85 GPa) is reached after heating Cr-C/Al_2O_3 composite coatings to 600°C. The co-deposition of Al_2O_3 particles inside Cr-C deposits improves wear resistance and decreases wear weight loss in coatings.

In **2019, Sadeghi and Najafisayar** [84] studied Cr-MoS_2 composite coatings were electrodeposited from Cr^{+6} baths containing various quantities of MoS_2 particles and various forms of surfactant in this sample (cationic and anionic). At various experimental conditions, the results revealed that the integration of MoS_2 particles into composite coatings is very small, and a Cr matrix with very low crystallinity can be electrodeposited. The presence of MoS_2 particles in the bath (up to an optimal value) causes composite coatings to form with lower surface roughness than traditional chromium coatings. While the solid content of the bath increases, more MoS_2 particles are introduced into the electrodeposits. Chromium can not be electrodeposited from baths containing

large quantities of MoS_2 particles. The use of a cationic surfactant encourages particle integration into the Cr metallic matrix. Furthermore, the presence of surfactant in the bath causes coatings to form with fewer microcracks. All of the composite coatings have higher hardness values than traditional chromium coatings; the coatings electrodeposited from baths with no surfactant have the highest hardness. Corrosion tests showed that smooth coatings with more MoS_2 particles and fewer micro cracks have better corrosion resistance than others.

In **2019, Zhang et al** [85] thermodynamic predictions of electrochemical reduction in a molten salt system containing NaCl, KCl, NaF, and Cr_2O_3 demonstrate that electrochemical deposition of a Cr coating on low carbon steel is conceivable. $Cr^{3+} + e \rightarrow Cr^{2+}$ and $Cr^{2+} + 2e \rightarrow Cr$ are the two steps in the electrochemical reduction of Cr(III) to Cr. according to the electrochemical reaction mechanism and electrocrystallization phase of chromium investigated at 1073 K by an electrochemical workstation. The electrochemical processes of Cr (III) and Cr (II) are quasi-reversible reactions, and the electrocrystallization process of Cr is an instantaneous hemispheroid three-dimensional nucleation process. On a low carbon steel substrate, a Cr coating with a thickness of 250μm was successfully deposited. The corrosion resistance of Cr-coated low-carbon steel is far higher than that of low-carbon steel, according to the results of the AC impedance process.

2.9 Literature review for Optimization

In **(2013), Jegan and Venkatesan** [86] the influence of pulse boundaries, such as frequency, pulse duration, and current density, on the crystal structure, hardness, and resistance to corrosion of nickel/nano-Al_2O_3 composite coatings generated by the pulse electrodeposition method was investigated on AISI

1018 steel samples electroplated in a Watt's type bath. The studies used Taguchi's L_{27} orthogonal array with various pulse factor configurations, and 27 trials were undertaken to see how pulse criteria affected sample hardness. The evaluation findings revealed that with a pulse frequency of 20 Hz, a service period of 30%, and a peak current density of 0.4 A/cm^2, the specimen has the highest hardness, which are the ideal characteristics in this instance. The service cycle has the largest effect on hardness, according to the ANOVA analysis, whereas current density has a little effect.

In **(2014), Gadhari and Sahoo** [87] with the use of Grey analysis and the Taguchi technique, attempts are made to explore the influence of process factors on the surface roughness of Ni–P–TiO_2 composite coatings. Ra, Rq, Rsk, Rku, and Rsm are some of the surface roughness metrics evaluated in the research. The coating criteria, which include nickel sulpahte as a nickel supplier, sodium hypophosphite as a reduction agent, and TiO_2 particle concentration as a secondary phase's particle, are installed into an L_{27} orthogonal array to identify the optimal level of process variables for limiting composite coating surface roughness. The experimental data observed that the amount of the secondary phase, namely titanium particles, has a substantial influence on managing the roughness parameters of composite coatings, whereas the amount of reducing agent has a minor effect.

In **(2017), Kumar and Narayanappa** [88] studied improving process parameters for Ni-WC electrodeposition on ferrous bearings for high wear resistance coatings. Based on Experimental method, electrochemical deposition criteria including electrolyte temperature (45, 50, and 55°C), agitating speed (200, 300, and 400 rpm), current density (3, 4, and 5 A/dm2), WC composition in electrolytic bath (1, 2, 3g/l), wear load (15, 20, 25 N), and

speed (60, 90, 120 rpm) were maximized (DOE). According to ANOVA analyses, the percentage share of variables are controlled for Ni-WC coatings was WC (45.96%), stirring speed (16.65%), current density (1.92%), temperature (1.6%), loading (10.00%), and velocity (11.72%). Stirring velocity 262.62 rpm, temperature 55 °C, current density 5 A/dm2, WC particulates 4 g/l, loading 24.19 N, and velocity 60 rpm are the optimal characteristics for high wear resistance and minimal friction, according to response surface technique.

In **(2018), Raghavendra et al** [89] this study is based on the response surface methodology. The coating parameters of composite coating on aluminum-based alloys were optimized via grey relation analysis. This model achieves the optimal coating parameter combination for maximal coating thickness, adhesive strength, microhardness, and wear rate. The effect of coating parameters at various levels has been discussed for each response. Temperature, 34 C; current density, 1 A/dm^2; and percentage of particle loading, (1.2)g/L are the best conditions for better composite coating performance based on Grey relation grade. The current density has statistical relevance on total composite coating performance at the 95% significance level.

2.10 Summery of Literature review

According to past research, the majority of them focused on the influence of coating process variables on the characteristics of the coating layer and its capacity to resist corrosion and wear when compared to the base metal as a kind of surface modification, as shown in table (2.5). To determine the properties of composite coating layers, most investigations used solutions and laboratory techniques. Composite coatings were studied in one of the concentrated sulfuric

acid plants, and the extent of resistance of this layer in the concentrated sulfuric acid solution was demonstrated.

Table (2.5): The electrodeposition studies

electrodeposition studies				
NO.	Years	Researchers	Substrate	Electroplating applications
1	1996	Ning	Stainless steel	Electrodeposited Cr-$A1_2O_3$ composite coating provides wear resistance.
2	2005	Surviliene	Carbon steel	The influence of SiC on the corrosion of chromium coatings
3	2011	Gao	Carbon steel	The research revealed that the Al_2O_3/SiC particles considerably improved the composite coating's corrosion resistance in a 0.05 M HCl solution.
4	2013	Juneghani	Carbon steel	The purpose of this study is to use conventional direct current electrocodeposition to evenly deposit SiC nanoparticles on a Cr metallic matrix to generate strong, crack-free Cr-SiC layers with improved wear and corrosion capabilities due to SiC nanoparticles' good corrosion and erosion properties.
5	2016	Lakra	Carbon steel	To improve the matrix and increase the (ZrO_2) content in the coating, greater pulse frequencies and pulsing were discovered. In addition to fine structure and dispersion, the crystallographic orientation of the Cr matrix influences hardness and wear characteristics. The wear mechanism in the case of DC deposition was discovered to be primarily abrasive.
6	2016	Liao	Carbon steel	Wear resistance of composite coatings is considerably improved and wear weight loss is reduced when Si_3N_4 nanoparticles are codeposition in the deposit.
7	2018	Sheu	Carbon	Improvement in the micro-hardness of (Cr-C/Al_2O_3) and an increase in wear

			steel	resistance and a decrease in the wear rate as a result of the heat treatment procedure of the composite coating layers.
8	2018	Sadegh	copper	Improving the hardness and corrosion resistance of the Chromium coating with MoS_2 particles.
9	2018	Zhang	Carbon steel	Increase corrosion resistance of carbon steel by Cr coating.

In table (2.6) shows the effect of electrodeposition process parameters that investigate the best performance depending on grey relational method.

Table (2.6): The Optimization studies

Optimization studies				
NO.	Years	Researchers	Substrate	Electroplating optimization
1	2013	Jegan	Carbon steel	The studies were carried out using Taguchi's L_{27} orthogonal array with various combinations of pulse parameters, and 27 trials were undertaken to evaluate the influence of pulse parameters in order to maximize the hardness of the specimen.
2	2014	Gadhari	Carbon steel	Using Grey analysis and the Taguchi approach, we studied the impact of process factors on the surface roughness of Ni–P–TiO_2 composite coatings.
3	2017	Kumar	Stainless steel	Optimize process parameters for Ni-WC electrodeposition on ferrous bearings for enhanced wear resistance coatings
4	2017	Raghavendra	Aluminium 6061	This method yields the optimal coating parameter combination for maximal coating thickness, adhesive strength, microhardness, and wear rate. The effect of coating parameters at various levels has been discussed for each

				response.

2.11 Current Research Trends

In the current research, the effect of adding micro-silicon carbide powder to the optimum chrome plating and the formation of composite coatings on the surface of carbon steel was studied, subjected to examination in concentrated sulfuric acid (98%) to show the extent of the ability of these coatings to achieve an improvement in corrosion resistance.

Chapter Three

Experimental Part

Chapter Three

Experimental Part

3.1 Introduction

The third chapter explains and clarifies the stages of the practical part, which include the operations of preparing all of the base metal and preparing it to perform the coating process on it, as well as providing equipment and materials to finish the electroplating operations, performing mechanical tests on the models that have been electrically plated, conducting corrosion tests on the job site at the concentrated sulfuric acid plant (98%), which involves two types of testing, the first for stagnation and the second for the flow of concentrated acid, as well as assessing the polarization of the samples. Surface coating tests, which include optical microscope, (SEM) and (AFM), as well as tests on the elements compounds and phases of the base metal (carbon steel), (XRF), metallic and composite coatings (EDS), and (XRD).Figure (3.1) depicts the steps of the practical section.

3.2 Materials

The materials used in the research include the metal on which the coating process was carried out, the materials that were used in the preparation of plating solutions and the powder that was used in the formation of composite coatings.

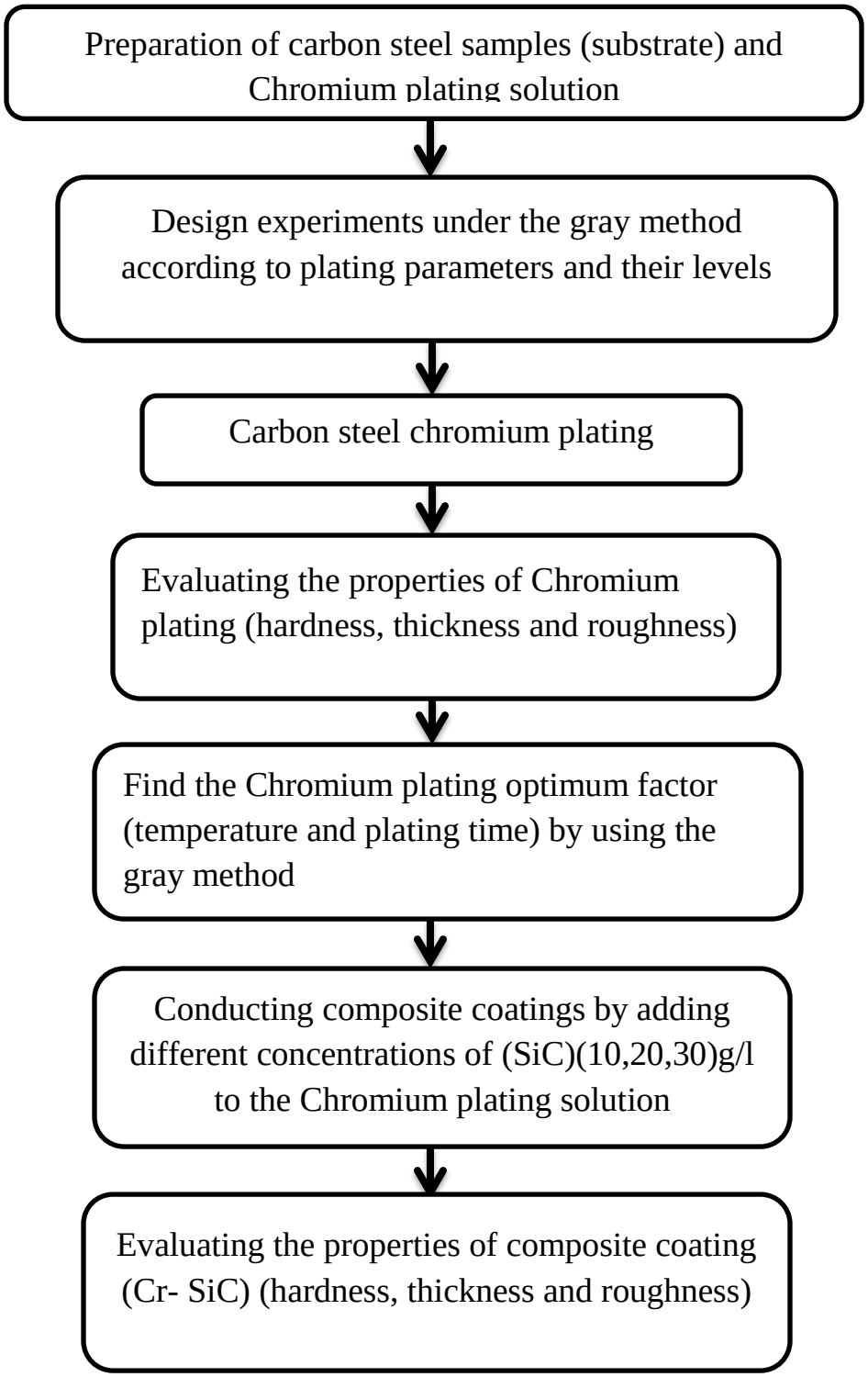
Preparation of carbon steel samples (substrate) and Chromium plating solution
Design experiments under the gray method according to plating parameters and their levels
Carbon steel chromium plating
Evaluating the properties of Chromium plating (hardness, thickness and roughness)
Find the Chromium plating optimum factor (temperature and plating time) by using the gray method
Conducting composite coatings by adding different concentrations of (SiC)(10,20,30)g/l to the Chromium plating solution
Evaluating the properties of composite coating (Cr- SiC) (hardness, thickness and roughness)

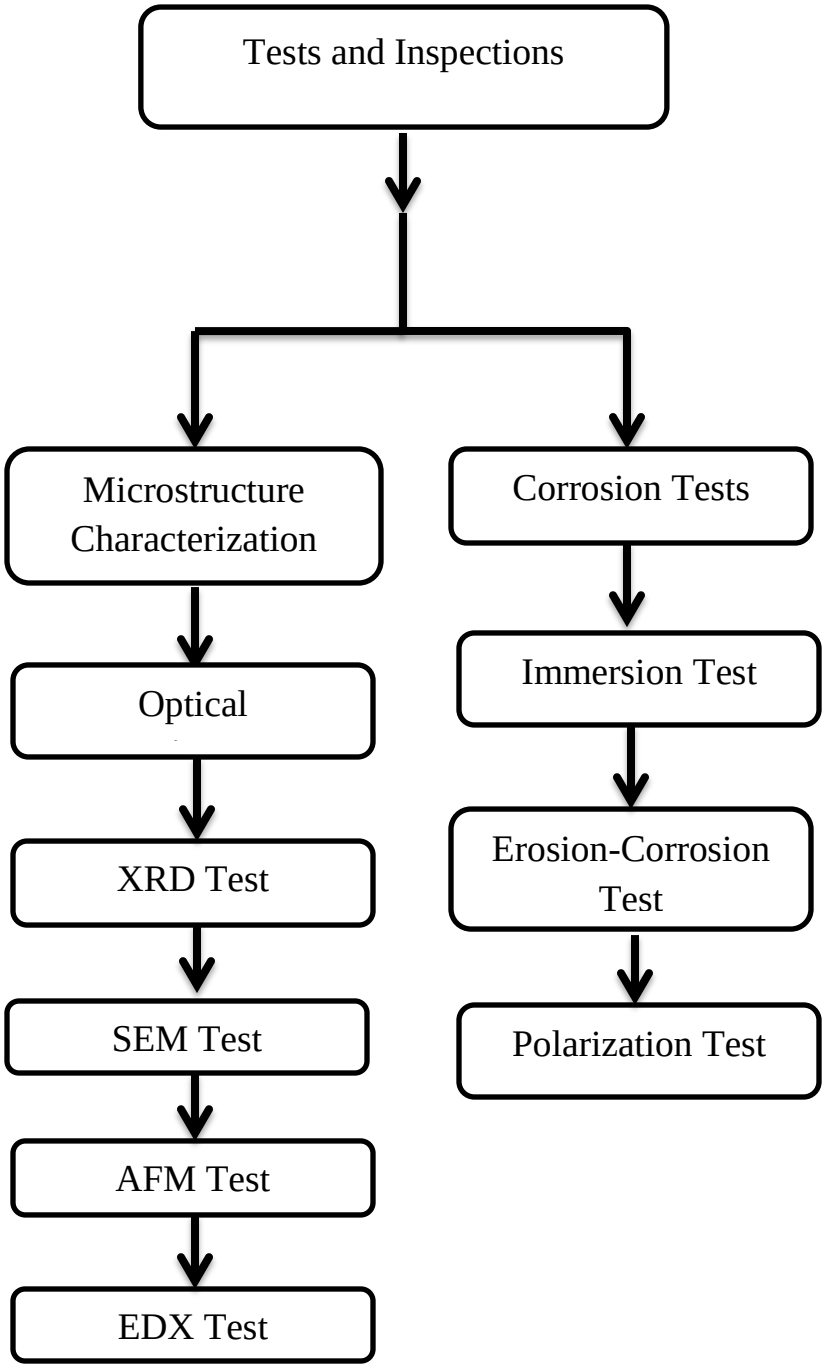

Figure (3.1): Diagram showing the steps of the practical part

3.2.1 Substrate material

The material to be coated is carbon steel obtained from Al-Furat State Company for Chemical Industries and Pesticides. It is a plate of medium carbon steel with dimensions of (20mm ×20mm ×5mm). Cut from a tube used to transport concentrated sulfuric acid from the factory to the acid storage tanks. The table (3.1) shows the proportions of the constituent elements of the substrate metal. Inspection being carried out by the General Company for Engineering Inspection and Rehabilitation in Baghdad.

Table (3.1): Chemical composition of carbon steel (tube)

Element %	C	Si	Mn ,	P	S	Cr	Mo	Ni	Cu	Fe
A	0.4	0.3	0.82 ,	0.01	0.01	0.08	0.02	0.13	0.19	rest

Because of the difficulty of preparing samples for the purpose of electroplating when the samples are in the form of a section of a tube and the thickness of the section is small, the shape of the base metal models was changed to a cylindrical shape by selecting four steel rods and conducting elemental analysis in the General Company for Engineering Examination and Qualification as listed in the table (3.2).

Table (3.2): Proportions of the constituent elements of metal rods

Element %	C	Si	Mn	P	S	Cr	Mo	Ni	Fe
1	0.2	0.307	0.526	0.0169	0.0123	0.0251	0.0032	0.036	Rest
2	0.385	0.24	0.917	0.0151	0.0289	0.148	0.0411	0.117	rest
3	0.433	0.357	0.758	0.007	0.0184	0.0577	0.019	0.0658	rest
4	0.382	0.283	0.423	0.008	0.0178	1.5	0.207	1.38	rest

The results of the chemical analysis of the rods indicate the convergence of sample (A) from table (3.1) with sample (3) from table (3.2) in terms of the chemical composition, and thus the sample (3) was chosen from table (3.2) to

be used as the substrate material for the purpose of conducting electrodeposition on it.

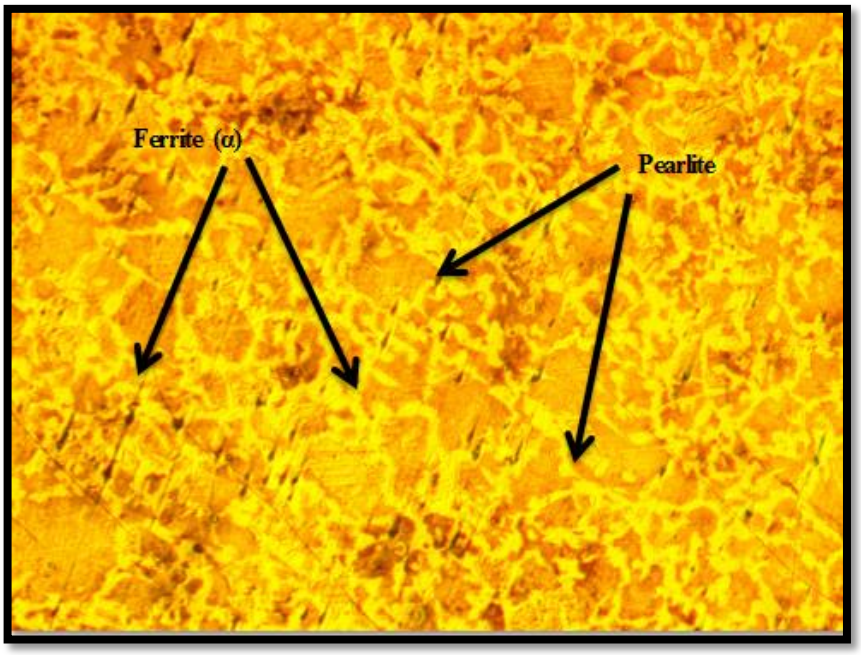

Figure (3.2): Microstructure of carbon steel (substrate material) (100x)

The microstructure of (pearlite), (α-Ferrite) can be seen in figure (3.2) as a result of an optical microscope on the substrate (carbon steel). microstructure of the steel sample consists of approximately equal amounts of ferrite and pearlite, which is expected for medium carbon steel with a percentage of carbon greater than (0.4%) carbon.

3.2.2 Trivalent Chromium oxide (Cr_2O_3)[63]

It is a dark red flaky granule as shown in figure (3.3). This is the source of the chromium metal for the purpose of depositing it on the metal (carbon steel).

Figure (3.3): Flaky of trivalent Chromium oxide (Cr_2O_3)[91]

3.2.3 Concentrated sulfuric acid (H_2SO_4)[62]

Concentrated sulfuric acid is used at a concentration (98%), as it is added to the solution consisting of trivalent Chromium oxide (Cr_2O_3) dissolved in distilled water.

3.2.4 Silicon Carbide powder (SiC)

Silicon carbide is a powdery greenish-green ceramic material. A material of high hardness, excellent corrosion and wear resistance. This material was used in this work for the purpose of forming composite coatings with chromium metal. Particle size was measured by a particle size analyzer in the laboratory of the department of Ceramic /Collage of Materials Engineering. The results of the particle size analysis for (SiC) powder are shown in Figure (3.4). The particle size of (SiC) powder varied from (0.909 µm to 23.68 µm), with a particle size, of (4.665 µm) on average.

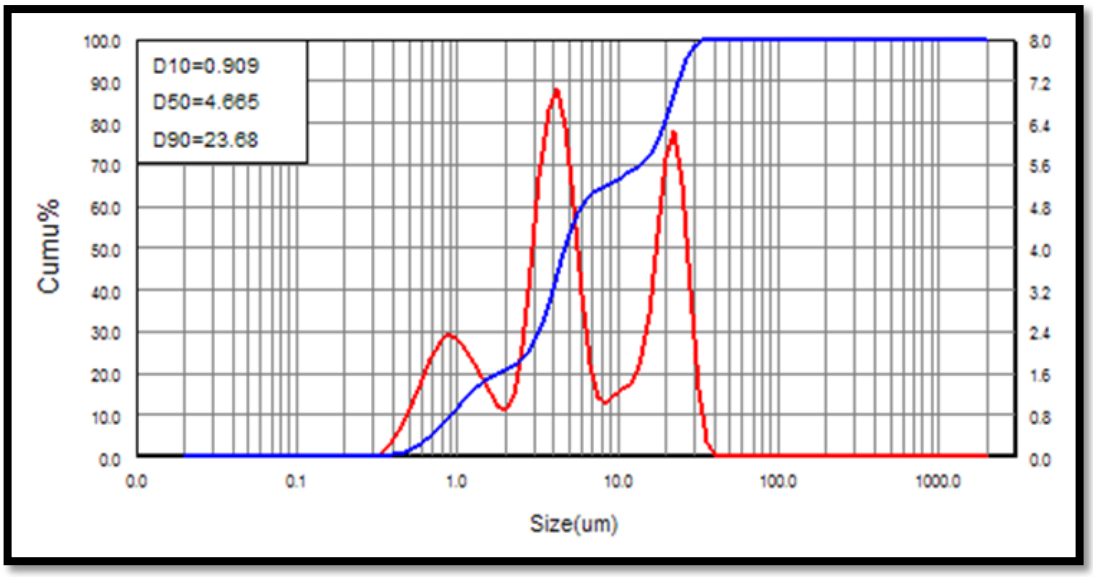

Figure (3.4): Particles size for silicon carbide (SiC)

Table (3.3) describes the details of the materials used in the electrodeposition process.

Table (3.3): The details of the materials used in the electroplating process

Material	Formula	Purity %	Origin
Trivalent Chromium oxide	Cr_2O_3	99.8	Canning(English)
Concentrated Sulfuric acid (98%)	H_2SO_4	99	PRS panreac (Spanish)
Silicon Carbide	SiC	99.78	CBC India

3.3 Samples preparation

Provide a carbon steel rod with a diameter of (1.4cm) and a length of (60cm). Following the removal of the oxide layer from the rod's perimeter by the lathe machine, samples of (0.6cm) in diameter,(1cm) in height and a reasonable number for the purpose of electrodeposition are cut. Surface preparation of samples began with graded smoothing using smoothing paper (silicon carbide paper) (220-2500). Deionized water would be used to wash all of the samples, then acetone, and then dried with an electro-dryer, and the samples were kept in containers with silica gel to avoid moisture. The stage of polishing the samples included the use of diamond paste in a gradual manner

(9, 3 and 1 microns), then washing with acetone to get rid of oily spots on the surface of the samples. Dip samples in an acetone solution to remove any oils left over from the diamond paste polishing process.

In order to ensure the cleanliness of the surface of the samples and to remove the oxides, the samples were immersed in hydrochloric acid at a concentration of (30%) for a time of (10) seconds in order to activate the carbon steel surface for electroplating process, followed by washing with distilled water, then drying by an electric dryer, then preservation in a container containing silica gel to absorb moisture and avoid oxidation in preparation for the electrodeposition process.

3.4 Preparation the electroplating bath

Dichromic acid ($H_2Cr_2O_7$) is the active ingredient to obtain chromium metal deposited on the part to be coated (carbon steel sample). dichromic acid is produced by dissolving triple chromium oxide(Cr_2O_3) in distilled water, where 300 grams of chromium tertiary oxide have been added to a liter of distilled water, followed by the addition of(98% concentrated sulfuric acid) at a ratio of (1:100) of oxide. Tables (3.4), shows bath solution for electroplating of chromium (Cr), figure (3.5) show Chromium coating bath solution.

Table (3.4): Chromium bath composition

Electroplating bath	Composition	Concentration
Chromium bath	Trivalent chromium oxide	300 g/l
	sulfuric acid	3 ml/l

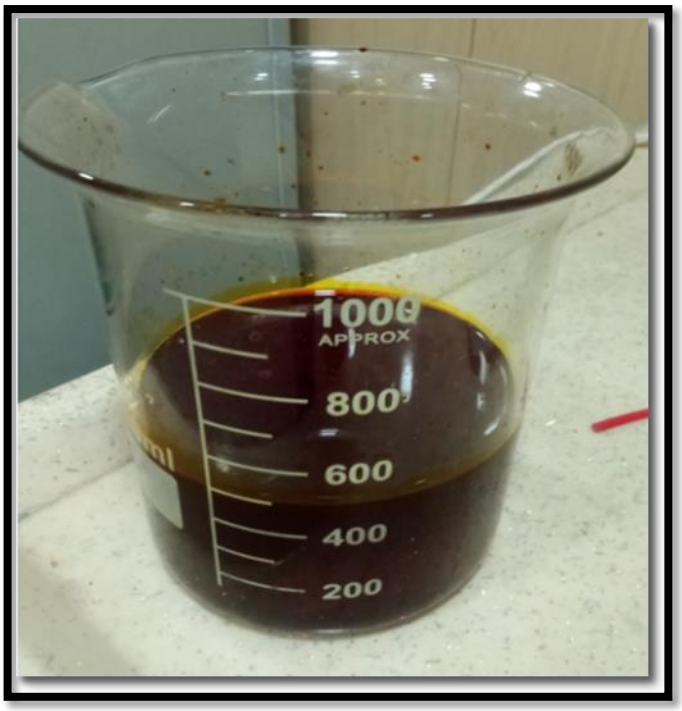

Figure (3.5): Chromium coating bath solution

3.5 Electroplating process

To achieve the electroplating process, a coating solution container has been prepared, which is a graduated glass cylinder. The glass cylinder is carried by a device known as a (hot plate and magnetic stirrer) which realizes the circulation of the solution and the control of the temperature of the solution as influencing factors during the electroplating process. The supply of electrical power is done by using a power supply with a current range of (0-6) Am, a voltage range of (0-20) V It contains a socket and connection wires where the negative electrode is connected to the carbon steel sample for the purpose of coating, while the anode is connected to two lead electrodes with dimensions 10cm for width and 20cm in length so that the carbon steel sample is in the middle of the distance between the two lead electrodes and the circular surface of the sample is parallel to both lead poles. So that the surface area of the lead electrodes (anode) is equal to or greater than the surface area of the steel

sample (cathode) where the surface area of the sample was (0.06) dm^2 and it is the electroplating current (1.2) Am. Table (3.5) shows the Chromium electrodeposition process conditions. Figure (3.6) shows the electroplating process for Chromium coating.

Table (3.5): Process conditions of Chromium electroplating

Process conditions	
PH	2
Deposition temperature(°C)	(40,50,60)
Deposition time (hours)	(1,1.5,2)
Distance between electrodes (cm)	5
Voltage (volts)	4.5
Magnetic stirring(rpm)(S.V.)	300
Current density (Am/dm^2)	20

For the purpose of depositing composite coatings (Cr-SiC) on the substrate (Carbon steel), the same conditions as for chromium coatings in table (3.5) are used, with the temperature of the depositing solution fixed at the value (50°C) and depositing time (2 hours), which are the optimal conditions that were obtained for metallic chromium plating based on the gray method as shown in table (3.6).

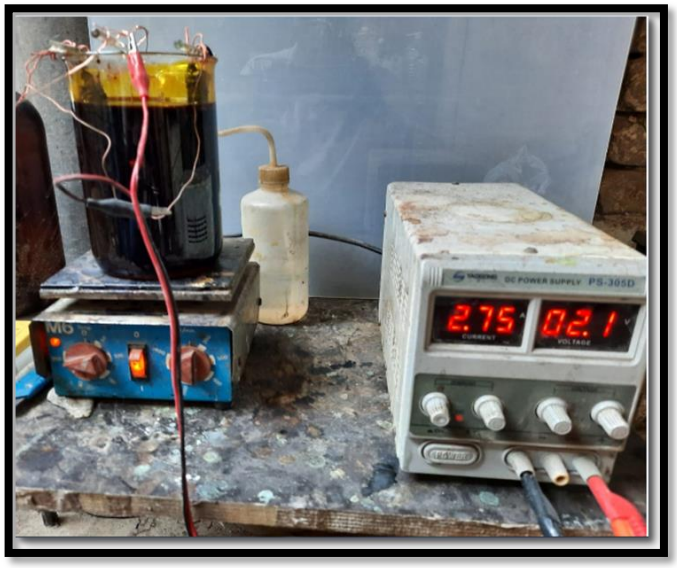

Figure (3.6): The electroplating process for Chromium coating

Table (3.6): Bath solution composition of composite coating

Composite coating bath	Composition	Concentration
Chromium-silicon Carbide	Trivalent Chromium oxide	300 g/l
	Concentrated Sulphuric acid	3 ml/l
	Silicon carbide	(10,20,30) g/l

The silicon carbide (SiC) is added to the chromium plating solution by weight relative to the volume of the solution and left for the purpose of dissolution in the plating solution for a period of 2 hours, and then the electrical power is prepared from the power supply to begin the process of depositing the coatings on the surface of the substrate (carbon steel).

Thus, the process of chromium plating and composite coatings of Silicon Carbide embedded in chromium metal were completed, as shown in figure (3.7).

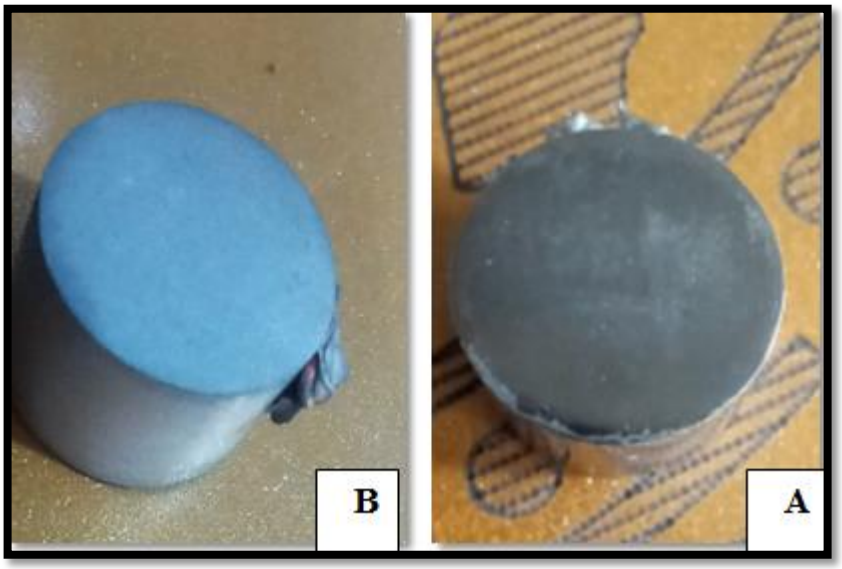

Figure (3.7): (A): Cr-coating, (B): (Cr-Sic) composite coating

3.6 Inspections

3.6.1 Optical microscopic examination

In order to obtain the microstructure of the carbon steel used as a substrate and take an image showing the composite coating thickness, the samples were prepared for this purpose by smoothing and polishing the surface, then immersion in Nital solution for (15) seconds, then the test samples were placed under the microscope to detect the microstructure. The test was conducted in the metallurgical laboratory of the College of Materials Engineering.

3.6.2 Measurements of coating thickness

The examination of the thickness of the coating layer according (ASTM B748) was carried out in the lab of the Department of Polymer Engineering and Petrochemical Industries/College of Materials Engineering-University of Babylon by using (Digital Coating Thickness Gavage (TT260)), where the thickness of the coating layer was measured and for six values of the surface for each model, the average thickness of the layer was extracted.

3.6.3 Surface roughness Measurement

The roughness of the surface of the coating layer was measured according (ASTM D7127-05) by using the roughness tester type (HSR210) in the (Lab of Metallurgical Engineering Department/College of Materials Engineering-University of Babylon).A roughness test of six readings was performed and the rate was taken for these readings. This technique was used in measuring the surface roughness of carbon steel (substrate) and measuring the roughness of metallic coatings consisting of Chromium metal for nine samples of

coating, which represent experiments in which optimal conditions for coating were obtained by relying on statistical analysis.

3.6.4 Hardness measurement for coating specimens

The micro-hardness test of Vickers according (ASTM E97-17) was performed in the lab of the Department of Ceramic and Building Materials Engineering/College of Materials engineering at the University of Babylon. There were three readings for each test sample and the average was taken for the readings. The load used in the micro-hardness test is equal to (25g) for 30 seconds as a load applying period.

3.6.5 Simple immersion weight loss test

This test was conducted on-site at Al-Furat State Company for Chemical Industries and Pesticides according to ASTM (G31). This test includes immersion of samples (carbon steel as a base metal, chromium-coated carbon steel and chromium-coated carbon steel with different concentrations of silicon carbide (Cr-(10, 20, 30) g/l SiC) in concentrated sulfuric acid (98%).

The steps for this test are as below:

- Measurement of the initial weights of the samples (W0). A high-accuracy sensitive balance (four decimal places) was used to achieve high weight accuracy as shown in figure (3.8) (A).
- Immerse the samples in concentrated sulfuric acid (98%) for a specified period at (25) °C as shown in figure (3.8) (B).
- After the specified period of immersion has passed, the samples are taken out, washed with distilled water, and dried in an electric oven at 65°C for one hour, as shown in figure (3.8) (C, D).

- Measuring the weight after immersion (W1) and calculating the difference in weight between the initial weight and the new weight after immersion.

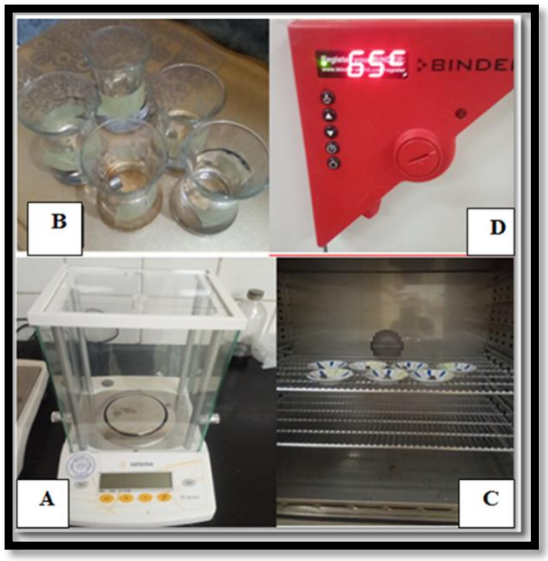

Figure (3.8): A: Balance which are used for weighting samples B: Immersion test of samples in acid, C: Drying samples in electric oven, D: Oven drying temperature

This mechanism is conducted on all samples and is repeated over time for the purpose of obtaining the rate of corrosion and drawing the relationship between the amount of weight loss with time for the purpose of comparing the samples and measuring the amount of weight loss in each experiment compared to the initial weight of samples. The readings of weight loss were recorded for each (3) days and for a period of time (30) days.

The corrosion rate is calculated by the weight loss method according to the equation (3.1) below: [99]

$$\text{Corrosion rate } (g/cm^2.day) = \frac{\Delta W}{t.A} \qquad \ldots\ldots\ldots\ldots\ldots\ldots\ldots\ldots\ldots\ldots \quad (3.1)$$

ΔW: It represents the difference in weight between the starting weight (W0) and the weight after immersion (W1), which is equal to (W0-W1).

A: Acid-exposed surface area (cm^2).

t: Acid exposure time (day).

3.6.6 Erosion-corrosion test in concentrated Sulfuric acid

This test was conducted at Al-Furat State Company for Chemical Industries and Pesticides according to ASTM (G73). This test involves exposing the samples to the effect of (Erosion-Corrosion) on the surface of the metal as a result of the movement of the concentrated acid (this test is the opposite case to the immersion test), which results in studying the behavior of the metal due to the impact of the acid mass on the surface as a physical action of movement with the chemical effect of the acid as a corrosive medium.

The testing mechanism depends on the presence of a tube to transfer the concentrated acid from the factory to a tank, where it is used to check the extent of (Erosion-Corrosion) resistance of the samples.

The acid transport tube has a diameter of (25) mm and a flow rate of (100) m^3/hr, a temperature of (65°C). The density of acid is (1.84) kg/m^3[36].

In order to fix the samples in the acid collection tank, stripes of Teflon resistant to concentrated sulfuric acid were used by cutting two symmetrical strips. Making holes in the Teflon strips with a diameter less than the diameter of the test samples and then fixing each stripe on a carbon steel plate with bolts and nuts as shown in figure (3.9).

Samples, Teflon strips and carbon steel plates are all one piece. The test system is suspended under a hollow cylinder located on a vertical line with the tube from which the concentrated acid comes out to be poured into the tank, and thus the acid will pass through the test samples and cause (Erosion-Corrosion) on the surface of the test samples as shown in figures (3.10),(3.11).(3.12) and(3.13) .

With this test mechanism, we have established similar conditions to what the acid transport tubes are exposed to in the test samples. The acid passes over the test samples under operating conditions similar to the acid flow in pipes in that it is a corrosive medium at a specific speed and temperature. To estimate the corrosion rate in this test, we use the equation (3.1) and apply the same steps as in calculating the corrosion rate in the immersion test.

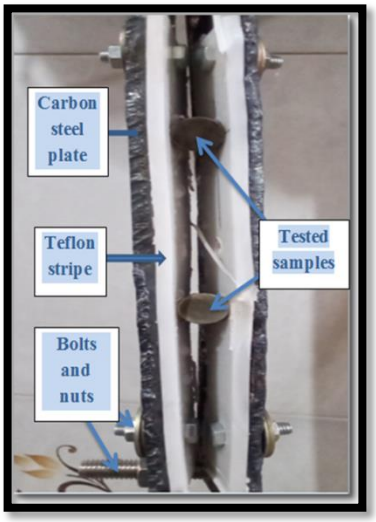

Figure (3.9): The mechanism of fixing samples for (Erosion-Corrosion) test in concentrated sulfuric acid

Figure (3.10): The mechanism for installing the sample examination system in the production tank for concentrated sulfuric acid for achieving the (Erosion-corrosion) test

Figure (3.11): Storage production that contains test samples

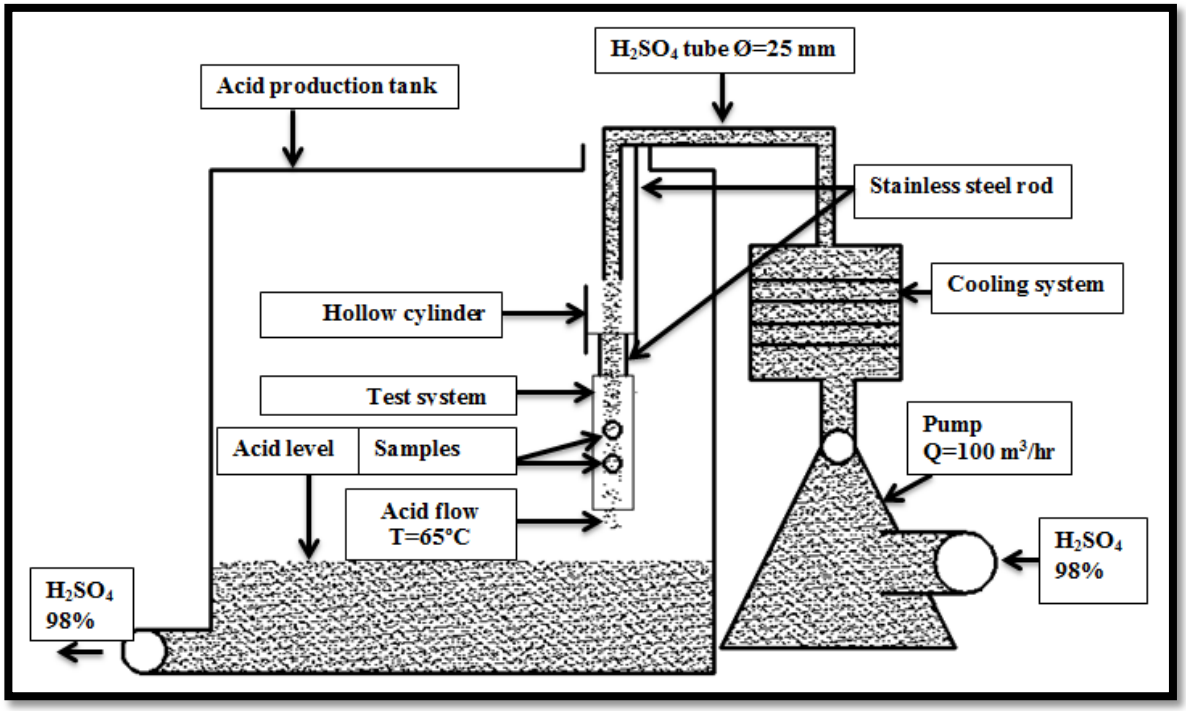

Figure (3.12): Diagram showing the mechanism of the (Erosion -corrosion) examination

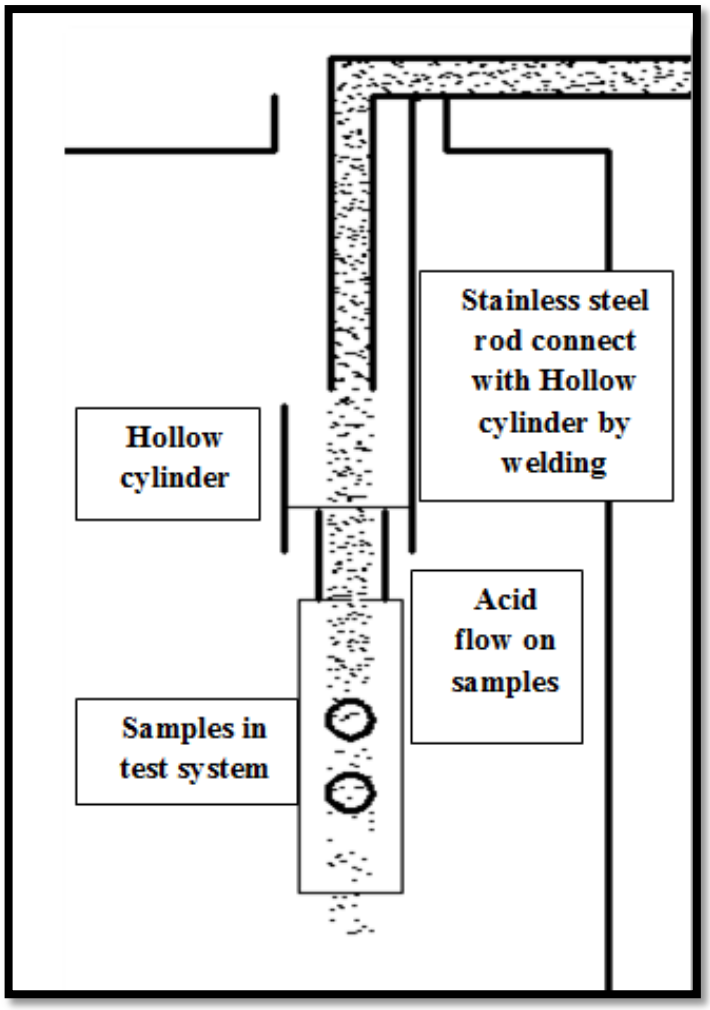

Figure (3.13): Diagram showing the samples test part with concentrated sulfuric acid flow

3.6.7 Electrochemical test (polarization test)

This type of examination includes the electrochemical test of the corrosion rate based on the find the value of the corrosion current and the corrosion potential difference for the samples under examination based on Tafel extrapolation as shown in Figure (3.14) where the test container contains (500 ml) of concentrated sulfuric acid as a solution in which the test was carried out and the first three electrodes It includes carbon steel (the base metal without a protective layer), carbon steel coated with chromium metal plating and the base metal coated with chromium composite coatings with different

concentrations of silicon carbide particles where this electrode represents the working electrode and the second platinum electrode as a counter electrode and the third electrode as a reference electrode from (Ag/AgCl). The linear potential sweep was done at a (-0.250 to +0.250) V potential range around the observed OCP, from the cathodic to the anodic side, at scan rates of (1) mV/s, to acquire polarization curves potentiodinamically. After immersion, the open circuit potential (OCP) was recorded, and polarization measurements were taken once the OCP stabilized. This test was conducted at the Borna Institute in Tehran, in the Islamic Republic of Iran.

Figure (3.14): Polarization test in concentrated Sulfuric acid

Corrosion current values can be calculated using electrochemical cells and polarization measures, such as Tafel extrapolations or polarization testing. We can calculate the corrosion rate of the samples, according to ASTM G102-89 [93]. This equation can be written as follows:

$$\text{Corrosion Rate (mpy)} = \frac{0.1288 \times \text{Icor.} \times (\text{EW})}{\text{A} \times \rho} \qquad \text{..... (3.2)}$$

Where:

0.1288: conversion factor for metric and time ((mpy g)/ (µA cm))

Icor. : Corrosion current (μA)

A: acid exposed area in (cm^2), which be equal for all samples (1.13) cm^2

ρ: Sample density (g/cm^3) for carbon steel (7.87 g/cm^3)[93].For Chromium coating (7.19g/cm^3)[93],for (SiC)(3.21g/cm^3)[93], Cr-10g/l SiC (6.47g/cm^3), Cr-20g/lSiC (6.59g/cm^3), Cr-30g/l SiC (5.36g/cm^3). The densities of Chromium coating and composite coating were estimated according ASTM G102 [109], depending on (EDS) Analysis for samples.

Calculation of (Cr-20g/lSiC) density:

ρ (Cr-20g/lSiC) = percent of (SiC) in (EDS) Analysis * ρ (SiC) + percent of (Cr) in (EDS) Analysis * ρ (Cr)

= 0,074 * 3.21 + 0.8831* 7.19 = 6.59 g/cm^3

EW: equivalent weight, these values can be calculated according to ASTM G102-89 as the formula below:[93]

$$EW = \frac{1}{\sum \frac{nifi}{wi}} \qquad \text{..... (3.3)}$$

fi: the element's mass fraction in carbon steel and electroplating samples.

wi: the element's atomic weight in carbon steel and electroplating samples.

ni : the element's valence in carbon steel and electroplating samples.

For carbon steel EW=19.4, for Cr-coating EW=26.7, for Cr-10g/l SiC (EW=19.9), for Cr-20g/l SiC (EW=13.3).for Cr-30g/l SiC (EW=6).

3.6.8 Diffraction of X-Rays (XRD)

This examination has been carried out at the Bim Gostar Institute in the Islamic Republic of Iran/Tehran.(Bim Gostar Institute). The crystalline phases of carbon steel (base metal) were identified using an X-ray with a copper tube (K radiation = 1.5406 A°). With a diffraction angle range of (5°-89°) and step duration of (1) second, the diffractometer's scanning speed was set at 2.4° per minute.

3.6.9 Energy-dispersive X-rayspectroscopy(EDS) test

This technique is used to obtain the elements ofsamples in order to determine the characteristics and behavior of the samples based on the type and amount of elements present in the samples.This examination was performed with a device (MIRA 3, TESCAN) at the (Bim Gostar Institute) in the Islamic Republic of Iran/Tehran. The components of the chemical composition of the substrate (carbon steel), metallic chromium plating (Cr-plating) and chromium composite coatings with different concentrations of silicon carbide (Cr-SiC) were examined to show the chemical composition of the components of the coating layers and their effect on the extent of corrosion resistance.

3.6.10 Scanning Electron Microscope (SEM)

This examination is characterized by greater accuracy than examination with a scanning electron microscope, as it uses electrons instead of light. Through this examination, the layers of coating that are deposited on the surface of the substrate were studied and the effect of the difference in the concentration of ceramic particles on the shape and appearance of the surface being analyzed. This examination was carried out with a device (MIRA 3, TESCAN) in the (Bim Gostar Institute) in the Islamic Republic of Iran/Tehran.

3.6.11 Atomic Force Microscopy (AFM)

Atomic force microscope (AFM) is a tool for examining and displaying the topography of exact surfaces. It is a high-powered microscope with analysis, and the concept of its operation is based on the fall of a laser beam onto a holder to which is attached a needle with micro-dimensions that moves over the surface whose topography is to be investigated. The reflected laser

beam is caught by the holder, which is dependent on the needle's height and decreases as it moves across the surface being studied. This examination was carried out in the Islamic Republic of Iran with a device (Bruker, ICON, USA origin).By this test, the surface roughness of five different samples representing the carbon steel sample (substrate), the surface roughness of the carbon steel coated with Chrome metallic plating, which represents the optimal sample, three samples representing the chromium composite coatings with different concentrations of carbide particles were examined.

Chapter Four

Results and Discussion

Chapter Four

Results and Discussion

4.1 Introduction

This chapter describes the results of the research's practical part, which include the results of properties for metallic and composite coatings, tests for the corrosive behavior of samples in cases of simple immersion and exposure to the flow of concentrated sulfuric acid (98%), testing of samples by polarization in concentrated acid, analysis and discussion of the results, and the results of the microstructural examination.

4.2 Substrate metal test results (carbon steel)

According to the analysis by (EDS) and (XRD) (JCPDS card No. 01-087-0721), figure (4.1) and (4.2) confirm that the constituent elements of the substrate metal are carbon steel.

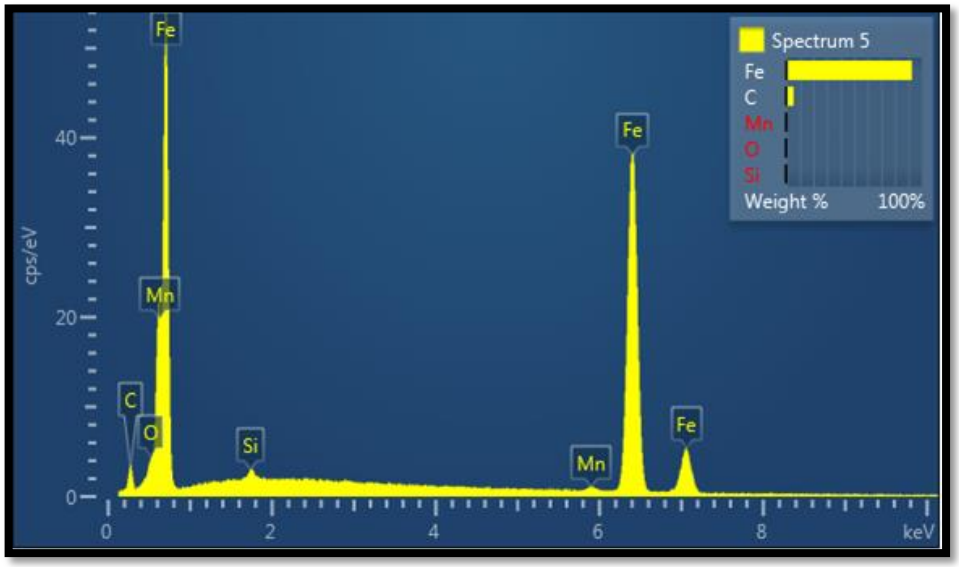

Figure (4.1): EDS analysis of substrate (carbon steel)

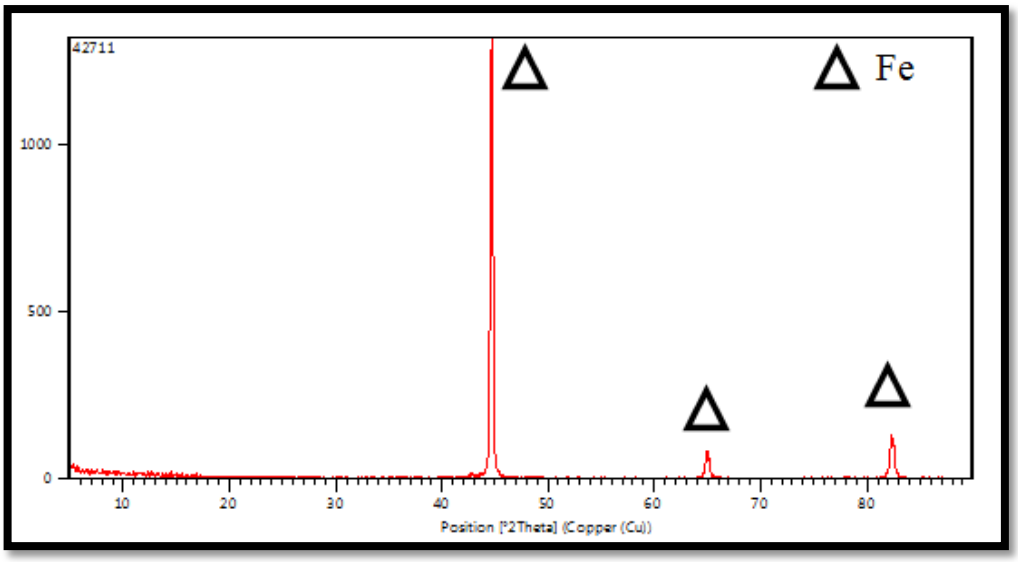

Figure (4.2): XRD patterns of carbon steel (substrate)

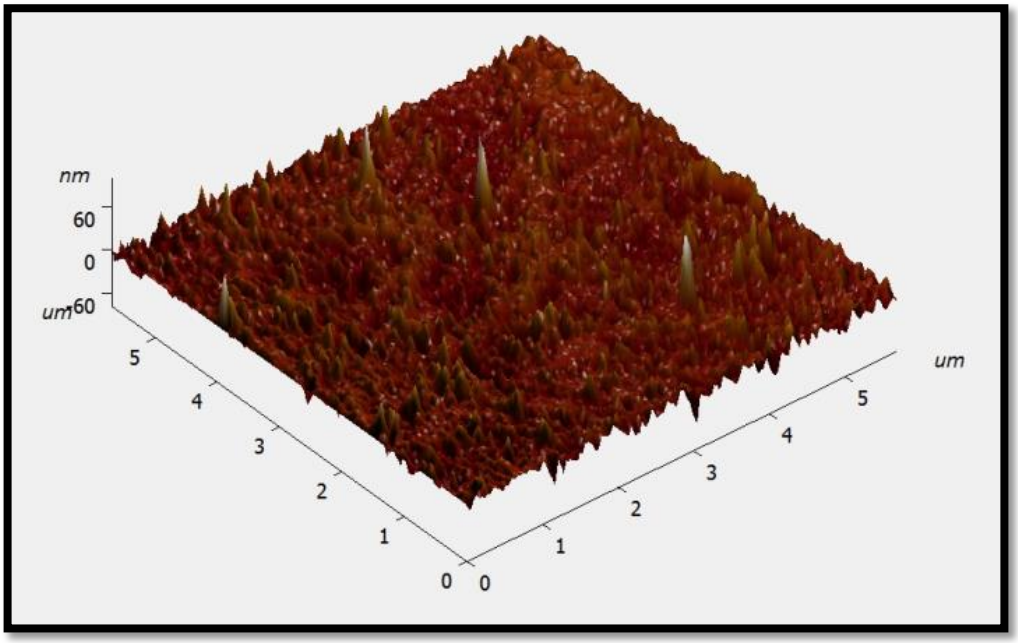

Figure (4.3): (AFM) for carbon steel surface

Figure (4.3) shows the scanning force microscope examination of the surface of the substrate metal (carbon steel), where the value of the surface roughness average was (0.010112) µm which was close to the value of the surface roughness we obtained through the mechanical roughness tester

(HSR210), which was (0.0112) µm and the maximum area peak height of (0.051209) µm.

4.3 Chromium plating results

The testing was conducted on the base metal's chrome plating layer (carbon steel) included (hardness, roughness and thickness) and according to the factors affecting the electroplating process (electroplating temperature and time) as shown in table (4.1).

Table (4.1): Influential variables and their levels

Parameters	**levels**		
Temperature (ºC)	40	50	60
Time (hour)	1	1.5	2

The gray method was chosen within Taguchi's design orthogonal array L_9 for designing the experiments under two variables at three levels, as shown in table (4.2). The ANOVA table (4.3) was estimated by using Minitab (17).

Table (4.2): Electroplating experiments and coating properties

Exp.No.	**Temp(ºC)**	**Time(hr.)**	**Hardness (Vickers) HV (Kg/mm^2)**	**Thickness(µm)**	**Roughness(µm)**
1	40	1	432	11.66	0.043
2	40	1.5	521	13.08	0.052
3	40	2	602	16.98	0.060
4	50	1	512	13.85	0.073
5	50	1.5	707	16.76	0.090
6	50	2	740	20.91	0.098
7	60	1	464	11.83	0.065
8	60	1.5	536	15.56	0.081
9	60	2	644	18.65	0.101
Carbon steel(substrate)			209		0.0112

Table (4.3): ANOVA Table for coating (hardness, thickness, roughness)

Output	Source	DF	Seq SS	Adj SS	Adj MS	F	P	Contribution%
Hardness	Temp	2	30040	30040	15020	13.16	0.017	33
	Time	2	56678	56678	28339	24.83	0.006	62.1
	Residual Error	4	4564	4564	1141			4.9
	Total	8	91283					100
	R-Sq.= 95%							
Thickness	Temp	2	16.081	16.081	8.0407	18.79	0.009	20.2
	Time	2	61.967	61.967	30.9835	72.40	0.001	77.7
	Residual Error	4	1.712	1.712	0.4279			2.1
	Total	8	79.76					100
	R-Sq.= 97.85%							
Roughness	Temp	2	0.002211	0.001105	0.002211	41.97	0.002	66.3
	Time	2	0.001016	0.000508	0.001016	19.29	0.009	30.5
	Residual Error	4	0.000105	0.000026	0.000105			3.2
	Total	8	0.003332					100
	R-Sq.= 96.84%							

4.3.1 Influence of electroplating process variables on Vickers Hardness

According to table (4.3), which was obtained by using Minitab 17 for statistical analysis, this includes the analysis of variance for the factors affecting the hardness of the chrome coating layer. As shown below:

- (P value) probability value for temperature (0.017) and time (0.006) that is smaller than (0.05) ($p< 0.05$) for both plating process variables (temperature, time), implying that (temperature, time) have a substantial effect on coating layer hardness.
- Time (24.83), temperature (13.16) (F- ratio). The values indicate the degree of the variance in the influence of the coating process parameters, as found that the time of the electroplating process has a bigger influence on the hardness of the chrome plating than the coating temperature.

- The contribution ratio to the variable components in the hardness of the chrome layer confirms the Fisher ratio values, with contribution ratios of 62.1% for time and 33% for temperature, as shown in the pie chart in figure (4.4).

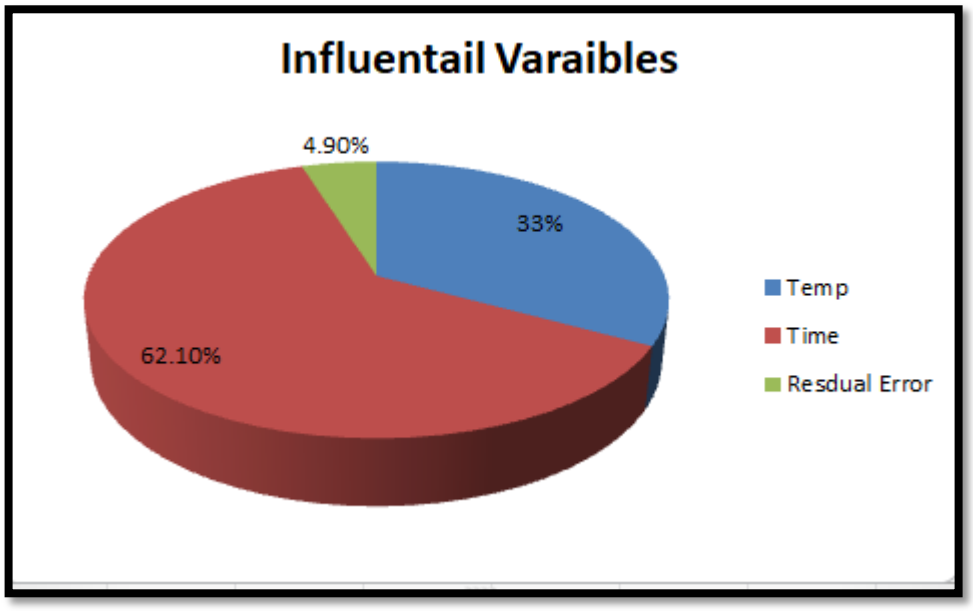

Figure (4.4): Percentage contribution of electroplating variables for hardness

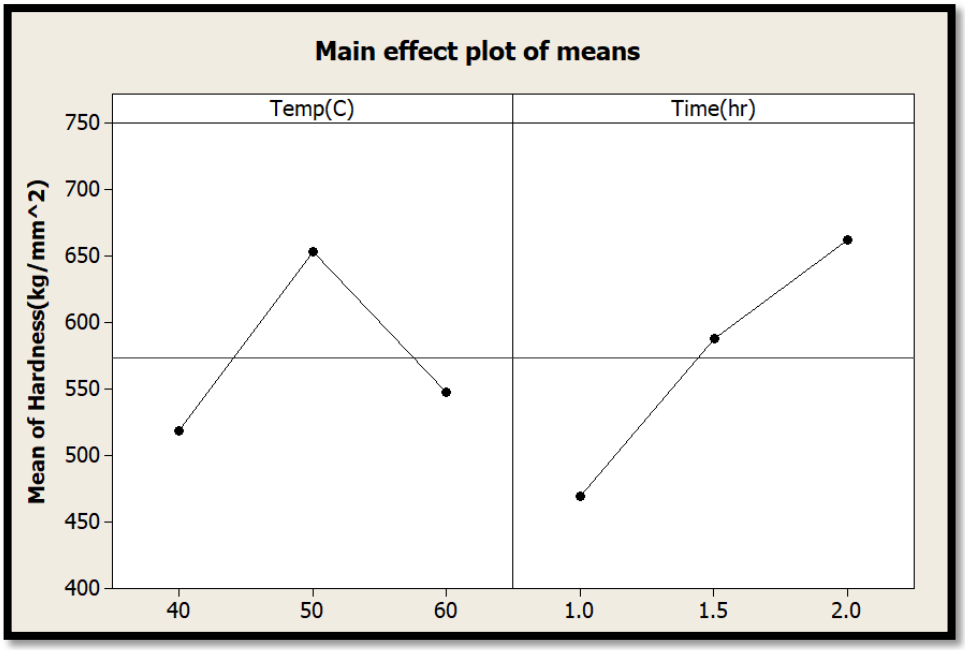

Figure (4.5): Main effect of factors on Vickers Hardness

- From figure (4.5), the hardness values of the chrome plating layer rise with the temperature up to (50°C) and then begins to decrease between (50-60) ºC. The reason for the decrease the hardness of chrome plating is the high temperature, which caused an increase in the size of the plating particles and led to a decrease in the amount of hardness [53]. Between 50 ºC and 60 ºC the results showed barely perceptible differences. This finding allows us to conclude that this electrochemical process could be carried out at 50°C without any important alterations in the resultant product, thus reducing the formation of acid mist typical at the higher temperature, with concomitant environmental benefits. [90]. As for the time factor, we notice that the hardness of chromium increases with the increase in the depositing time, as the time will be sufficient to precipitate the largest amount of chromium ions on the surface of the piece to be coated. [53].

4.3.2 Influence of electroplating process variables on coating thickness

The analysis of variance for the factors affecting the thickness of the chromium coating layer is included in table (4.3).

- The probability value for both plating process factors (temperature, time) is ($p< 0.05$), indicating that (temperature ($p=0.009$) and time ($p=0.001$) have a significant impact on the thickness of the coating layer.
- 'The (F-ratio) number represents the amount of variation in the influence of coating process parameters on the thickness of the chrome coating layer, as shown by the fact that the electroplating process time (F-ratio=72.4) has a greater influence on the chrome coating layer thickness than the coating temperature (F-ratio=18.79).

- The Fisher ratio validates the values of the contribution to the variable factors in the thickness of the chrome coating layer, where the contribution ratio is for time (77.7%) and temperature (20.2%), as shown in the pie chart in figure (4.6).

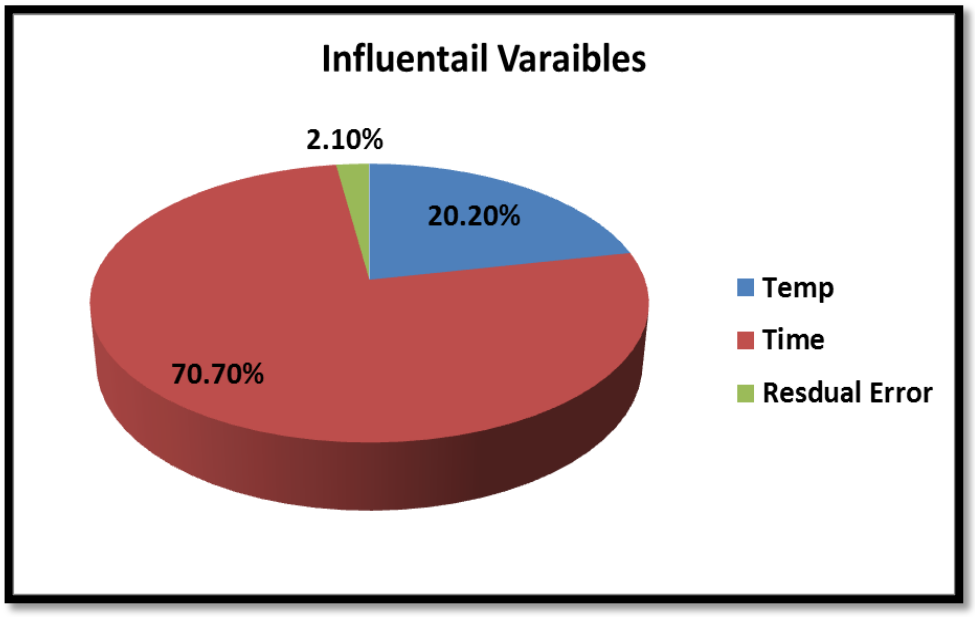

Figure (4.6): Percentage contribution of electroplating variables for thickness

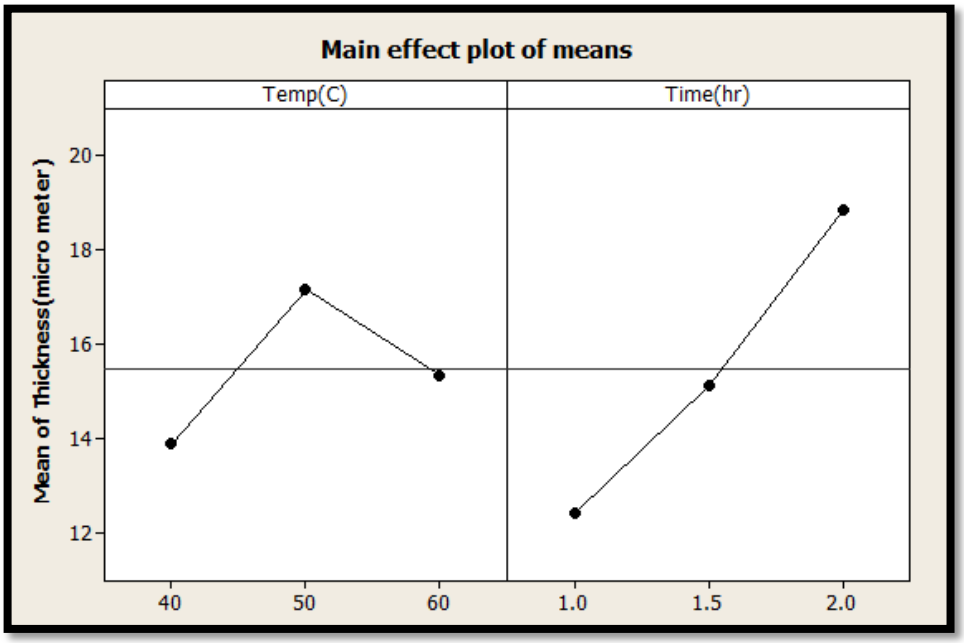

Figure (4.7): Main effect of factors on coating thickness

- As shown in figure (4.9), the thickness of the chromium coating layer increases with increasing temperature up to 50°C, then the thickness decreases with increasing temperature to 60°C. The drop in cathodic film thickness as temperature rises is owing to a decrease in the viscosity of the cathodic film, which promotes a more uniform distribution and a faster rate of dissolution [90]. The thickness of the coatings grows as the coating duration increases. According to Faraday's law, as the amount of coating time rises, the thickness of the coated metal increases [53].

4.3.3 Influence of electroplating process variables on coating roughness

According to table (4.4), which was obtained by using Minitab (17) for statistical analysis, this includes the analysis of variance for the factors affecting the Roughness of the chrome coating layer.

- (P value) probability value is ($p < 0.05$) for both variables of the plating process (temperature ($p=0.005$), time ($p=0.018$)), which gives us the conclusion that (temperature, time) have a significant effect on the roughness of the coating layer.
- (F- ratio). This value gives an indication of the extent of the variation in the influence of the parameters of the coating process as we found that the temperature (F-ratio=41.97) of the electroplating process has a greater effect than the time (F-ratio=19.29) of the coating on the roughness of the chrome coating layer.
- The ratio of the contribution to the variable factors in the roughness of the chrome coating layer confirms the values of the Fisher ratio, where the contribution ratio is for temperature (66.3%) and for time (30.5%) as shown in the pie chart in figure (4.8).

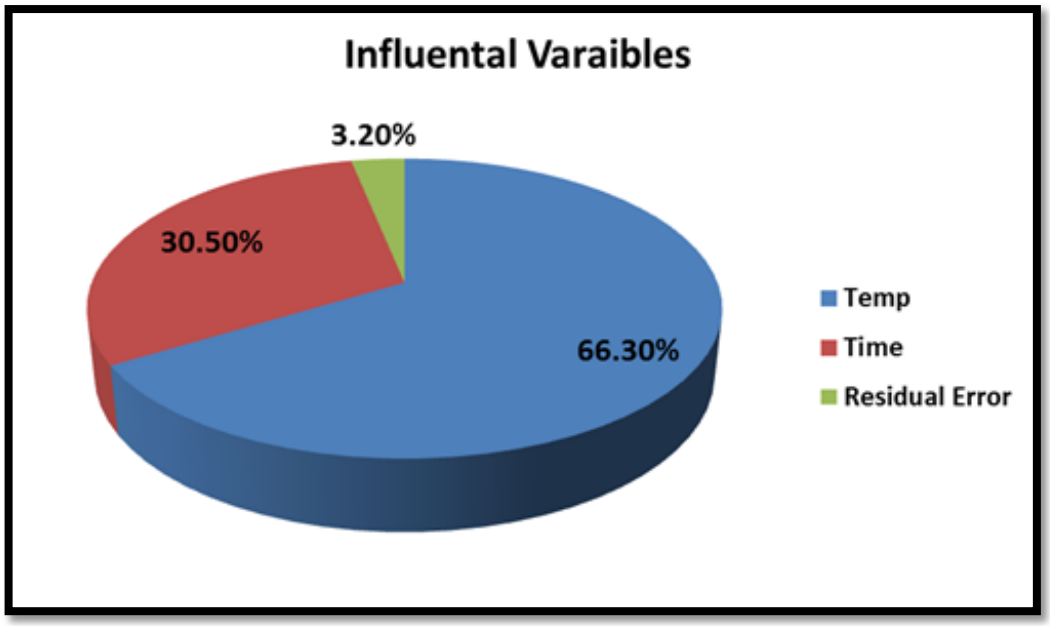

Figure (4.8): Percentage contribution of electroplating variables for roughness

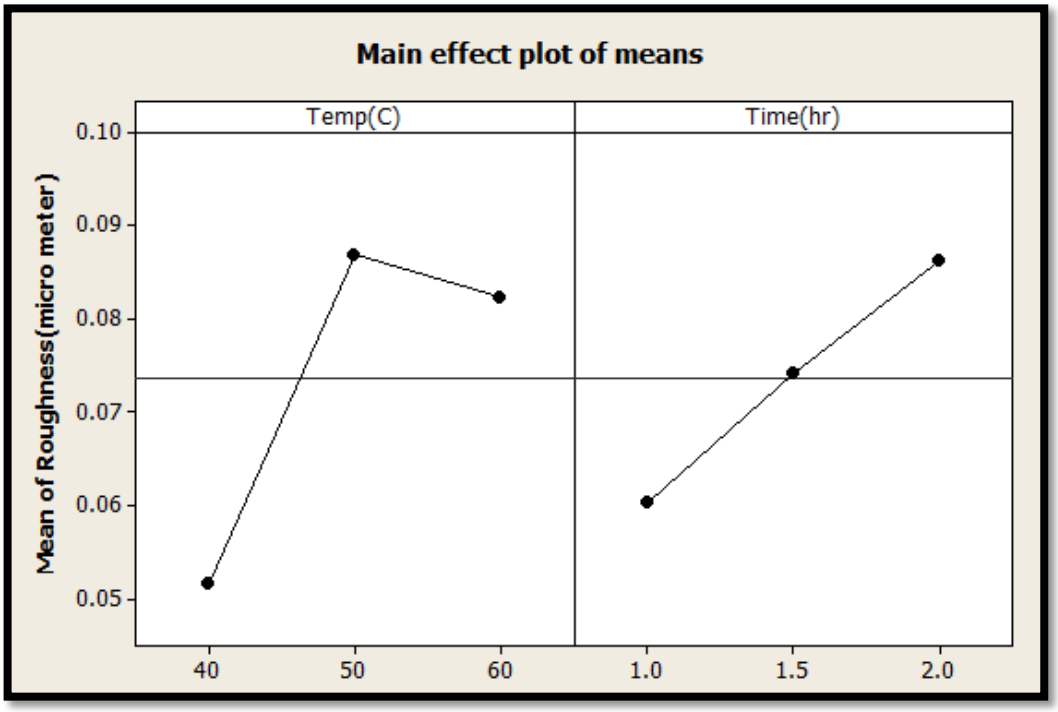

Figure (4.9): Main effect of factors on coating roughness

- As shown in figure (4.9) the surface roughness increases with increasing temperature (40-50) °C, then be decreased at (60) ºC. As the temperature of the chromium plating solution increases, the surface

roughness values of the plating layer rise as a result of the process of depositing chromium ions on the surface of the cathode (the work piece), but a decrease in the amount of surface roughness occurs when the temperature rises above (50) ºC . When electroplating hard chrome, the temperature should be higher than 50°C. These high temperatures are essential to avoid the formation of abrasive deposits at elevated sedimentation rates [91]. The relationship of the surface roughness of chrome plating is directly proportional with deposition time, as the surface roughness increases with the growth of chromium granules with an increase in the time of deposit of chromium granules on the surface of the plating sample [92].

4.3.4 Predicted regression equation for each response characteristic

As a function of influential variables Temperature (T), time (t), the predicted regression equation for each response characteristic (Hardness (H.V.), Thickness and Roughness) as shown in equations (4.1), (4.2), (4.3).

Hardness (H.V.) = -2855 + 120.6* T + 436* t - 1.198*T^2 – 89* t^2+
0.50 T*t …… (4.1)

Thickness = - 49.8+ 2.506 *T- 3.51*t-0.02547*^2+2.05t^2+
0.0750^T^2 …….. (4.2)

Roughness = -0.4658 + 0.02011* T - 0.0095*t-0.000200 T^2 - 0.00400 t^2 +
0.000950 T*t …….. (4.3)

4.3.5 Checking the model's accuracy

In addition to the use of analysis of variance (ANOVA) in table (4.4), which provided evidence of the mathematical model's suitability in examining the outputs and the influence of the coatings factors on them.

Another criterion for determining the model's suitability is the determinant's coefficient (R^2). For Hardness, thickness, and roughness, the estimating values of (R^2) are (95%), (97.85%), and (96.84%), respectively. All of these R^2 values are greater than 95%, indicating that the regression models are more than acceptable.

Drawing scatter diagrams is used to test the validity of the regression models that have been generated. The observed and expected response values are dispersed along the 45° line, demonstrating a near-perfect match of the empirical models established. Figures (4.10),(4,11) and (4,12) show typical scatter diagrams for all of the models.

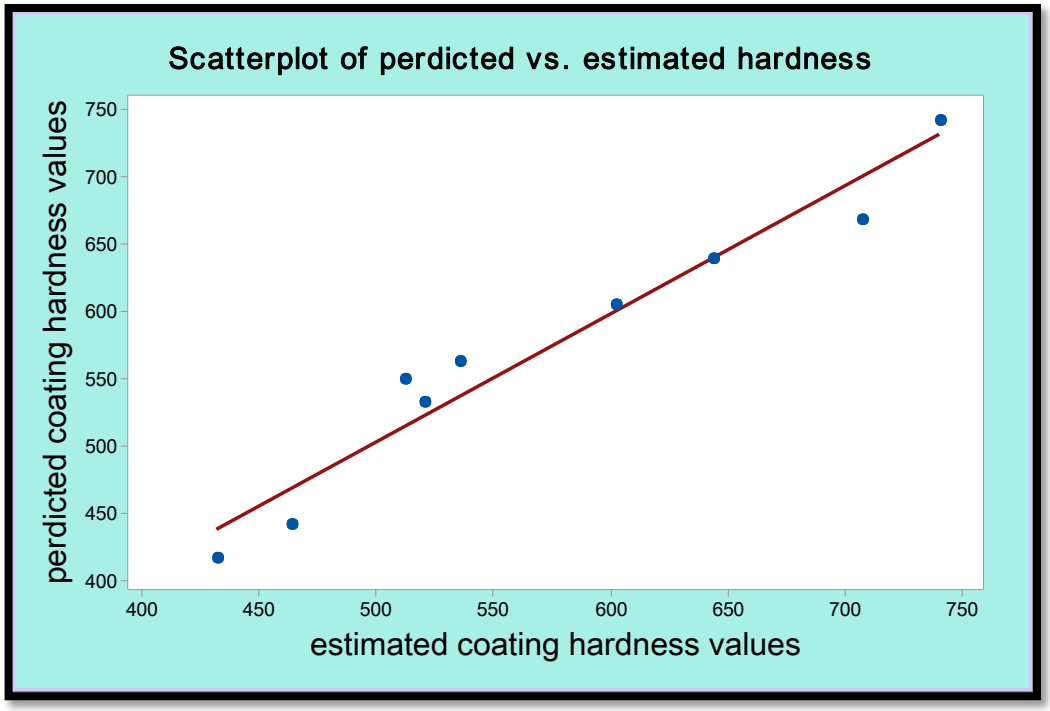

Figure (4.10): Coating hardness scatter diagram

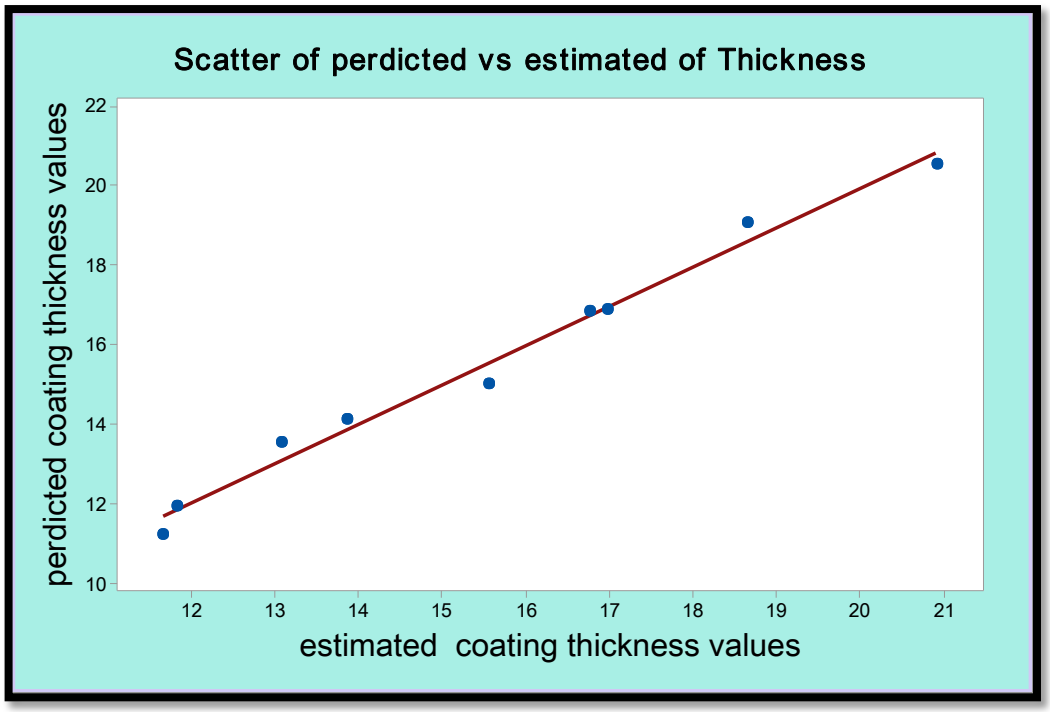

Figure (4.11): Coating thickness scatter diagram

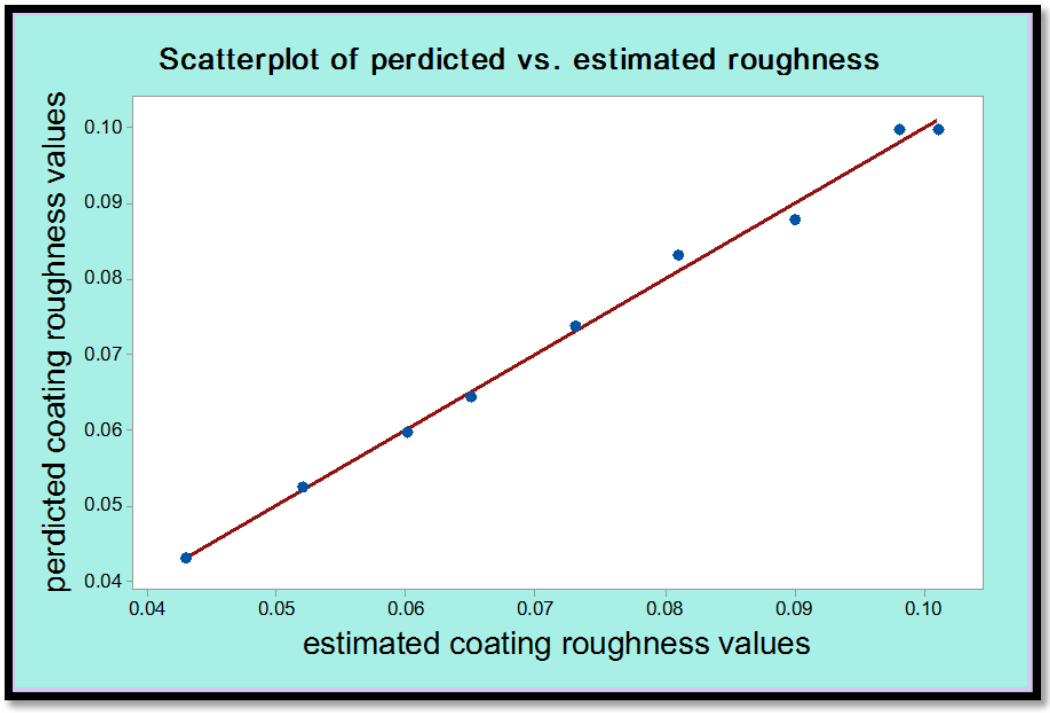

Figure (4.12): Coating roughness scatter diagram

4.3.6 Influential variables optimization

The Taguchi design orthogonal array (OA) was utilized in conjunction with the GRA approach to determine the values of the optimum factors (temperature, duration) that create the best attributes of the chrome plating layer. The output values of the coating layer must be normalized in GRA to be in the range of (0) to (1).When the sequence's objective directions are different or the range of sequence scatter is too broad, data pre-processing is necessary. Data pre-processing is the process of transferring the original sequence to a similar arrangement. As a result, the experimental results are normalized.

According to equations (2.16) and (2.17) the output values of the chromium plating process have been modified in order to unify all the output values for each experiment between (zero to one) where the equation (2.16) is used for the values of hardness and thickness of the coatings, considering that the preferred values for these larger outputs are the best and the equation (2.17) is used for the surface roughness values for coatings on the basis that the smaller is the best, as shown in the table (4.4).

Table (4.4): Adjusted values of the outputs of the chromium plating process

Exp. No.	Hardness	Thickness	Roughness
1	0	0	1
2	0.288961	0.153514	0.844828
3	0.551948	0.575135	0.706897
4	0.25974	0.236757	0.482759
5	0.892857	0.551351	0.189655
6	1	1	0.051724
7	0.103896	0.018378	0.62069
8	0.337662	0.421622	0.344828
9	0.688312	0.755676	0

In experiment (1) in table (4,4) the normalize value of Hardness (Larger is better) (H_1*) calculated as the equation below:

$$H_1^* = \frac{H1-Hmin}{Hmax-HMIN} = \frac{432-432}{740-432} = 0$$

And for the normalize value of Thickness (Larger is the better) (Th_1^*) calculate as the equation below:

$$Th_1^* = \frac{Th1-Thmin}{Thmax-Thmin} = \frac{11.66-11.66}{20.91-11.66} = 0$$

And for the normalize value of Roughness (Small is the better) (Rou_1^*) calculate as the equation below:

$$Rou_1^* = \frac{Rou(max)-Rou1}{Roumax-Roumin} = \frac{0.101-0.043}{0.101-0.043} = 1$$

The deviation sequence was calculated using equation (2.18), and the results are shown in Table (4.5).

Table (4.5): The sequences of deviations

Exp. No.	Δ0i (Hardness)	Δ0i(Thickness)	Δ0i(Roughness)
1	1	1	0
2	0.711039	0.846486	0.155172
3	0.448052	0.424865	0.293103
4	0.74026	0.763243	0.517241
5	0.107143	0.448649	0.810345
6	0	0	0.948276
7	0.896104	0.981622	0.37931
8	0.662338	0.578378	0.655172
9	0.311688	0.244324	1

GRC (Grey Relational Coefficient §i (k)) is computed from the normalized data after data pre-processing to build a relationship between the preferred and real data. Where using the eq. (2.19) to find a value for the output values Grey Relational Coefficient as listed in table (4.6).

Table (4.6): Grey relational coefficient values

Exp. No.	Grey Relational Coefficient (GRC)(§i(k))		
	(§i(1))Hardness	(§i(2))Thickness	(§i(3)Roughness
1	0.333333	0.333333	1
2	0.412869	0.371337	0.763158
3	0.527397	0.54062	0.630435
4	0.403141	0.395807	0.491525
5	0.823529	0.527066	0.381579
6	1	1	0.345238
7	0.35814	0.337468	0.568627
8	0.430168	0.463659	0.432836
9	0.616	0.67175	0.333333

According to equation (2.20), table (4.6) contains the values of the Grey Relational Coefficient. We'll calculate the Grey Relational Grade for each experiment (GRG).Experiment number six has the greatest GRG, indicating that it is the most successful. Table (4.7) shows the results.

Table (4.7): Values of Grey Relational Grade (GRG) for experiments

Exp. No.	Grey Relational Grade (δi)	Rank
1	0.555556	4
2	0.515788	6
3	0.566151	3
4	0.430158	8
5	0.577391	2
6	0.781746	1
7	0.421412	9
8	0.442221	7
9	0.540361	5

Figure (4.13) shows the GRG obtained under multiple configurations. The GRG indicates that, primarily, the higher the GRG, the closer the product's quality will be to the ideal value. As a result, the larger GRG is prized for its superior performance. As a result, the value of the coating temperature (50°C) and the coating time (2 hours) that

achieve the highest value of (GRG) are the optimal factors for the coating process from which we obtain the best properties of the coating layer.

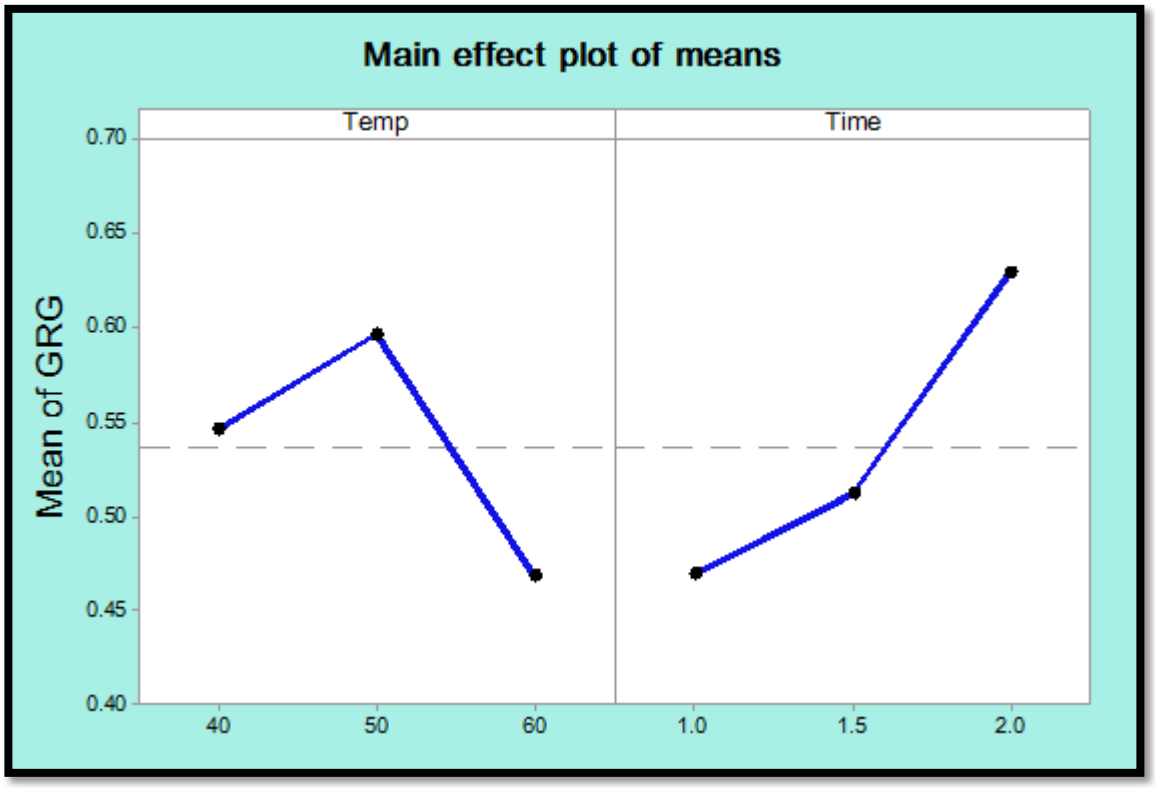

Figure (4.13): Main effecct of factors on GRG

The ideal process parameters are at the level with the highest GRG (Minitab program) , as shown in table (4.8).

Table (4.8): Table of responses for the grey relationship grade

Parameters	**Grey Relational Grade**			**Main effect(Max-Min)**	**Rank**
	Level 1	**Level 2**	**Level 3**		
Time	0.4827	0.5313	**0.6448***	0.1621	1
Temp	0.5611	**0.6075***	0.4903	0.1172	2
The grey relational grade's total mean value β_m= 0.552866 (*)optimal GRG levels					

At optimal factors (Temperature (50°C), Time (2 hr.), table (4.9) shows the estimated values of the properties of the coating layer by taking advantage of the equations (4.1),(4.2) and (4.3) compared to the practically calculated values along with the predicted error which is obtained from the equation (4.4).

$$\text{Predicted error \%} = \frac{\text{Experimental value} - \text{Predicted value}}{\text{Experimental value}} \quad \ldots\ldots\ldots (4.4)$$

Table (4.9): Experimental and prediction for Chromium coating value

Cr coating property	Experimental value	Predicted value	Predicted error %
Vickers hardness(kg/mm^2)	740	741.889	0.255
Thickness(µm)	20.91	20.5444	1.748
Roughness(µm)	0.098	0.0996667	1.02

4.4 Optimal Chromium sample test results

The results of testing on the optimum sample of metallic chromium plating on carbon steel (substrate),were collected using the gray method of factor analysis and getting the optimum factors that produce the best chrome plating qualities include: (EDS) and (AFM).

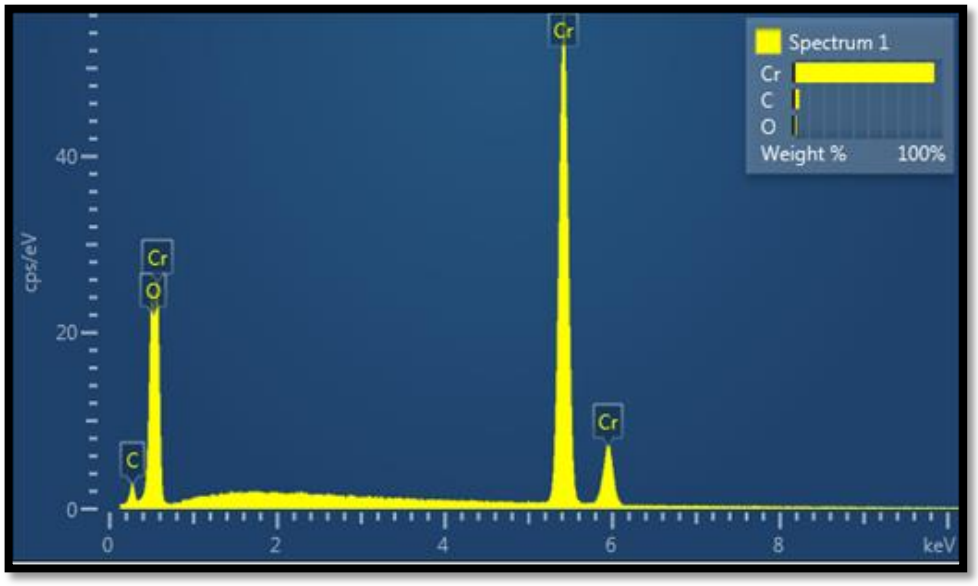

Figure (4.14): EDS analysis of Chromium coating

The elemental analysis of the surface in figure (4.14), which confirms the achievement of metallic chromium plating. This phase is expected to

appear in metallic chromium coatings, which confirms the analysis (EDS) of the surface of the chromium plating sample.

Figure (4.15) shows the atomic force microscope examination of the surface of the Chromium plating, where the value of the surface roughness average was (0.093337) µm which was close to the value of the surface roughness obtained through the mechanical roughness tester (HSR210), which was (0.098) µm and the maximum peak height of (0.0499085) µm.

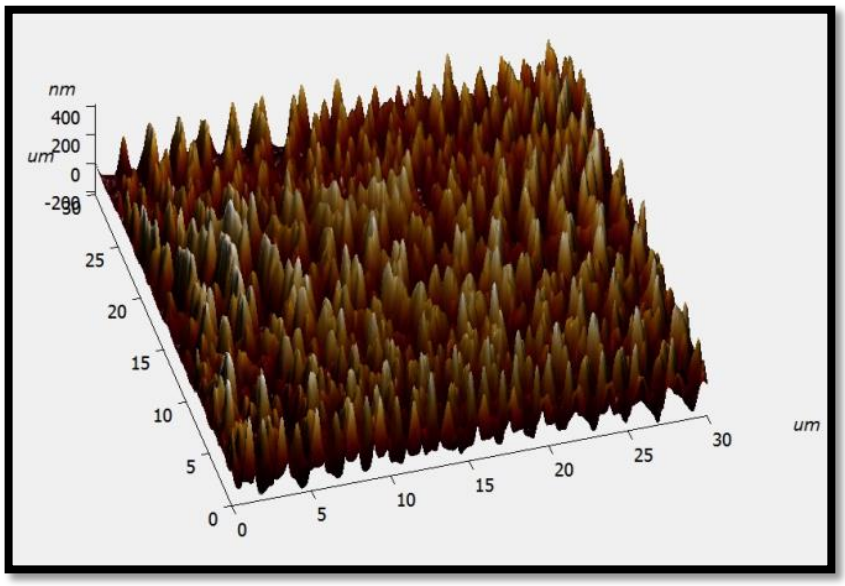

Figure (4.15): AFM of Chromium plating surface

4.5 Chromium-Silicon Carbide composite coating

4.5.1Composite coatings electrodeposition

For the purpose of obtaining composite coatings, chromium plating was carried out with silicon carbide particles based on the optimum factors for chromium coatings (temperature and time of the plating process), which were extracted by using the gray method for statistical analysis, where the deposited temperature was (50°C) with deposited time (2 hours). With a change in the proportions of silicon carbide (SiC)

added, the values of the tests for the layer of composite coatings (Cr-SiC) are shown in table (4.10).

Table (4.10): (Cr-SiC) composite coating properties

Cr-Sic (g/l)	Vickers Hardness H.V. (Kg/mm^2)	Roughness(µm)	Thickness(µm)
10	766	0.087	10.67
20	902	0.421	17.74
30	665	0.158	12.9

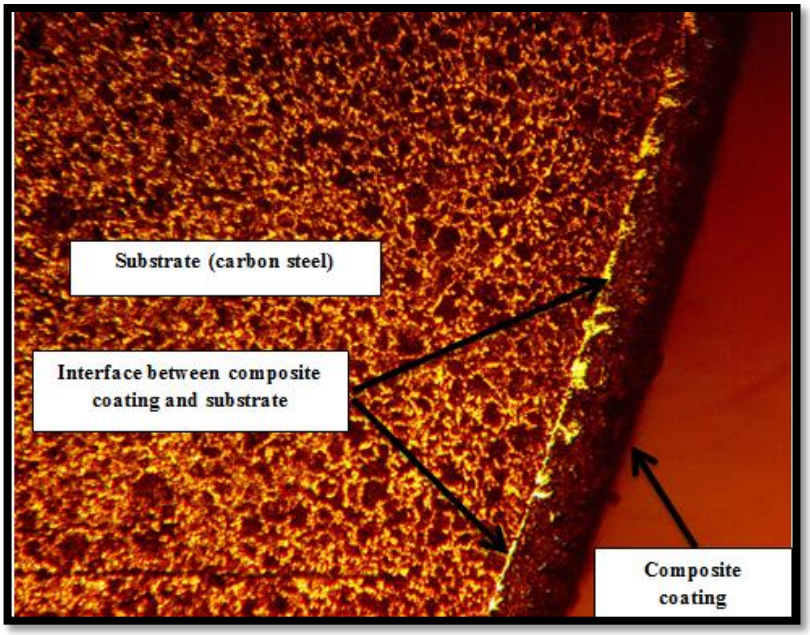

Figure (4.16): An image showing composite coating thickness (100x)

In figure (4.16), an image was taken by an optical microscope to show the thickness of the composite coatings (Cr-SiC) on the metal of the substrate, where the indicator of the interface between the coatings and the substrate is clearly visible.

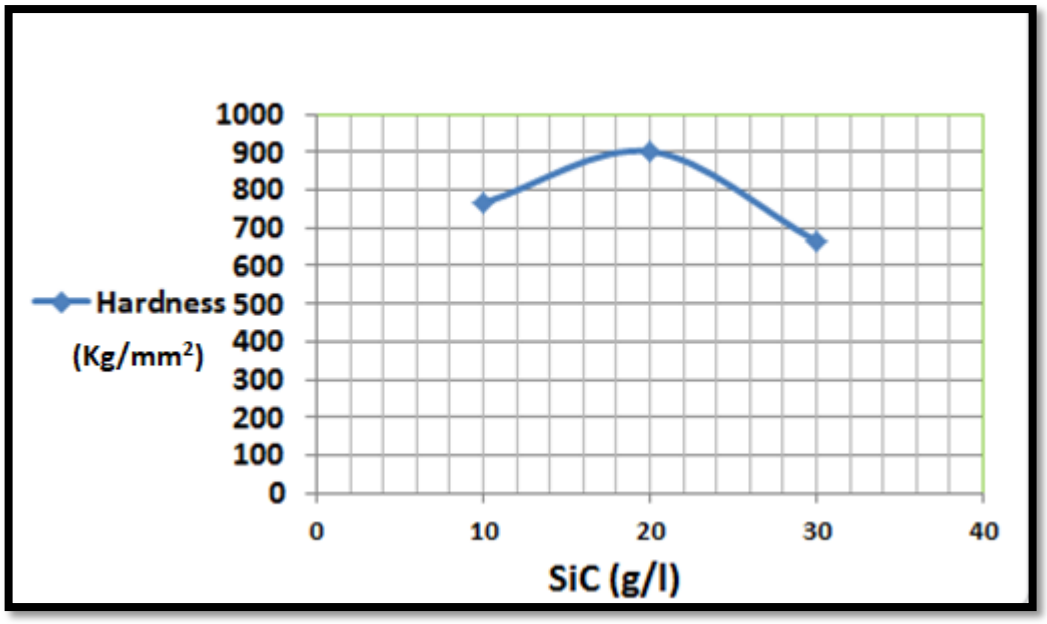

Figure (4.17): The effect of SiC concentration on coating hardness

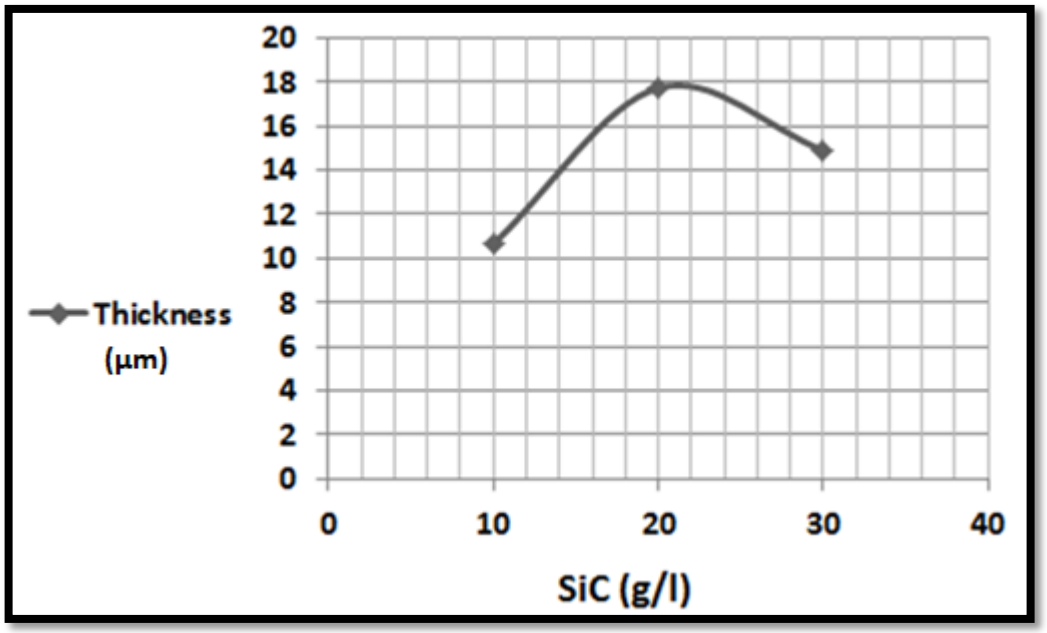

Figure (4.18): The effect of SiC concentration on coating thickness

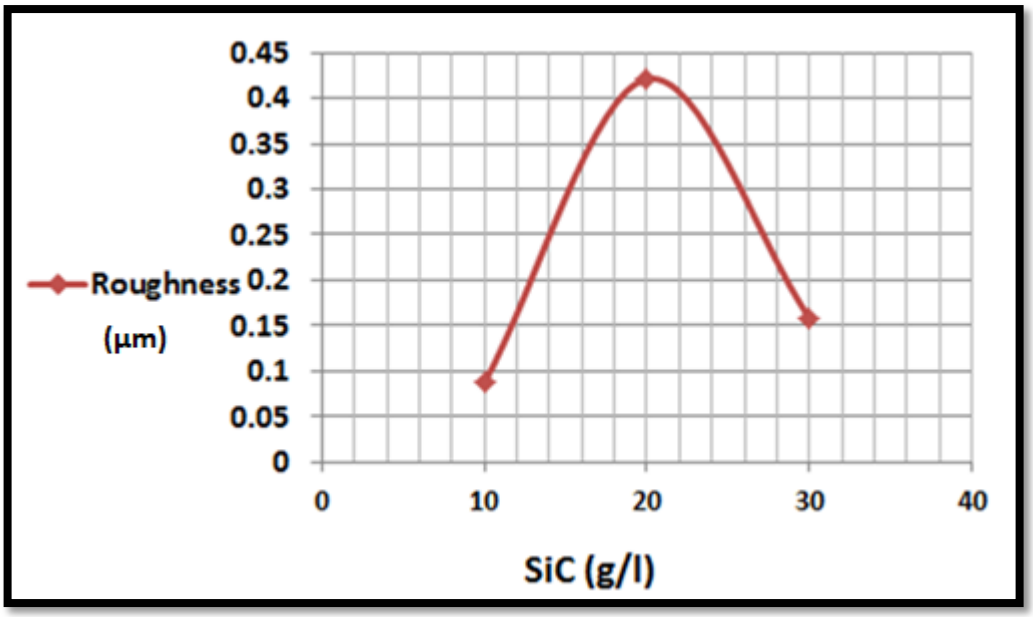

Figure (4.19): The effect of SiC concentration on coating roughness

In figures (4.17), (4.18)and (4.19) that show the effect of (SiC) added concentrations of silicon carbide particles to the chromium plating solution on the properties of the formed composite coatings, notice that (hardness, thickness and roughness) values have increased as a result of adding (20g/l) of Silicon Carbide in comparison with the values of these properties when the amount of addition (10g/l) where the thickness and roughness increase as a result of the increase in the concentration of silicon carbide in the solution. As a result, as the concentration of SiC rises, the number of adsorption Cr^{+3} ions on the surface of SiC particles increases. SiC particles migrate towards the cathode surface due to an electric current, where the adsorbed Cr^{+3} ions discharge and deposit on the carbon steel surface, encasing and embedding the SiC particle. As for the hardness of the composite coatings, it increases slightly (766 HV) than the hardness of the metal chromium plating (740HV) when the concentration of carbides is (10g/l), but by increasing the concentration to (20g/l), where the rise in hardness is greater due to the increase in the amount of particles deposited with chromium ions on the

surface of the carbon steel (cathode electrode). The high hardness is due to the diffusion of silicon carbide particles through chromium metal. These particles are obstacles to the movement of dislocations and thus enhance the properties of the coating, involving the hardness of the coating surface [80].

In figures (4.20) and (4.21) which show the results of examining the surface of the composite coatings with a scanning electron microscope, where we notice from the images that the composite coatings resulting from the addition of (20g/l SiC) with the presence of some small unincorporated masses in the ground layer of chromium metal, while the case is the opposite in the case of the layer consisting of adding (10g/l SiC) of carbide particles, the reason for this is that the concentration of carbides in the coating solution is lower than it was in increasing its concentration to (20g/l SiC).

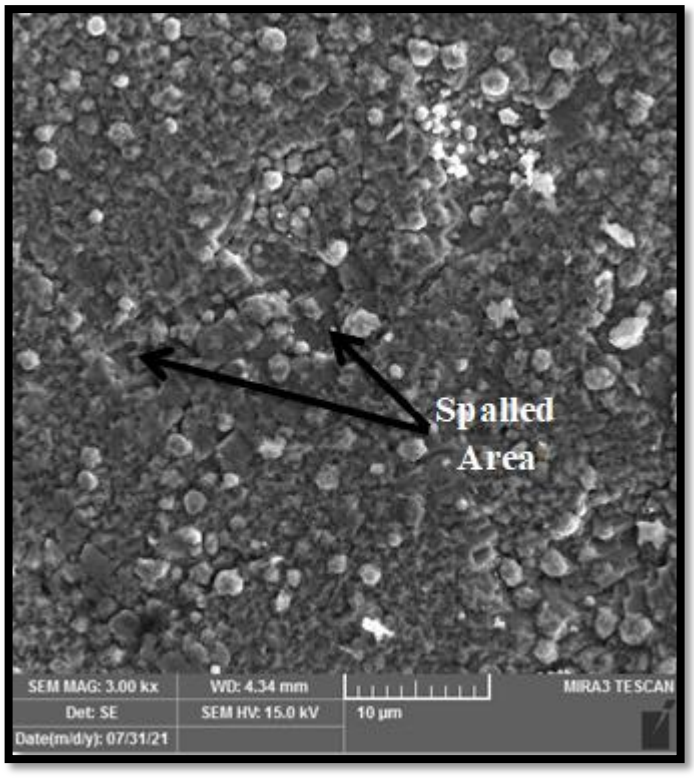

Figure (4.20): SEM image for surface morphology of (Cr-10 g/l SiC)

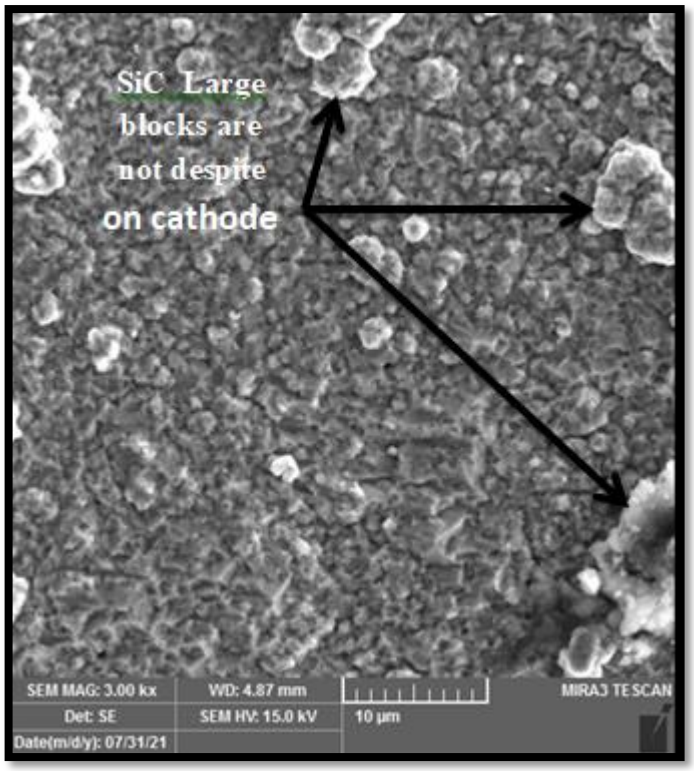

Figure (4.21): SEM image for surface morphology of (Cr-20 g/l SiC)

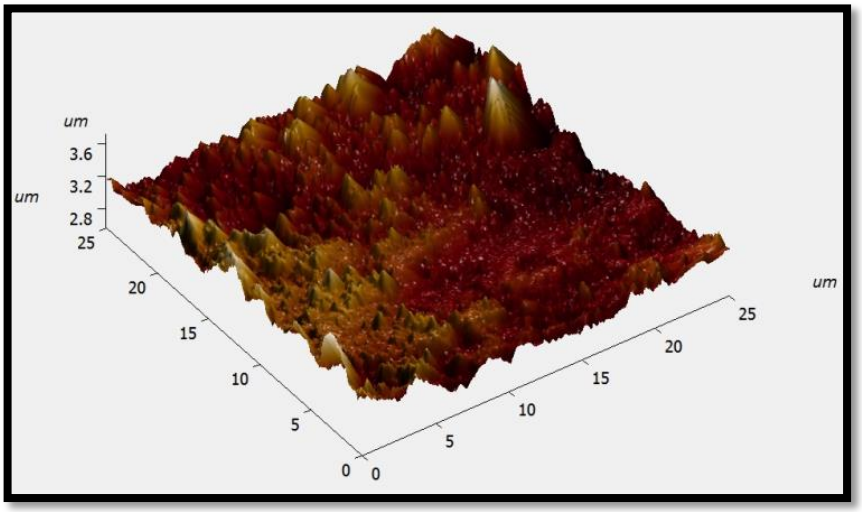

Figure (4.22): (AFM) for (Cr-10g/l SiC)

In figures (4.22 and 4.23) shows the examination (SFM) of the surface of the composite coatings, where we notice the effect of silicon carbide deposition on the surface according to the different concentration of carbide particles in the coating solution, where the roughness rate (0.087)µm with the

maximum height of the peaks was (0.694)µm when the concentration of carbide was (10 g/l SiC) while it increases these values are to (0.421)µm as the average surface roughness with the increase of the maximum height of the peaks to (2.59)µm when the amount of silicon carbide concentration is increased to (20 g/l SiC), where these values increase due to the high concentration of carbides in the solution [80].

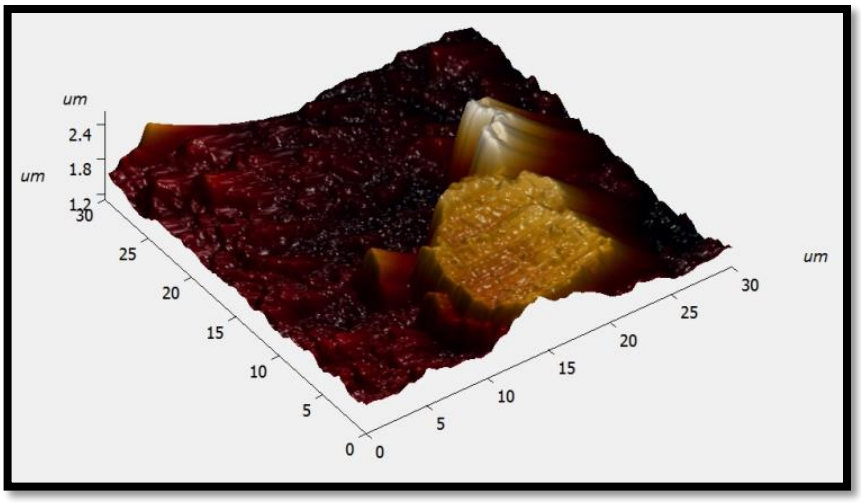

Figure (4.23): (AFM) for (Cr-20g/l SiC)

Referring to figures (4.17, 4.18 and 4.19), we notice that the values of the properties of the layer of composite coatings decrease when the concentration of silicon carbide particles becomes (30g/l), so that the hardness, thickness, and roughness decrease from their values when the concentration of the addition of silicon carbide (20g/l) and the reason for this is that the constant velocity of solution movement (stirrer rate) with increasing concentration for silicon carbide, so that it is not able to transfer large amounts of carbide particles to the surface of carbon steel, where when its concentration in the solution increases, its amount decreases in the coating layer due to a decrease or weakness in hydration and its agglomeration inside the solution[86], as illustrated infigure (4.24).

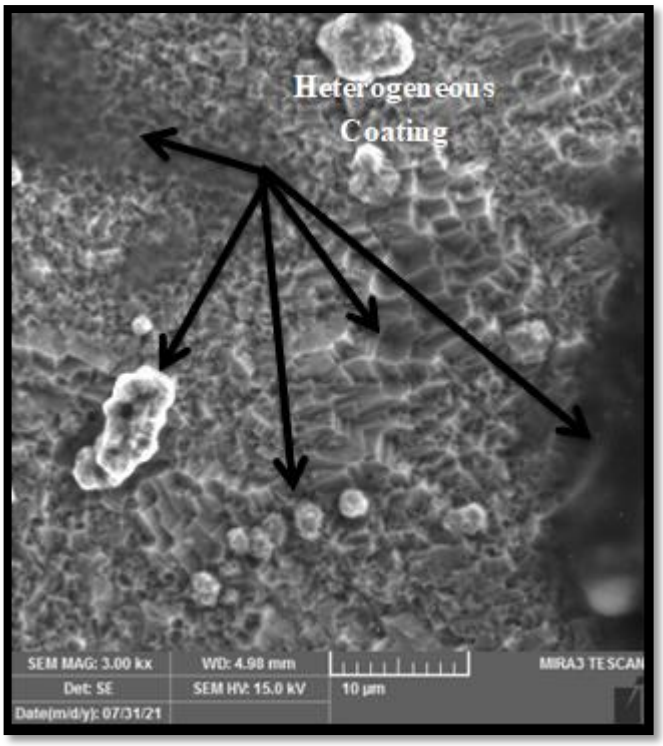

Figure (4.24): Image by SEM for the surface morphology of (Cr-30g/l SiC)

Figure (4.25) represents (AFM) examination of the surface of the composite coatings when the concentration of silicon carbide was increased to (30g/l SiC), where the surface roughness rate decreases to (0.158) µm and the maximum height of the peaks (1.35) µm from what it was when the carbide concentration (20g/l SiC) was evidence when the deposition occurred carbide with high efficiency.

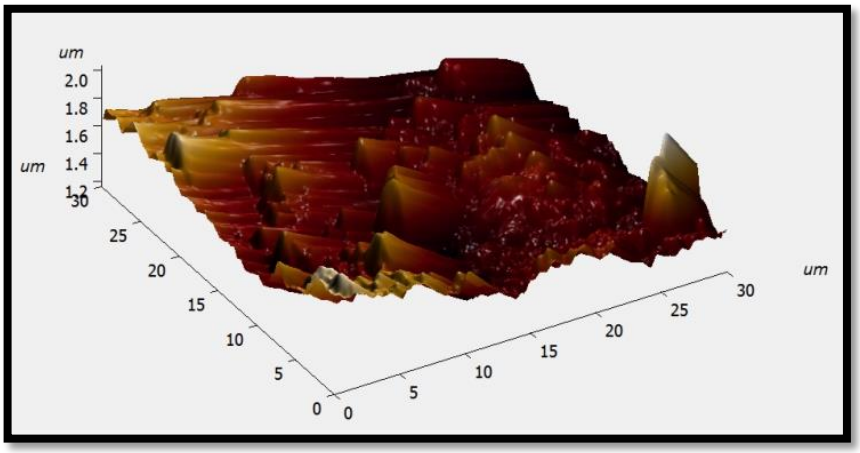

Figure (4.25): (AFM) for (Cr-30g/l SiC)

4.5.2 EDS results for Composite Coating

In figures (4.26, 4.27 and 4.28), (EDS) analysis of layers of chromium composite coatings and different concentrations of silicon carbide particles. These analyses confirm the components from which the composite coatings are formed.

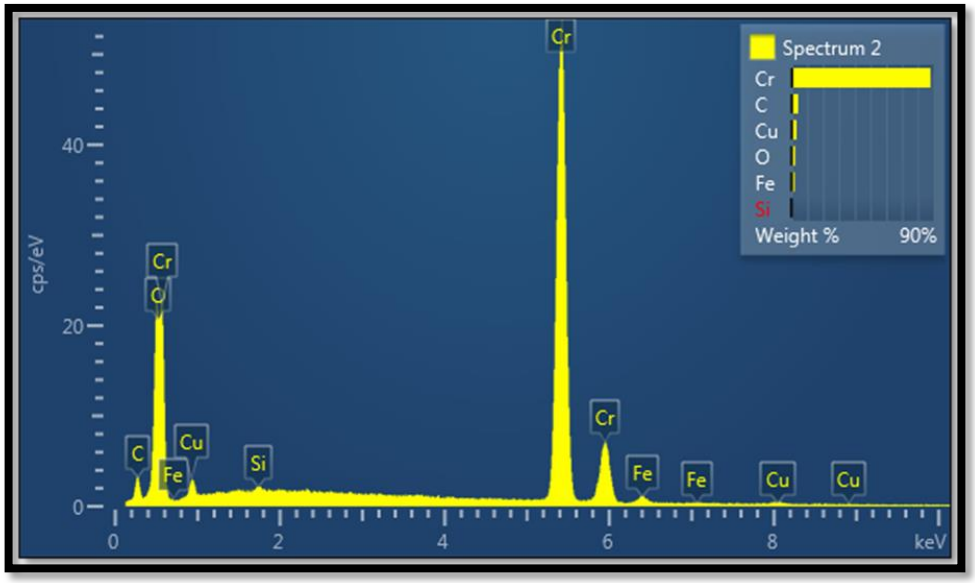

Figure (4.26): EDS analysis of (Cr- 10 g/l SiC)

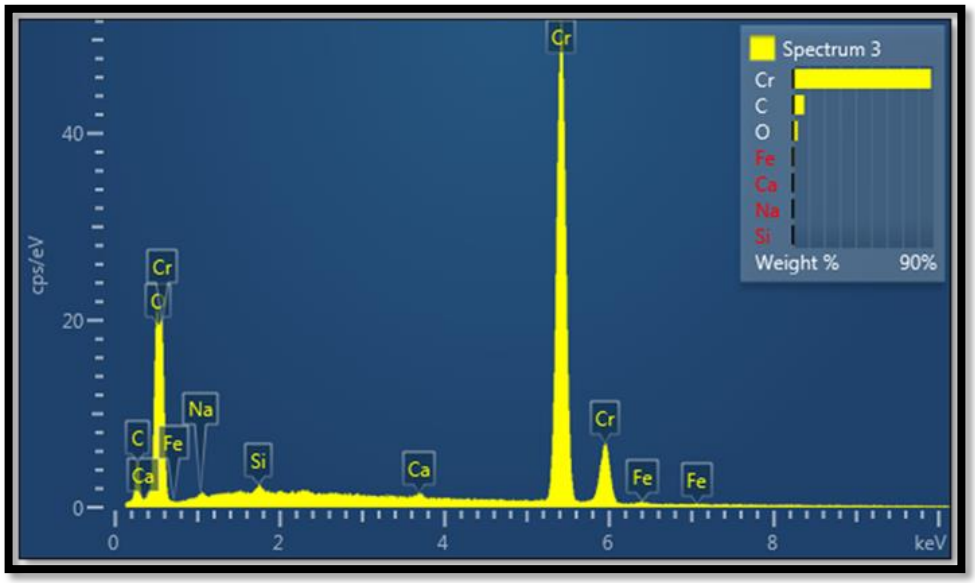

Figure (4.27): EDS analysis of (Cr-20g/l SiC)

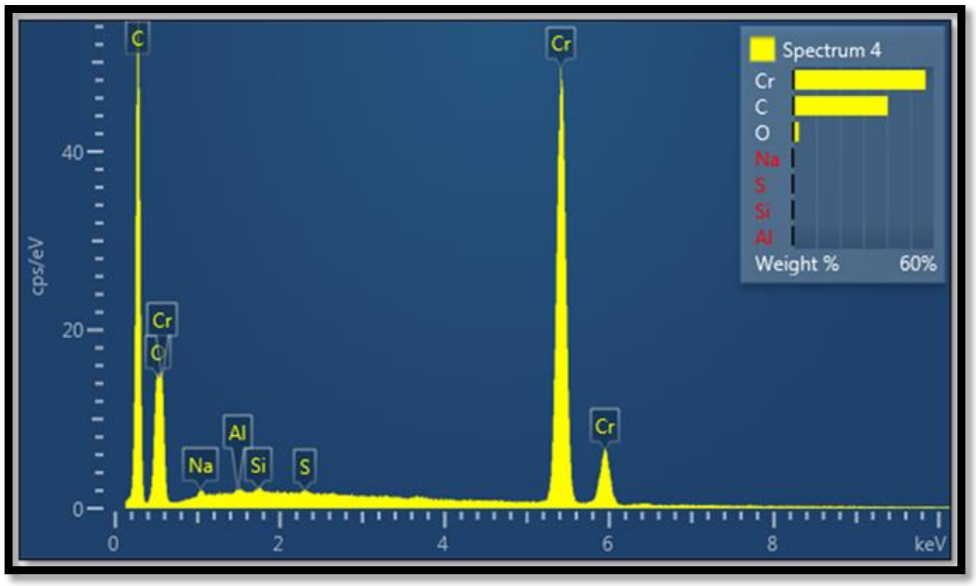

Figure (4.28): EDS analysis of (Cr-30g/l SiC)

4.6 Results of corrosion tests

4.6.1 Results of Erosion- Corrosion test

In table (4.11) the values of corrosion rates in the (Erosion-Corrosion) test in concentrated sulfuric acid under flow conditions and a temperature of (65)°C to show the effect on the samples under the effect of acid flow depending on the amount of weight loss during the area exposed to the acid in a time of (30) days for each sample and extracting the corrosion rate of the samples during one day with drawing a relationship between the amount of corrosion rate over time as shown in figure (4.29).

Table (4.11): Corrosion rate for (Erosion – Corrosion) test

Samples	Corrosion Rate($g/cm^2.day$)	IP%
Carbon steel	152×10^{-5}	–
Chromium coating	114.7×10^{-5}	24.53
Chromium coating- 10 g/l SiC	41.7×10^{-5}	72.56
Chromium coating- 20 g/l SiC	30×10^{-5}	80.26
Chromium coating- 30 g/l SiC	61×10^{-5}	59.86

Figure (4.30) shows a bar-shaped diagram for the purpose of comparing the models in the corrosion rate in the test of (Erosion-Corrosion), which clearly shows the extent of the difference in the rates of corrosion and decline for the samples protected by composite coatings compared to the base metal without any type of protection.

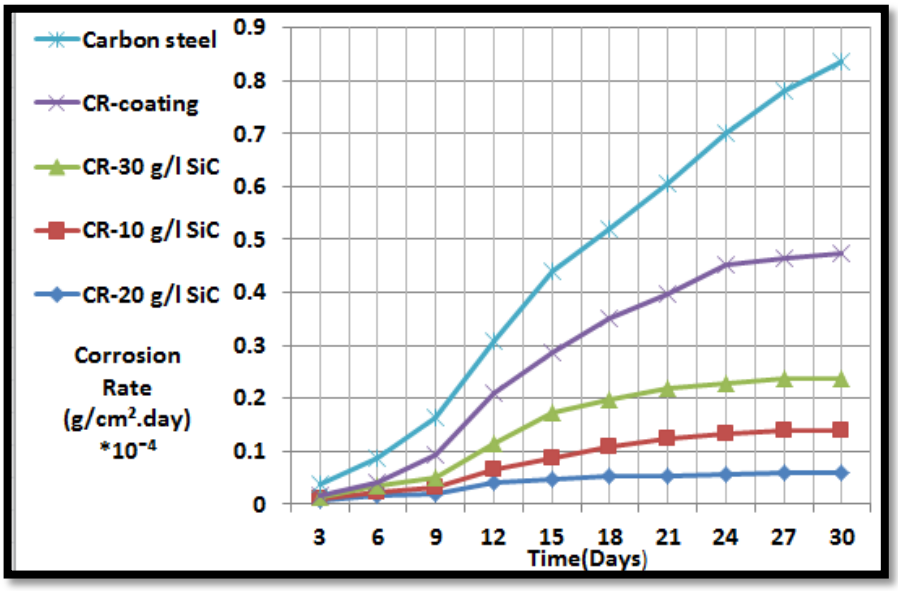

Figure (4.29): The relationship between corrosion rates for samples with time in (Erosion-Corrosion) test

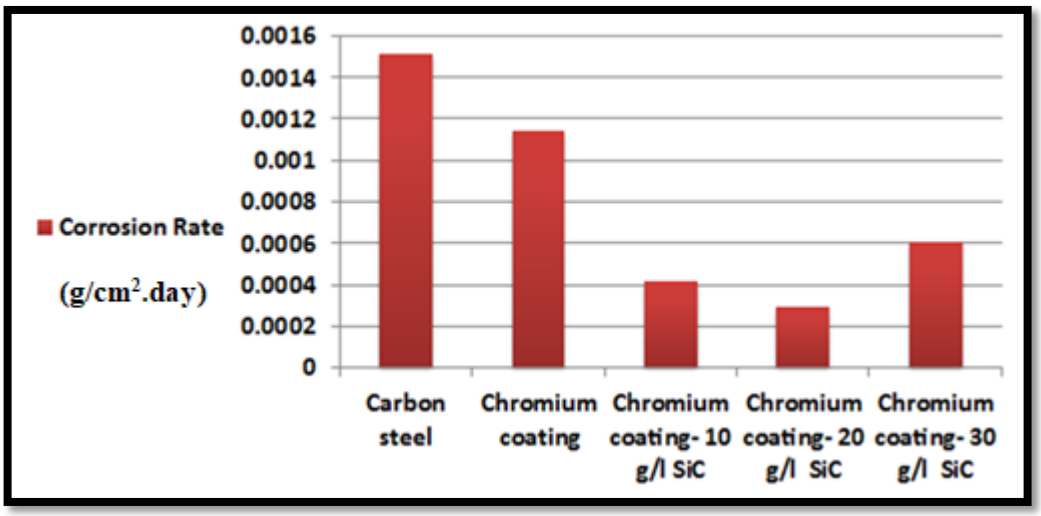

Figure (4.30): Bar chart showing comparison between samples in the rate of corrosion ($g/cm^2.day$) during (Erosion-Corrosion) test

Figure (4.29), which shows the amount of the corrosion rate over time for five samples as indicated in the figure. This test is considered one of the most important tests to indicate the extent of the corrosion rate in concentrated sulfuric acid (98%), which is the result of the exposure of the samples subjected in this test to the effect of the corrosive medium flowing at a speed similar to the flow rate of the concentrated acid in the tubes carrying the acid. The embodiments in this test include carbon steel as a base material without a layer of corrosion protection, carbon steel protected by a layer of chromium metal, carbon steel and carbon steel protected by a layer of chromium-composite coatings added to it with different amounts of silicon carbide.

As for the corrosion curve for carbon steel, we notice that the corrosion rate is constantly rising, indicating the continuation of weight loss over time. This is due to the absence of a protective layer of ferrous sulfate ($FeSO_4$) due to the high flow rate of the concentrated acid on the surface of the samples and the high temperature (65) °C where the intrusiveness of the sulfate layer is affected by the high temperature of the acid and leads to its fracture [36], so that the steel is unprotected, which is the rate of corrosion for this test (0.00152 g/cm^2.day).

In the corrosion curve of carbon steel coated with chromium, we notice a decrease in the corrosion rate compared to carbon steel without coating, which has a corrosion rate of (0.001147) and an improvement percentage of (24.53%).The reason for this behavior is the formation of a layer of chromium oxide, which is a barrier that reduces the corrosion rate due to the chromium oxide layer and the ability to rebuild the layer due to the effect of acid on it; this is consistent with previous studies [60].

For curves representing the behavior of composite coatings consisting of silicon carbide particles of different concentrations embedded in the chromium plating layer.

In general, we note that all of these curves are according to the different concentrations of silicon carbide particles, where the corrosion rate is low in the first (15) days of testing, then the curves take the form of almost a straight line, especially in the sample (Chromium coating-20g/l SiC), where the amount of corrosion rate is very small over time. The reason for this is that the composite coatings of chromium and silicon carbide give high wear resistance, as they outperform metallic coatings of chromium alone in acidic environments in improving corrosion resistance, as shown in table (4.11). Due to the formation of chromium oxide, which is a protective layer for the base metal, and silicon carbide particles, which is an inert and high-hardness material that resists wear and erosion [63, 80].

4.6.2 Immersion corrosion result

Table (4.12), which includes the results of the corrosion rates of samples in the immersion test in concentrated sulfuric acid (98%), where the results depend on the amount of weight loss of the area exposed to the acid during a time of (30) days of each sample. Also, a relationship was drawn between the corrosion rates of the samples over time, as shown in the figure (4.31).

Table (4.12): The Corrosion Rate for (Immersion Corrosion) test

Samples	Corrosion Rate($g/cm^2.day$)	IP%
Carbon steel	31.2×10^{-5}	–
Chromium coating	13.5×10^{-5}	56.73
Chromium coating- 10 g/l SiC	10.2×10^{-5}	67.3
Chromium coating- 20 g/l SiC	7.19×10^{-5}	76.95
Chromium coating- 30 g/l SiC	14.6×10^{-5}	53.2

Figure (4.31) shows the representation of corrosion rates in the bar diagram of the corrosion rates of metal and composite coatings compared to carbon steel in concentrated sulfuric acid.

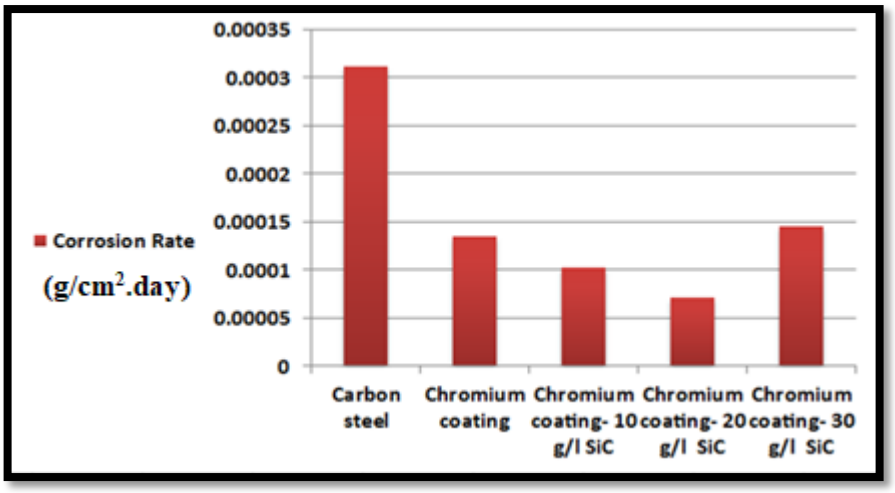

Figure (4.31): Bar chart showing comparison between samples in the rate of corrosion (g/cm^2.day) during (Immersion Corrosion) test

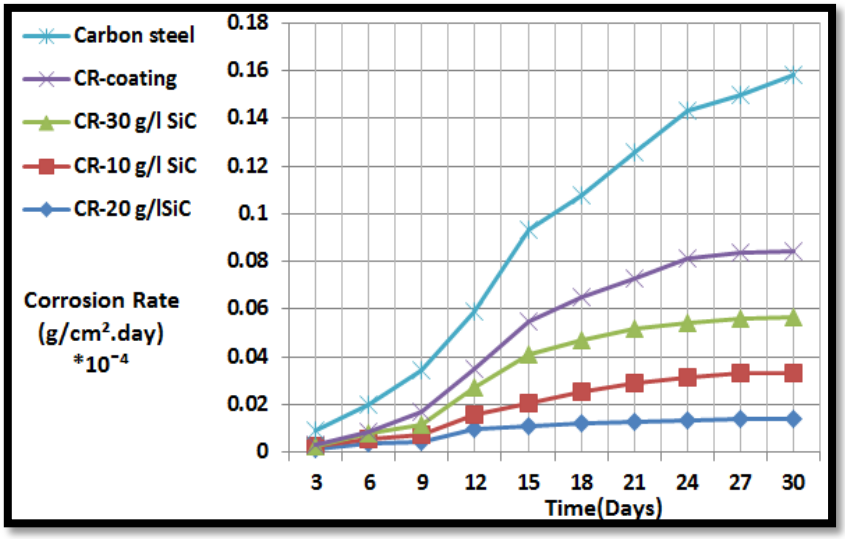

Figure (4.32): The relationship between corrosion rates for samples with time in (Immersion Corrosion) test

Figure (4.32), which represents the corrosion rates of samples under sulfuric acid conditions by immersion test and at ambient temperature, that is, the effect of acid on the samples is as a stagnant corrosive medium. We note, according to the figure, that all samples (carbon steel, Cr-coating, Cr-10 g/l SiC, Cr-20 g/l SiC, and Cr-30 g/l SiC) suffer from corrosion in sulfuric acid. All samples protected by composite coatings and metallic chromium coatings have low corrosion rates compared to the bare protection (substrate) carbon steel.

This behavior is expected for metallic and composite coatings in concentrated sulfuric acid (98%) where they have high corrosion resistance due to the formation of a valuable layer of chromium oxide related to the metal coating and the presence of corrosion-resistant silicon carbide particles embedded in chromium metal to form the composite coatings [80].

Carbon steel (substrate) in the immersion test in concentrated sulfuric acid is subjected to corrosion, but the corrosion rate is low compared to the corrosion rate in the case of acid flow and the temperature is higher than the ambient temperature. This is due to the formation of a protective layer of ferrous sulfate ($FeSO_4$) and its stability on the surface of carbon steel as long as the concentrated acid (98%) is stationary or moving at low speed and at natural temperatures close to the temperature of the external environment [36].

In figure (4.33) a comparison of the sample of carbon steel as a result of exposure to concentrated sulfuric acid in the case of the immersion test, as shown in the image (A) where the corrosion rate was (0.000312 g/cm^2.day) while the image (B) represents the exposure of carbon steel to the concentrated acid in the test (Erosion-Corrosion) where the corrosion rate was equivalent to(0.00152 g/cm^2.day) meaning that the amount of the corrosion rate in the test (Erosion-Corrosion) is five times the corrosion rate in the immersion test.

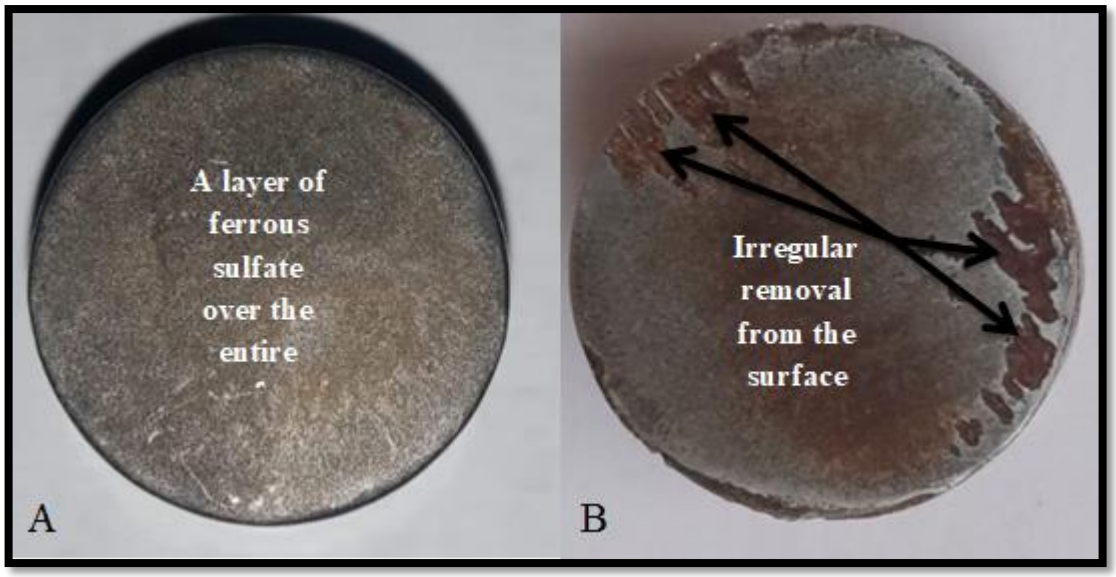

Figure (4.33): Shows a comparison of the effect of concentrated sulfuric acid on carbon steel (A: Immersion test, B :(Erosion-Corrosion) test)

The two images in the figure (4.33) represent the behavior of carbon steel when exposed to concentrated sulfuric acid, where the image (A) represents the behavior of steel in the case of stagnation of the acid or movement at a low speed and ambient temperature as in concentrated sulfuric acid tanks While the picture (B) represents the behavior of carbon steel at high flow velocities and high temperatures, and it represents the same conditions for acid flow in pipes conveying to acid production tanks.

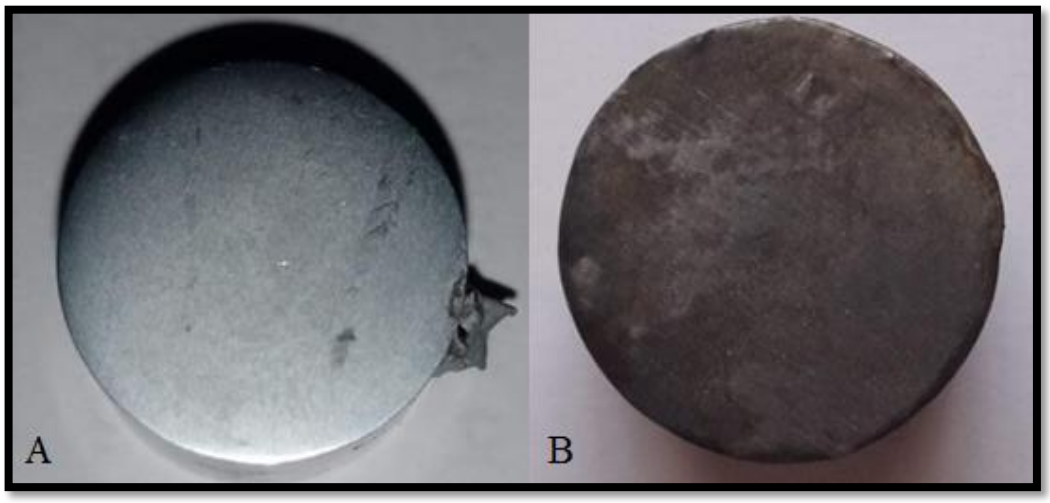

Figure (4.34): The composite coating (Cr-20 g/l SiC) sample before and after exposure to concentrated sulfuric acid

Figure (4.35) (A): Represents carbon steel coated with composite coatings of (Cr-20g/l SiC before exposure to concentrated sulfuric acid. Figure (4.35)(B): Represents carbon steel coated with composite coatings of (Cr-20g/l SiC) after (30) days of exposure to concentrated sulfuric acid flow.

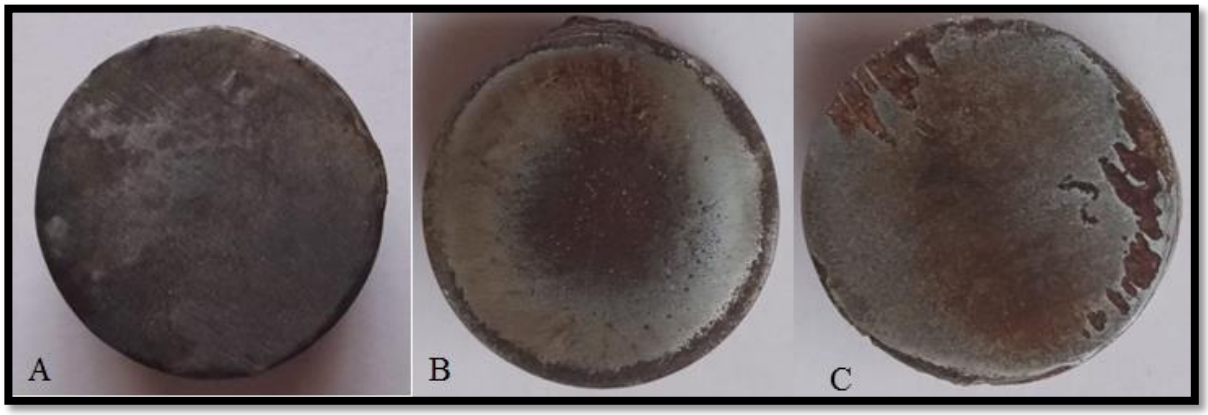

Figure (4.35): Comparison of tested samples (Erosion-Corrosion) in concentrated Sulfuric acid (A: (Cr-20 g/l SiC) coating, B: (Cr- coating), C: Carbon steel (substrate)

In the figure (4.35) which shows the effect of samples with concentrated sulfuric acid in the test (Erosion-corrosion), where the difference in the surface parameters of unprotected carbon steels, carbon steels protected by metallic coatings and carbon steels protected by composite coatings are noted.

4.6.3 Polarization test results

The polarization test for samples in concentrated sulfuric acid (98%) includes obtaining voltage readings (V) and current (A) where the relationship between the voltage and the logarithm of the current is drawn, and then a Tafel extrapolation is made on the resulting curve by the intersection of the contact lines for both the cathode and anode curves, where the coordinates of the intersection point represent the corrosion voltage and the corrosion current by dropping the point on the axis of voltage and axis of current, respectively As shown in the figures below.

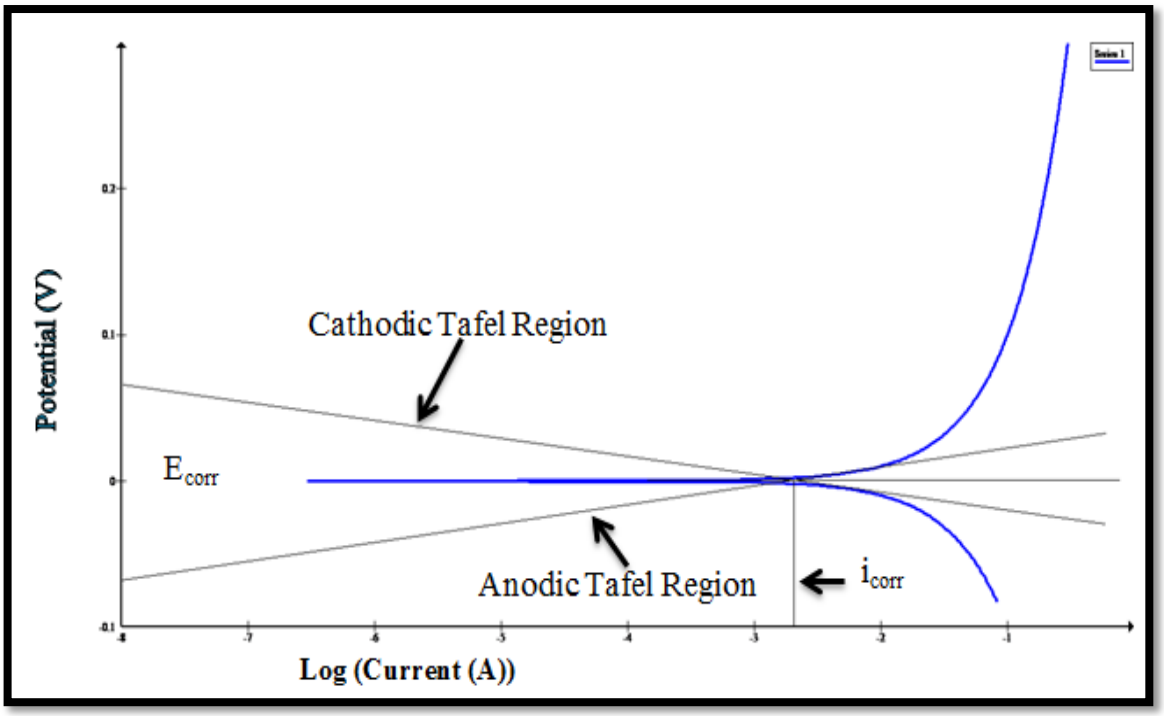

Figure (4.36): Polarization curve for carbon steel (substrate)

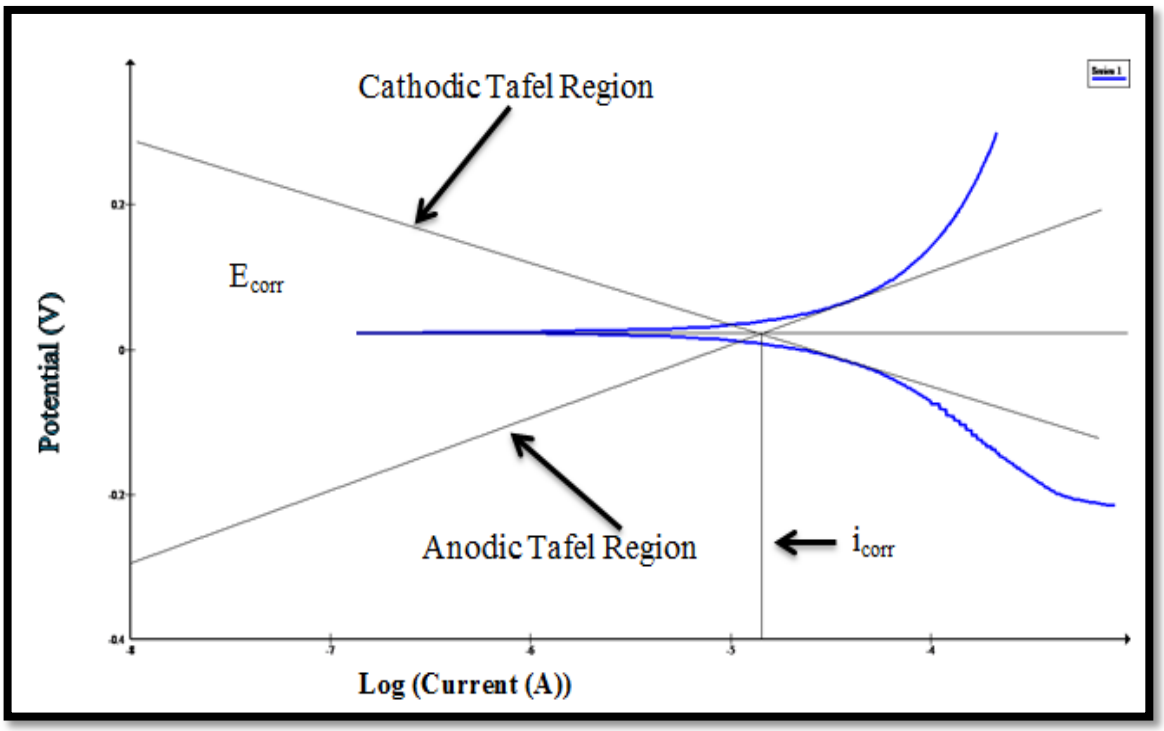

Figure (4.37): Polarization curve (Cr-coating)

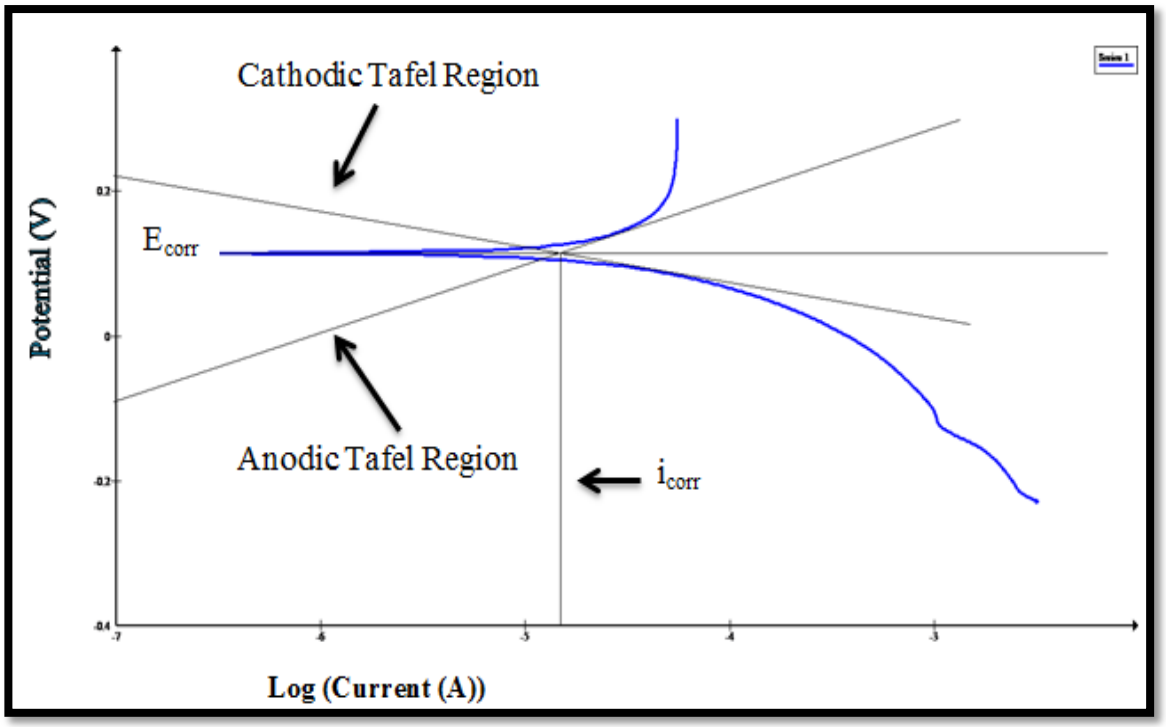

Figure (4.38): Polarization curve (Cr-10g/l SiC) Composite coating

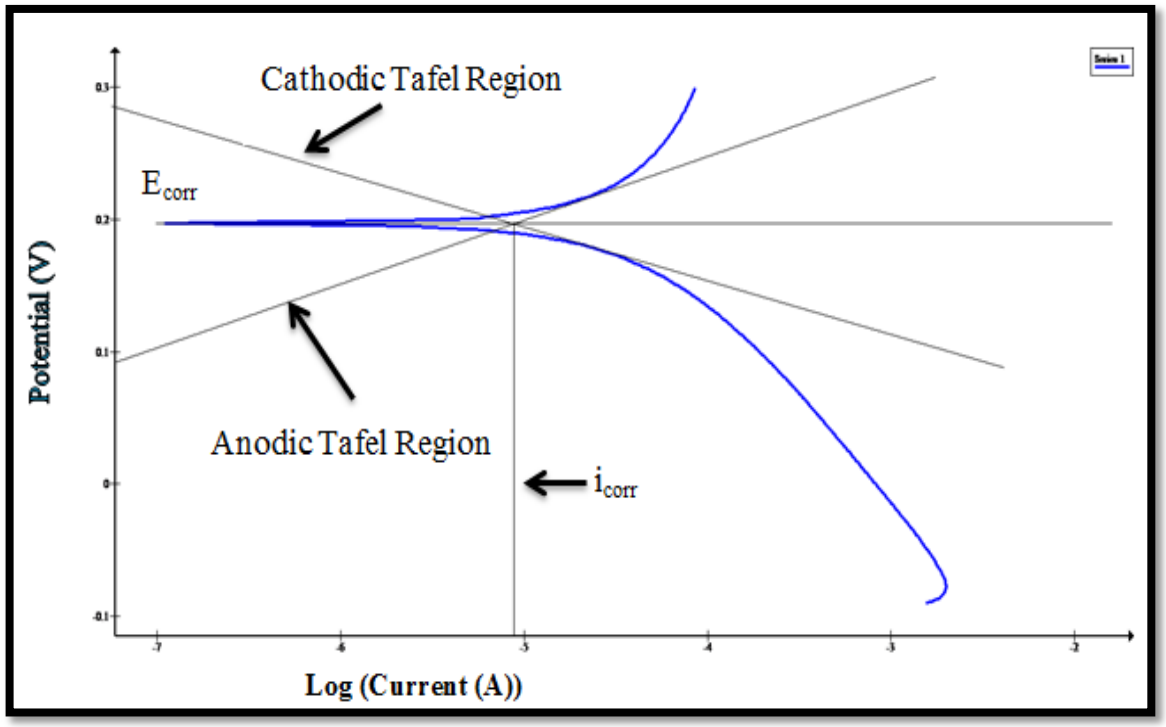

Figure (4.39): Polarization curve (Cr-20g/l SiC) Composite coating

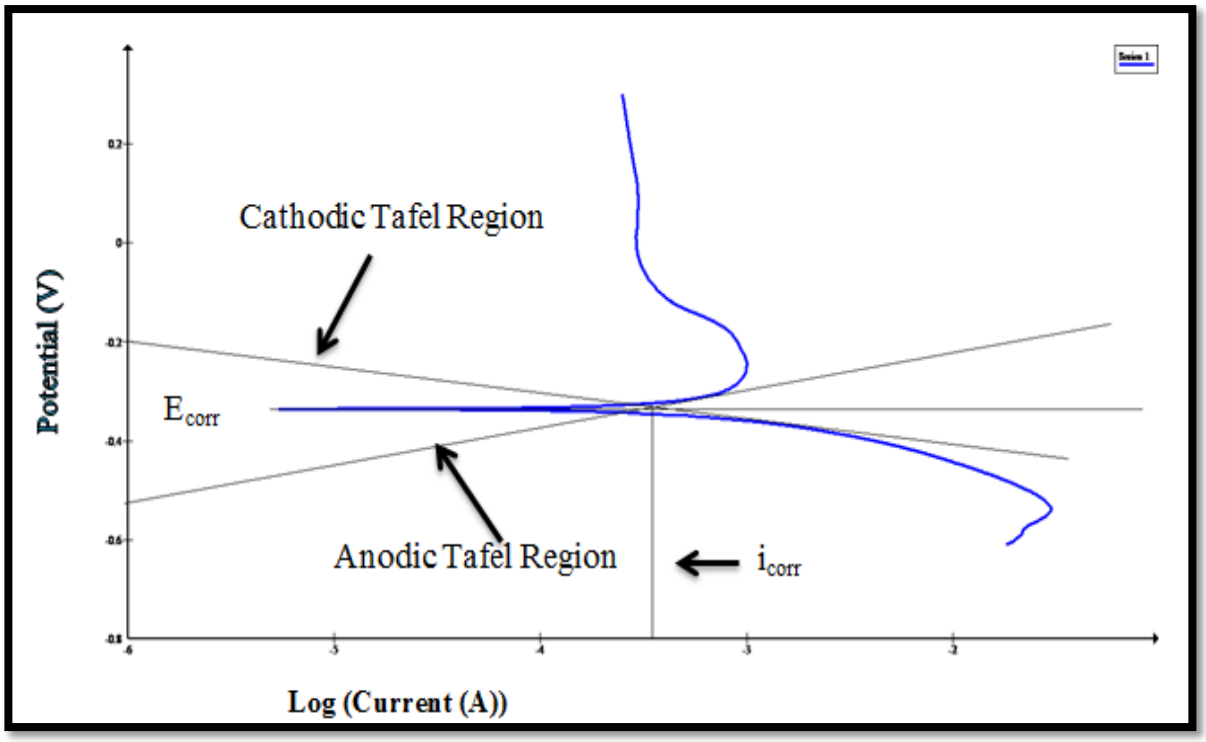

Figure (4.40): Polarization curve (Cr-30g/l SiC) Composite coating

Table (4.13): Polarization test factors and Corrosion rates for the models

Samples	Corrosion Current (µA)	Current density(µA/cm^2)	Corrosion rate(mpy)	IP%
Carbon steel	1412	1249	396.55	-
Cr-coating	19.95	17.65	8.44	97.8
Cr-10 g/l SiC	17.78	15.73	6.23	98.4
Cr-20 g/l SiC	7.94	7	1.82	99.5
Cr-30 g/l SiC	398	352.2	45.36	88.5

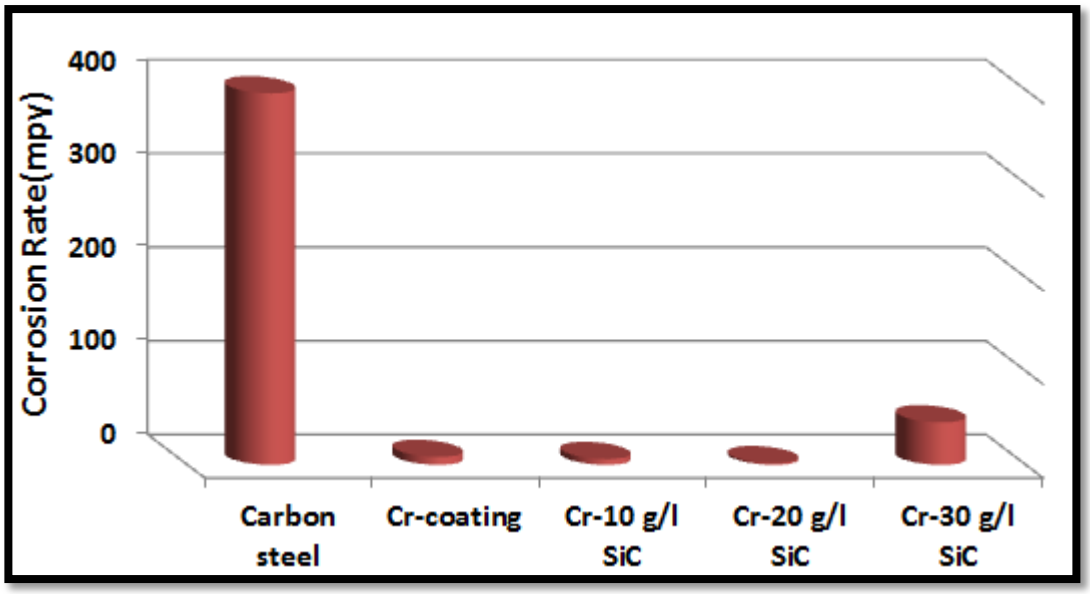

Figure(4.41): Shows a representation in cylindrical columns of the corrosion rate of carbon steel, chrome metal plating, chrome composite coatings, and silicon carbide particle concentrations (10, 20, 30)g/l

In table (4.13), the values of corrosion current, current density, and corrosion rates in addition to the percentage of improvement that occurred due to the use of metallic and composite coatings in comparison to carbon steel that is not protected from corrosion in concentrated sulfuric acid (98%).

There is significant improvement in reducing the corrosion rate as a result of the use of chromium metal coatings and composite coatings of micro-particles of silicon carbide embedded in chromium in comparison to the corrosion rate of the base metal (carbon steel without coating), where the micro-particles of silicon carbide have a significant function in enhancing the corrosion resistance in concentrated sulfuric acid because it forms a protective layer on the surface of carbon steel, isolates the metal from the attack of concentrated acid, and prevents or limits the emergence of defects on the surface of carbon steel.

Reinforcement distribution particles in the chromium coating led to the development of many corrosion micro-cells; with SiC particles acting as cathodes and chromium acting as anodes (the standard potential of SiC is higher than that of

chromium). These corrosion micro cells aid in anodic polarization. As a result, in the presence of SiC, localized corrosion is hindered, and predominantly uniform corrosion happens [80].

In the figures below, images of the scanning electron microscope show the difference in surface for carbon steel, metallic chromium plating, chromium and SiC micro particles composite coatings, before and after the polarization test in concentrated sulfuric acid.

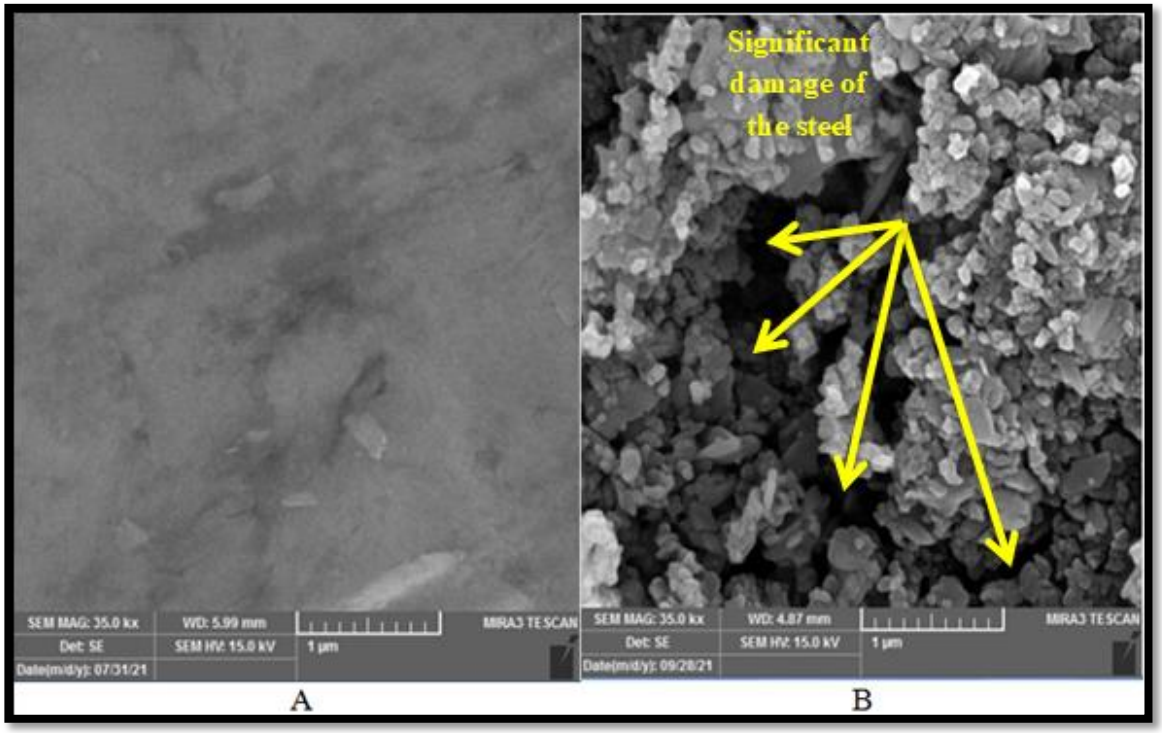

Figure (4.42): SEM images for carbon steel (A: Before polarization test, B: After polarization test)

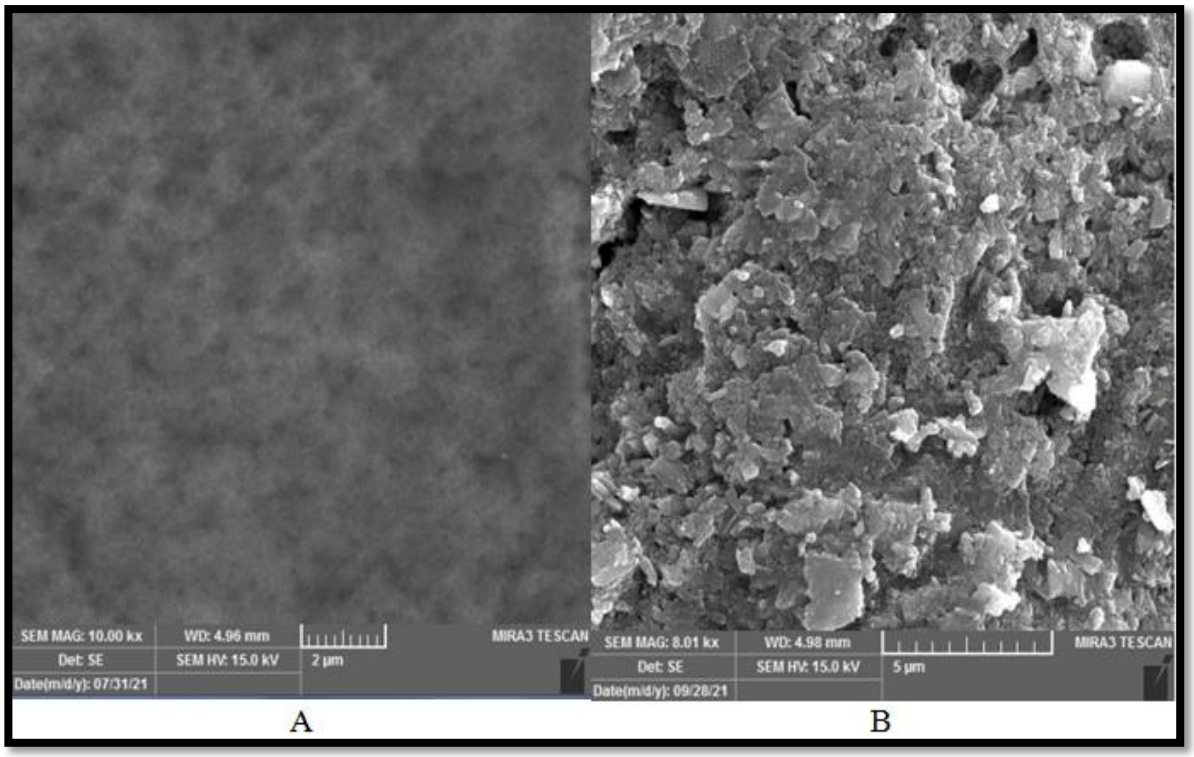

Figure (4.43): SEM images for Cr-coating (A: Before polarization test, B: After polarization test)

In figures (4.42) and (4.43), we note through images (SEM) the extent of the difference in the effect of the surface of carbon steel without any protection layer and carbon steel coated with chrome metal. Metal textures, while in acid, the effect of acid on chrome plating is a surface effect that falls within the uniform surface effect of corrosion.

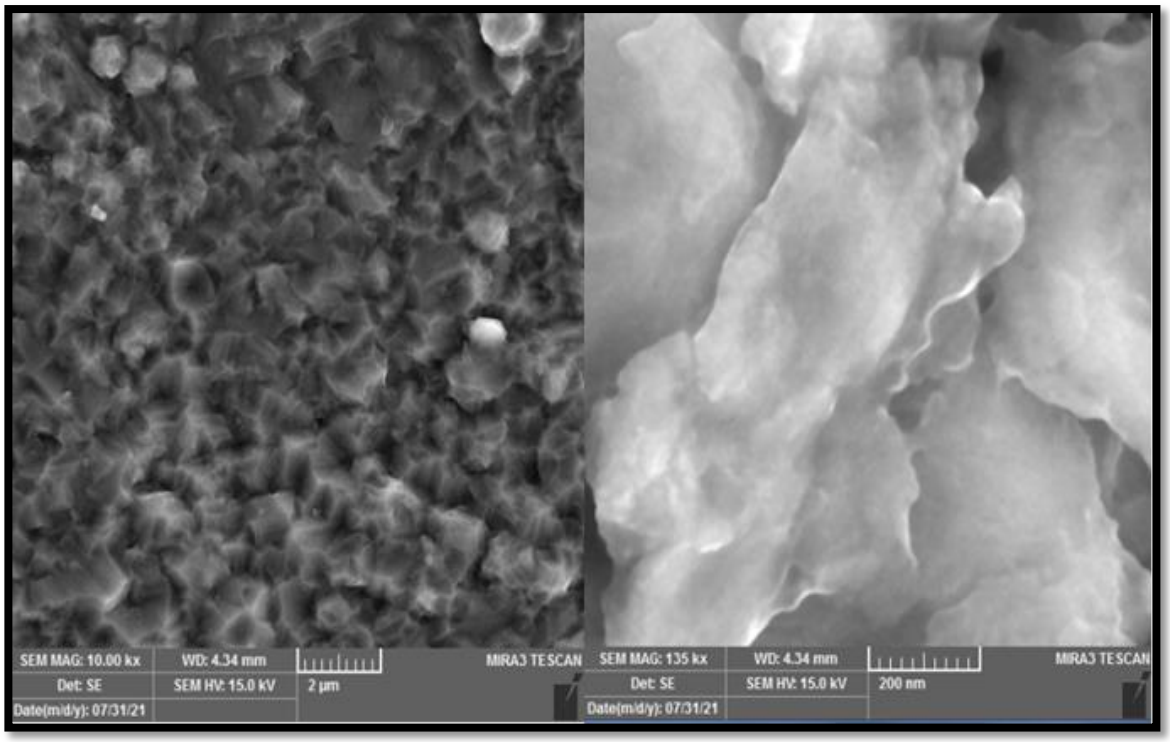

Figure (4.44): SEM images for Cr-10g/l SiC composite coating before polarization test

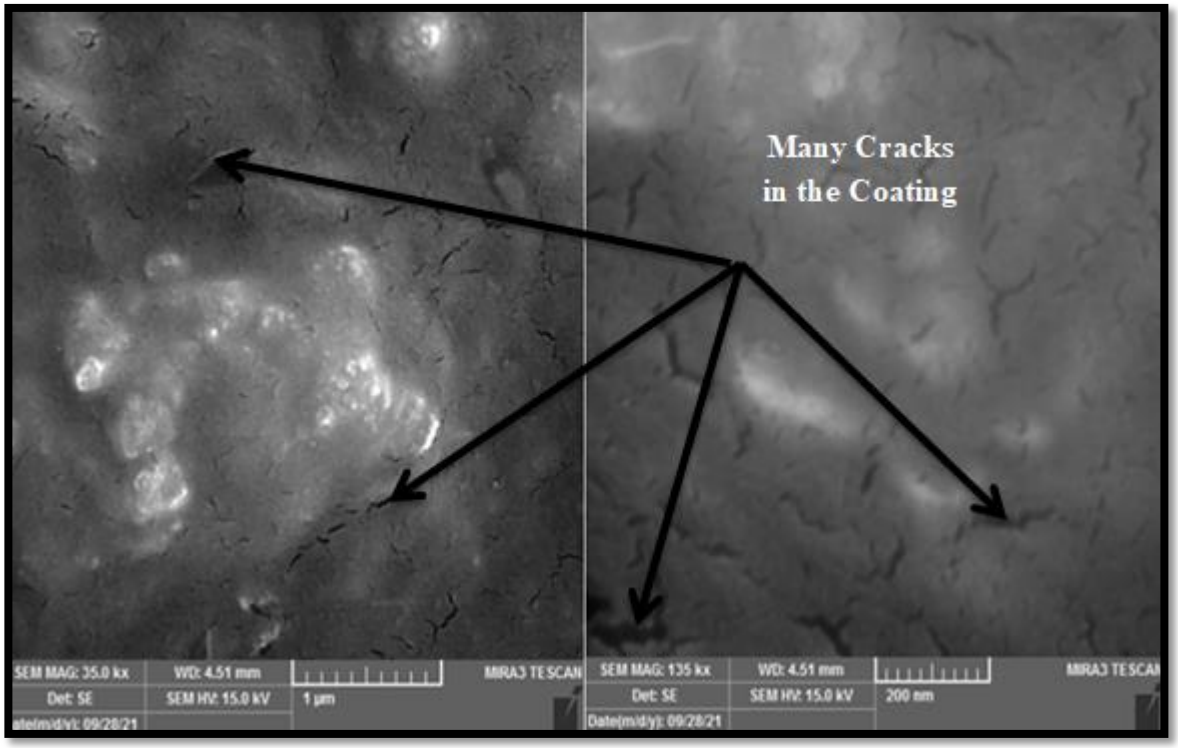

Figure (4.45): SEM images for (Cr-10 g/l SiC) composite coating after polarization test

In the figure(4.45) that shows an image of the composite coating (Cr-10g/l SiC), although the corrosion is uniform on the surface of the coating, we notice that there are cracks in the surface of the coating when exposed to concentrated acid as a result of the low concentration of silicon carbide in the coating layer. As a result, this type of coating causes an improvement in corrosion resistance that is very high compared to unprotected carbon steel, and its corrosion rate is close to that of chrome plating.

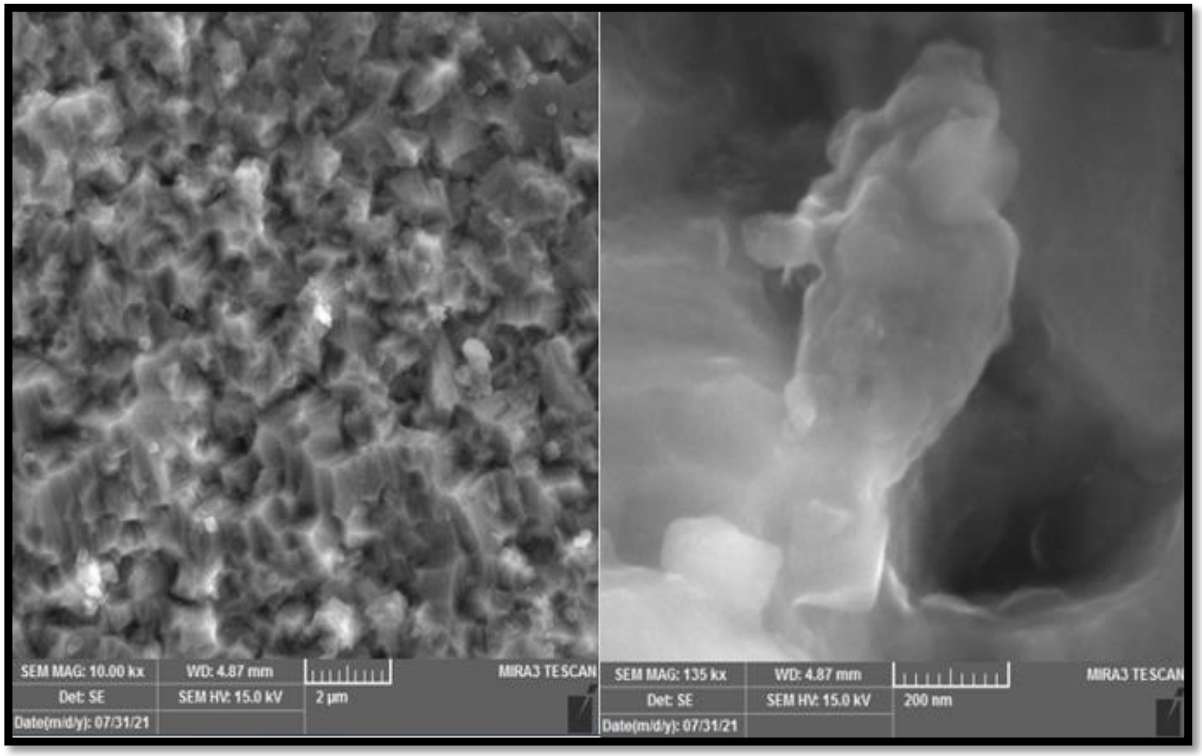

Figure (4.46): SEM images for (Cr-20g/l SiC) composite coating before polarization test

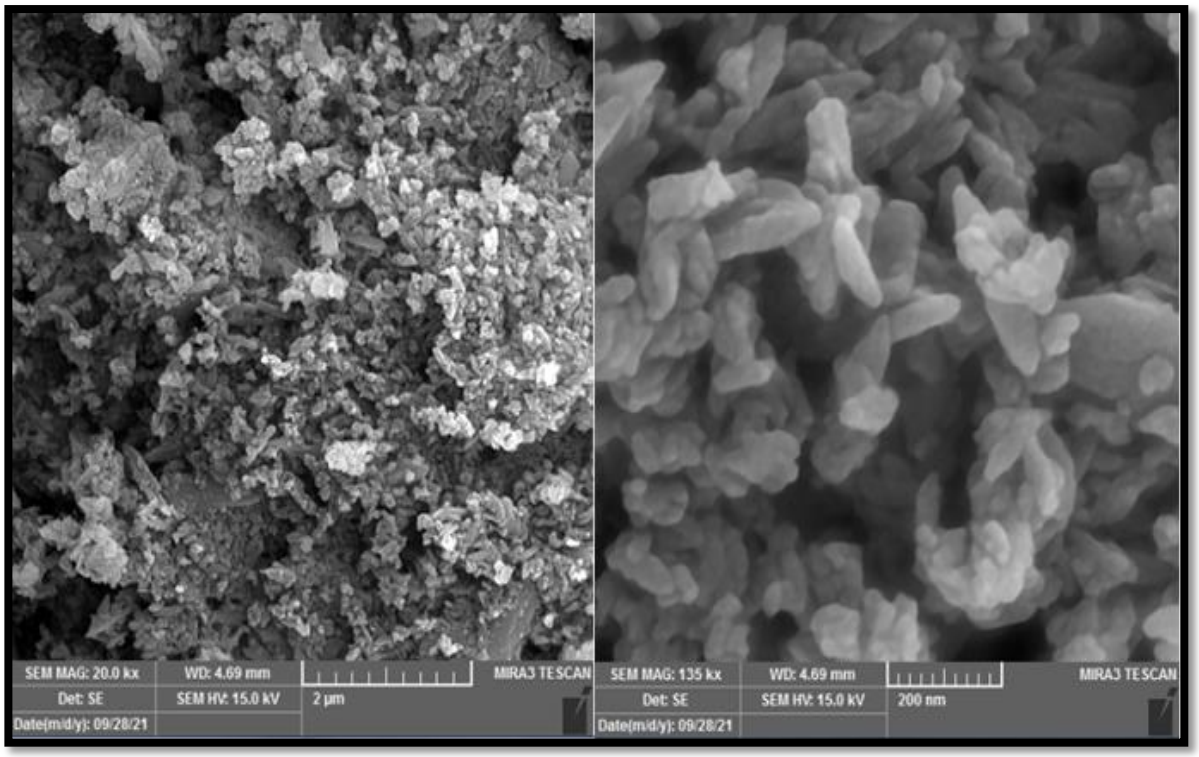

Figure (4.47): SEM images for (Cr-20g/l SiC) composite coating after polarization test

In the figure (4.47) show (SEM) image, which shows the surface of the composite coatings (Cr-20g/l SiC) after polarization test, we notice the homogeneous distribution of silicon carbide particles in chromium metal, which is the reason for a significant decrease in the corrosion rate upon exposure to concentrated sulfuric acid compared to the base metal (carbon steel) and the rest of the coatings with different concentrations of silicon carbide and chrome metal plating.

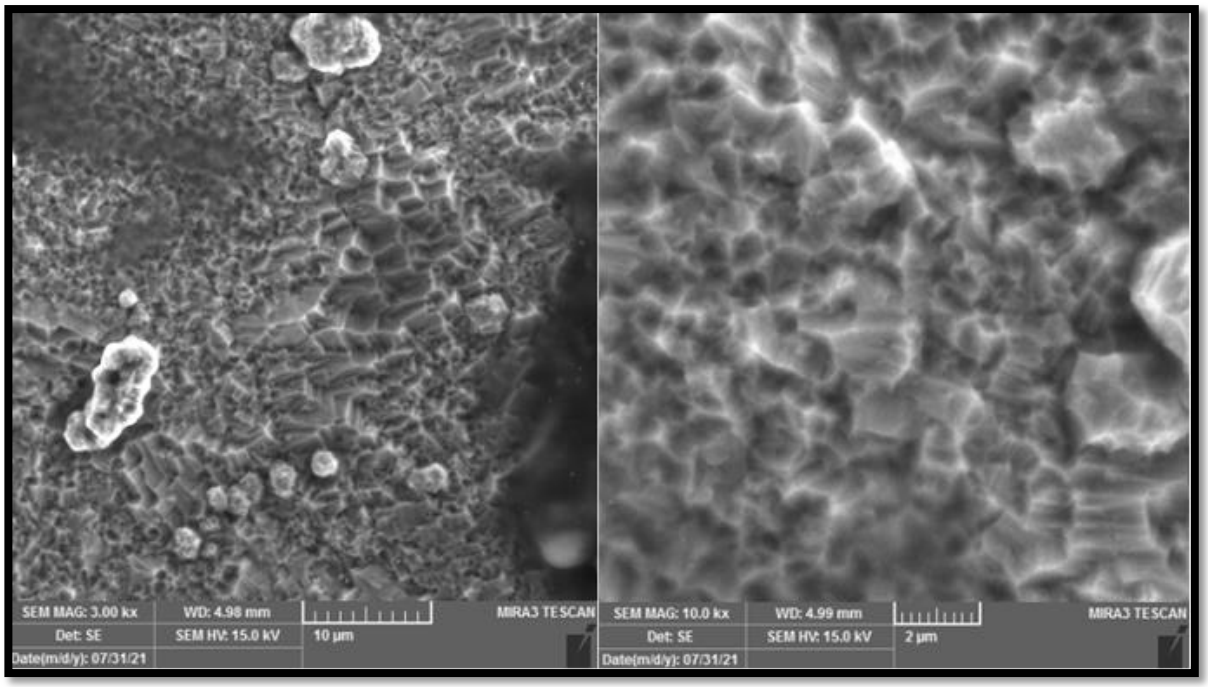

Figure (4.48): SEM images for (Cr-30g/l SiC) composite coating before polarization test

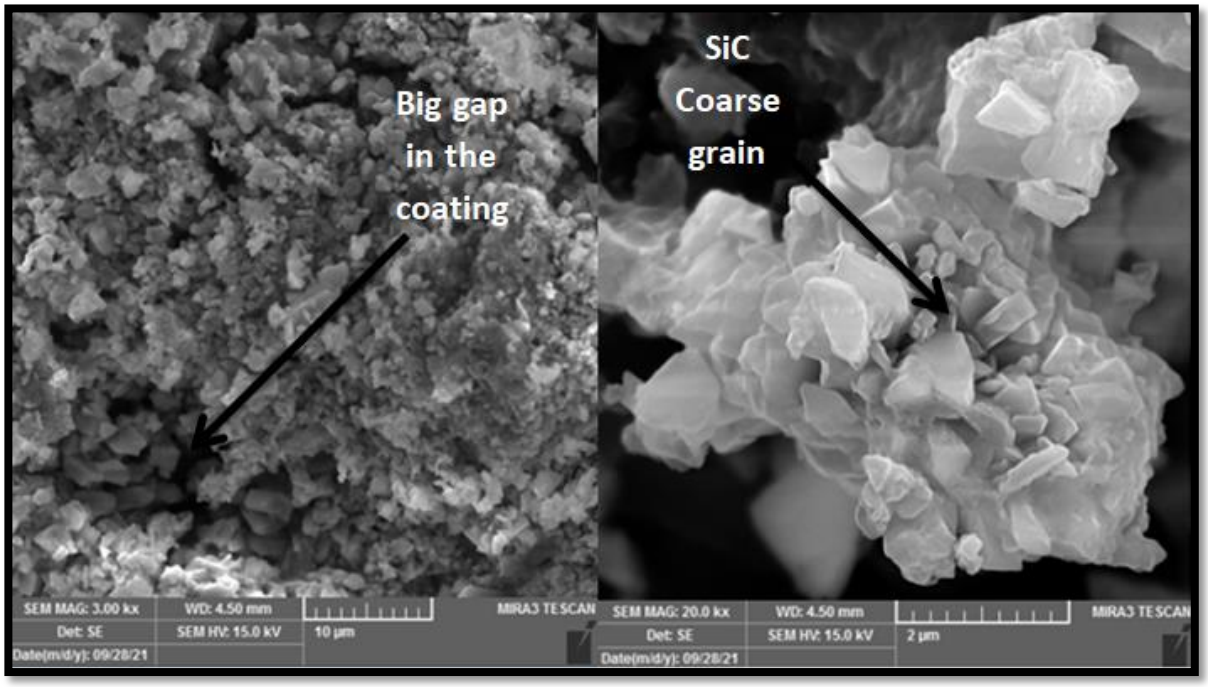

Figure (4.49): SEM images for (Cr-30g/l SiC) composite coating after polarization test

In the figure (4.49) SEM images of the composite coatings (Cr-30g/l SiC) after polarization test, we notice the lack of homogeneity in the distribution of silicon carbide particles in chromium metal with the presence of agglomerations of carbide particles that cause the inefficient work of the composite coatings as a barrier to the surface of carbon steel. Although the corrosion rate was low compared to non-carbon steel protected, at the same time, the corrosion rate was high compared to metallic chrome plating and the rest of the other composite coatings (Cr-10g/l SiC) and (Cr-20g/l SiC).

By comparing our current research with the research (JUNEGHANI (2013), in which the researcher used a solution (0.05 mol/l HCL) with Hexavalent-chromium oxide, silicon carbide nanoparticles While in our research (Trivalent-Chromium oxide) was used with silicon carbide microparticles in concentrated sulphuric acid (98%) as a medium for corrosion, the results were consistent in terms of a decrease in the corrosion rate with an increase in the concentration of silicon carbide particles to (20g/l), but when the percentage was higher than (20g/l), a higher percentage occurred. In the corrosion rate in both studies, the reason for this increase in the corrosion rate is the lack of high mixing speed to raise the silicon carbide particles to the surface of the cathode, taking into account the avoidance of turbulent movement of the particles.The results of the corrosion test for the composite coating (Cr-20g/l SiC) for both studies were as follows: the current research (1.82 mpy) and the research (0.96 mpy) where the increase in the corrosion rate of the current research for research (JUNEGHANI (2013) and this is expected due to the intensity of the corrosive medium (concentrated sulphuric acid (98%)) compared to the solution (0.05 mol/l HCL).

Chapter Five

Conclusions & Suggestions

Chapter Five

Conclusions & Suggestions

5.1 Conclusions

The following are the conclusions that obtained from the result of this research:

1. The optimum coating qualities for metallic chrome metal were in the coating solution temperature (50) °C, coating time (2) hours, and current density ($20A/dm^2$), as this coating obtained effective improvement in concentrated sulfuric acid(98%) when employed on grade(A830-1045)carbon steel.
2. The time of metallic chrome plating had the largest influence on the coating layer's qualities (hardness and thickness), whereas the temperature of the coating solution had the greatest effect on the surface roughness of the metallic chrome plating.
3. The corrosion resistance of the uncoated base metal (carbon steel) was improved by chromium composite coatings with a concentration of micro-silicon carbide particles (20)g/l, where the carbide particle distribution was homogeneous.
4. The composite coatings (Cr-30g/l SiC) performed poorly in terms of corrosion protection when compared to the other coatings (Cr-10g/l SiC) and (Cr-20g/l SiC), because their high concentration caused an increase in agglomeration within the coating solution resulting in heterogeneous deposition.

5. The composite coatings (Cr-20g/l SiC) were the best at improving the corrosion resistance in all equipment and parts of a concentrated sulfuric acid plant (98%).

5.2 Suggestions

1. Study of the use of chromium composite coatings with silicon carbide nanoparticles and comparison with the results obtained in this research.
2. The use of other types of ceramic particles in the deposition of composite coatings in chrome metal such as (SiO_2, ZrO_2) and the comparison between the efficiency of corrosion protection and cost.
3. Study of the corrosion resistance relationship of composite coatings of chromium and micro-silicon carbide with different concentrations of chromium plating solution.
4. Examine the usage of different ways of corrosion protection, such as selecting a material with high corrosion resistance (Duplex stainless steel), and compare the properties and costs with the results of this study.
5. The effect of electroplating deposition parameters (current density and stirring speed) on the attributes of composite coatings and comparison with chromium and silicon carbide composite coatings.

References

[1] Dwivedi, D., Lepková, K., & Becker, T. (2017). "Carbon steel corrosion: a review of key surface properties and characterization methods". RSC Advances, Vol.7,No.8, p 4580–4610.

[2] Mozetic, M. (2019). "Surface Modification to Improve Properties of Materials. Materials". Vol.12, No.3, pp441 .

[3] CEPHA Imaging Pvt. Ltd.(2006)." Introduction to Corrosion", India ISBN: 0750659246. .

[4] Marsh, G. N., & Chew, C. (1984). "Well man clinic in general practice". In British Medical Journal (Vol. 288, Issue 6412).

[5] Iliyasu, I., Yawas, D. S., & Aku, S. Y. (2012). "Corrosion Behavior of Austenitic Stainless Steel in Sulphuric Acid at Various Concentrations". Advances in Applied Science Research, Vol.3, No.6, 3909–3915.

[6] Edmonds, D. V., & Cochrane, R. C. (2005). "The effect of alloying on the resistance of carbon steel for oilfield applications to CO_2 corrosion". Materials Research, vol.8, No.4, pp. 377–385.

[7] Liu, M., Cheng, X., Li, X., Pan, Y., & Li, J. (2016). "Effect of Cr on the passive film formation mechanism of steel rebar in saturated calcium hydroxide solution". Applied Surface Science, 389, 1182–1191.

[8] Walsh, F. C., & Ponce De Leon, C. (2014). "A review of the electrodeposition of metal matrix composite coatings by inclusion of particles in a metal layer": An established and diversifying technology. Transactions of the Institute of Metal Finishing, Vol.92, No2, pp.83–98.

[9] Santosa, B., Gale, B. K., Beane, R. J., Ilayaraja, M., Mohan, S., Gnanamuthu, R. M., Saravanan, G., Ahmad, Y. H., Mohamed, A. M. A., Sharma, A., Das, S., Das, K., By, P., Boukhouiete, A., Creus, J., Prinsip, E., Kaedah, A. D. A. N., Manurung, C., Zong-jun, T., Corbacioglu, B. D. (2015). "Pulse-Electroplating: Process Parameters and Their Influence on the Formed Microstructure". International Journal of Chemistry, Vol.2, No.3, pp.124.

[10] Shaw, B. A., & Kelly, R. G. (2006). "What is corrosion". Electrochemical Society Interface, Vol.15, No.1, pp. 24–26.

[11] Raja, P. B., & Sethuraman, M. G. (2008). "Natural products as corrosion inhibitor for metals in corrosive media - A review". Materials Letters, Vol.62, No.1, pp.113–116.

[12] Makhlouf, A. S. H., Herrera, V., & Muñoz, E. (2018). "Corrosion and protection of the metallic structures in the petroleum industry due to corrosion and the techniques for protection". In Handbook of Materials Failure Analysis. Elsevier Ltd.

[13] P.A.Schweitzer.(2007), "Corrosion Engineering HandBook" 2 nd edition, Taylor and Francis Group,LLC.

[14] William Hawkes. (2020). "The_Principle_Mechanisms_of_Corrosion".

[15] Bardal, E. (2007)." Different Forms of Corrosion Classified on the Basis of Appearence",Corrosion and Protection. pp. 89-191.

[16] Barker, D. (1993). "The Strategy for Corrosion Prevention. ".

[17] Burstein, G. T., Liu, C., Souto, R. M., & Vines, S. P. (2004). "Origins of pitting corrosion". Corrosion Engineering Science and Technology, Vol.39,No.1, pp.25–30.

[18] Strehblow, H. H., & Marcus, P. (2011). Fundamentals of corrosion. In Corrosion Mechanisms in Theory and Practice: Third Edition.

[19] Linda Gaverick ,(1994)." Forms of Corrosion in the Petrochemical Industry".

[20] Perez, N. (2004)."Forms of corrosion". Electrochemistry and corrosion science .Springer. ISBN: 978-1-4020-7860-6.

[21] Scully,J.R.(2003)."Intergranular Corrosion".Encyclopedia of Electrochemistry, V, 810–827.

[22] Kuruvila, R., Kumaran, S. T., Khan, M. A., & Uthayakumar, M. (2018). "A brief review on the erosion-corrosion behavior of engineering materials". Corrosion Reviews, Vol.36,No.5, pp.435–447.

[23] Zhang, J., Kang, J., Fan, J., & Gao, J. (2016). "Study on erosion wear of fracturing pipeline under the action of multiphase flow in oil & gas industry". Journal of Natural Gas Science and Engineering, Vol.32, No.1,pp.334–346.

[24] Rajahram, S. S., Harvey, T. J., & Wood, R. J. K. (2009)." Erosion-corrosion resistance of engineering materials in various test conditions". Wear, Vol.267,No.(1–4), pp.244–254.

[25] Stack, M. M., & Pungwiwat, N. (2004). "Erosion-corrosion mapping of Fe in aqueous slurries": Some views on a new rationale for defining the erosion-corrosion interaction. Wear, Vol.256,No.(5), pp.565–576.

[26] Liu, J. G., BaKeDaShi, W. L., Li, Z. L., Xu, Y. Z., Ji, W. R., Zhang, C., Cui, G., & Zhang, R. Y. (2017). "Effect of flow velocity on erosion–corrosion of 90-degree horizontal elbow. Wear, 376–377, 516–525.

[27] Islam, M. A., & Farhat, Z. (2017). "Erosion-corrosion mechanism and comparison of erosion-corrosion performance of API steels". Wear, 376–377, 533–541.

[28] Uzorh, E. A. (2013). "Corrosion Properties of Plain Carbon Steels". The International Journal Of Engineering And Science (IJES) Volume, 2(11), 18–24.

[29] Gandy, D. (2007). "Carbon Steel Handbook". Carbon, 3(3), 172.

[30] Stamatis, D. H. (1997). "TQM Engineering Handbook". TQM Engineering Handbook

[31] Revie, R.W. (2008),"Corrosion and corrosion control": an introduction to corrosion science and engineering", John Wiley & Sons.

[32] Liu, Y., Wang, Z., & Wei, Y. (2019)." Influence of seawater on the carbon steel initial corrosion behavior". International Journal of Electrochemical Science, Vol.14,No.2, pp.1147–1162.

[33] Handoko, W., Pahlevani, F., & Sahajwalla, V. (2018). "The effect of low-quantity Cr addition on the corrosion behaviour of dual-phase high carbon Steel". Metals, Vol.8,No.(4), pp.2–12.

[34] Ferrer, F., Faure, T., Goudiakas, J., & Andrés, E. (2002). Acoustic emission study of active-passive transitions during carbon steel erosion-corrosion in concentrated sulfuric acid. Corrosion Science, Vol.44,No.(7),pp. 1529–1540.

[35] Menu, M., Index, S., & Guide, U. (1998). "Corrosion Control ".

[36] Panossian, Z., Almeida, N. L. de, de Sousa, R. M. F., Pimenta, G. de S., & Marques, L. B. S. (2012). "Corrosion of carbon steel pipes and tanks by concentrated sulfuric acid: A review". Corrosion Science, 58(August 2018), 1–11.

[37] Michael, D. (2011). "Alloy selection for service in sulphuric acid".

[38] Azam, M. A., Ibrahim, M. F., & Zaimi, M. (2014). "Corrosion Analysis of Carbon Steel Pipeline: Effect of Different Sulfuric Acid Concentrations". Applied Mechanics and Materials, Vol.699,No.1,pp. 215–220.

[39] VGO inspection engineer. (2015)." Case Study : Failure Analysis of Sulfuric Acid Supply Line". (Issue 503, pp. 1–11).

[40] Maaß, P. (2011). "Corrosion and Corrosion Protection". Handbook of Hot-Dip Galvanization, 1–19.

[41] Nazal, M. K., & Jafar Mazumder, M. A. (2019). "Anticorrosive Coating". 883–909.

[42] Pierre R. Roberge. (2000). "Handbook of Corrosion Engineering" Library of Congres .P 1129.

[43] Wilds, N. (2017). Corrosion under insulation. In Trends in Oil and Gas Corrosion Research and Technologies: Production and Transmission. Elsevier Ltd.

[44] Kelly, G. J. (1984). Corrosion Engineering - Practices VS Principles. In CEA, Chemical Engineering in Australia (Vol. ChE9, Issue 2).

[45] Zaki Ahmad. (2006)." Principles of Corrosion Engineering and Corrosion Control" • Publisher: Elsevier Science & Technology Books (Issue September).

[46] Yahalom, J. (2001). "Corrosion Protection Methods". Encyclopedia of Materials: Science and Technology, pp.1710–1713.

[47] Bardal, E. (2003). "Corrosion and protection against corrosion". In Pumps (Issues 148, Jan.1979).

[48] Paunovic, M., & Schlesinger, M. (2005). "Fundamentals of Electrochemical Deposition: Second Edition", pp.1–373.

[49] Sharma, A., Cheon, C.-S., & Jung, J. P. (2016). "Recent Progress in Electroless Plating of Copper". Journal of the Microelectronics and Packaging Society, Vol.23,No.(4), pp.1–6.

[50] Postigo, M. V. (2010). "New methods for the analytical control of a nickel electroplating bath". Application of chemometric techniques.

[51] S.A.Calbeto,(2011)"Nickel matrixmicro/nano SiC composite electrodeposition" MSc. thesis , Escola Tecnica Superior D'enginyeria Industrial De Barcelona.

[52] Munford, M. L. (2006). "Encyclopedia of Chemical Processing". 821–832.

[53] Kumar, S., Pande, S., & Verma, P. (2015). "Factor Effecting Electro-Deposition Process"International Journal of Current Engineering and TechnologyVol.5, No.2.

[54] Haque, E., Hoque, A., & Islam, M. (2017). Effect of Various Operating Parameters on Trivalent Chromium Electroplating. Vol.13,No.3, pp.1–9.

[55] Tracton, A. a. (2001). "Coatings Technology Handbook, Third Edition - CRC Press" Book. 2–3.

[56] El-hallag, I. S., Moharram, Y. I., Darweesh, M. A., & Tartour, A. R. (2020). "Factors Affecting Nucleation and Growth of Chromium Electrode- posited from Cr^{3+} Electrolytes Based on Deep Eutectic Solvents". Vol.11,No.3, pp.291–309.

[57] Raj, L. M. I., Sathishkumar, J., Kumaragurubaran, B., & Gopal, P. (2013). "Analysis of Hard Chromium Coating Defects and its Prevention Methods". Vol.5, 427–432.

[58] Hoque, A. (2015). "Electroplating of Chromium From Cr (III) Aqueous Solutions on the Mild Steel" : Optimization of Bath Constituents. International Journal of Innovation in Science and Mathematics. 3(2).

[59]Yli,Pentti,(2014)." Electroplating and Electroless Plating".Comprehensive Materials Processing, Volume 4. P (277-306).

[60]Latif, S. (2010). "Carbide Reinforced Metal-Matrix Composite Coatings by Carburizing of Electrodeposited Amorphous and Nanocrystalline Alloys". ph.D. A thesis, Department of Metallurgy and Materials Engineering Pakistan Institute of Engineering and Applied Sciences Islamabad, Pakistan October.

[61] Spyrellis, N., Pavlatou, E. A., Spanou, S., & Zoikis-Karathanasis, A. (2009). "Nickel and nickel-phosphorous matrix composite electrocoatings". Transactions of Nonferrous Metals Society of China (English Edition), Vol.19,No.4, pp.800–804.

[62] Losiewicz, B. (2015). "Electrodeposition mechanism of composite coatings". Solid State Phenomena, 228, 65–78.

[63] Lekka, M. (2018). "Electrochemical deposition of composite coatings". In Encyclopedia of Interfacial Chemistry: Surface Science and Electrochemistry. Elsevier.

[64] Low, C. T. J., Wills, R. G. A., & Walsh, F. C. (2006). "Electrodeposition of composite coatings containing nanoparticles in a metal deposit". Surface & Coatings Technology 201, 371–383.

[65] Yang, X. (2013). "Engineering Optimization and Industrial Applications". School of Science and Technology. 393–412.

[66] Sha, M., & Xie, Y. (2016). "The Applications of Mathematical Modeling Based on MATLAB"Department of Mathematics, Kunming University. Icassr 2015, 526–529.

[67] Liu, S., Forrest, J., Yang, Y., & Liu, S. (2014). Grey Systems : Theory and Application A brief introduction to grey systems theory A brief introduction to grey systems theory.

[68] Huang, S., Chiu, N., & Chen, L. (2008). "Integration of the grey relational analysis with genetic algorithm for software effort estimation". European Journal of Operational Research. 188, 898–909.

[69] Ertugrul, I., & Prof, A. (2016). Grey Relational Analysis Approach In Academic Performance Comparison Of University : A Case Study Of Turkish Universities. 7881(June), 128–139.

[70] Kuo, Y., Yang, T., & Huang, G. W. (2008). "The use of grey relational analysis in solving multiple attribute decision-making problems". Computers and Industrial Engineering, Vol.55,No.(1), pp. 80–93.

[71] Das, P. P., Diyaley, S., Chakraborty, S., & Ghadai, R. K. (2018)." Multi-Objective Optimization of Wire Electro Discharge Machining (WEDM) Process Parameters Using Grey-Fuzzy Approach". 1–10.

[72] Patil, A. N. (2019)."Grey Relation Analysis Methodology and its Application". Volume-04. Issue-02. ISSN: 2455-3085.

[73] Nair, A., Govindan, P., & Ganesan, H. (2014). "A Comparison between different Optimization Techniques for CNC End Milling Process". Procedia Engineering, 97, 36–46.

[74] Puh, F., Jurkovic, Z., Perinic, M., Brezocnik, M., & Buljan, S. (2016). "Optimization of machining parameters for turning operation with multiple quality characteristics using Grey relational analysis". 2, 377-382.

[75] Natoli, C. (2017). "Understanding Analysis of Variance"

[76] Zoda, H. H. H. (2020). "Multiple Optimization of Mechanical and Machining Properties of Hybrid MMCs".A Thesis Submitted to the council of the College of Materials Engineering / University of Babylon. Multiple Optimization of Mechanical.

[77] Sun Ke-Ning , S., Xin-ning, H., & Ji-ren, W. (1996)." Electrodeposited Cr-A1203". Wear, 1648(95), 3–5.

[78] Surviliene, S., Lisowska-Oleksiak, A., Jasulaitiene, V., & Češuniene, A. (2005)." Effect of SiC on the corrosion behaviour of chromium coatings". Transactions of the Institute of Metal Finishing, Vol.83,No.(3), pp. 130–136.

[79] Gao, J., & Suo, J. (2011). "Preparation and characterization of the electrodeposited Cr-Al_2O_3 /SiC composite coating". Applied Surface Science, 257(22), 9643–9648.

[80] Juneghani, M. A., Farzam, M., & Zohdirad, H. (2013). "Wear and corrosion resistance and electroplating characteristics of electrodeposited Cr-SiC nano-composite coatings". Transactions of Nonferrous Metals Society of China (English Edition), Vol.23,No.(7),pp. 1993–2001.

[81] Lakra, S., Maharana, H. S., & Basu, A. (2016). "Synthesis and Characterization of Cr-ZrO2 Composite Coating Formed by DC and Pulse Electrodeposition". Materials and Manufacturing Processes, Vol.31,No.(11), pp.1447–1453.

[82] Liao, C. W., Lee, H. Bin, Hou, K. H., Jian, S. Y., Lu, C. E., & Ger, M. Der. (2016). "Characterization of the Cr-C/Si3N4 Composite Coatings Electroplated from a Trivalent Chromium Bath". Electrochimica Acta, Vol.209, pp. 244–253.

[83] Sheu, H. H., Hong, T. Y., Lin, T. Te, & Ger, M. Der. (2018). "The effect of heat treatment on the corrosion resistance, mechanical properties and wear resistance of Cr-C Coatings and Cr-C/Al_2O_3 composite coatings electrodeposited on low carbon steel". International Journal of Electrochemical Science, Vol.13,No.(10), pp.9399–9415.

[84] Sadeghi-dehsahraee, M., & Najafisayar, P. (2019). "Electrodeposition and Characterization of Cr-MoS_2 Composite Coatings". Journal of Materials Engineering and Performance, Vol.28,No.9, pp.5674–5690.

[85] Zhang, S., Li, Y., Wang, C., & Zhao, X. (2019). "Preparation of a Cr coating on low-carbon steel by electrodeposition in a NaCl-KCl-NaF-Cr_2O_3 molten salt". International Journal of Electrochemical Science, Vol.14,No.1, pp.91–101.

[86] Jegan, A., & Venkatesan, R. (2013). "Characterization and optimization of pulse electrodeposition of Ni/nano-Al2O3 composite coatings". International Journal of Minerals, Metallurgy and Materials, Vol.20,No.5, pp.479–485.

[87] Gadhari, P., & Sahoo, P. (2014). "Influence of process parameters on multiple roughness characteristics of Ni-P-TiO2 composite coatings". Procedia Engineering, 97, 439–448.

[88] Narayanappa, B.S. P. K. and K. M. (2017). "Optimization of Electrodeposition Process Parameters on Wear Properties of Ni-Wc Coated Ferrous Alloy". International Journal of Current Engineering and Technology, Vol.7,No.1, pp.223–227.

[89] Raghavendra, C. R., Basavarajappa, S., & Sogalad, I. (2018). "Multi-objective Optimization of Electrodeposition of Ni–Al2O3 Nano Composite Coating on Al6061 Substrate". Transactions of the Indian Institute of Metals, Vol.71,No.9, pp.2119–2132.

[90] Salvador Barbato, R., Jilberto Ponce, F., Marcelo Jara, V., Jacqueline Cuevas, S., & Rodrigo Egaña, A. (2008). "Study of the effect of temperature on the hardness,

grain size, and yield in electrodeposition of chromium on 1045 steel". Journal of the Chilean Chemical Society, Vol. 53, No. 1, pp. 2–5.

[91] Bashar, S. N. (2020). "Erosion Corrosion Prediction for Industrial Pumping Station with Optimization".College of Materials Engineering.Department of Metallurgical Engineering.

[92] S. Mahdavia, S.R. Allahkaramb, A. Heidarzadehc, (2018)." Characteristics and properties of Cr coatings electrodeposited from Cr(III) baths". Research Center for Advanced Materials, Faculty of Materials Engineering, Sahand Universityof Technology, 5133511996, Tabriz, Iran.

[93] ASTM-Standards. (1999)." Standard practice for calculation of corrosion rates and related information from electrochemical measurements". Astm G 102-89, 89(Reapproved), pp.1–7.

Appendix

Appendix A
(Statistical analysis software application)

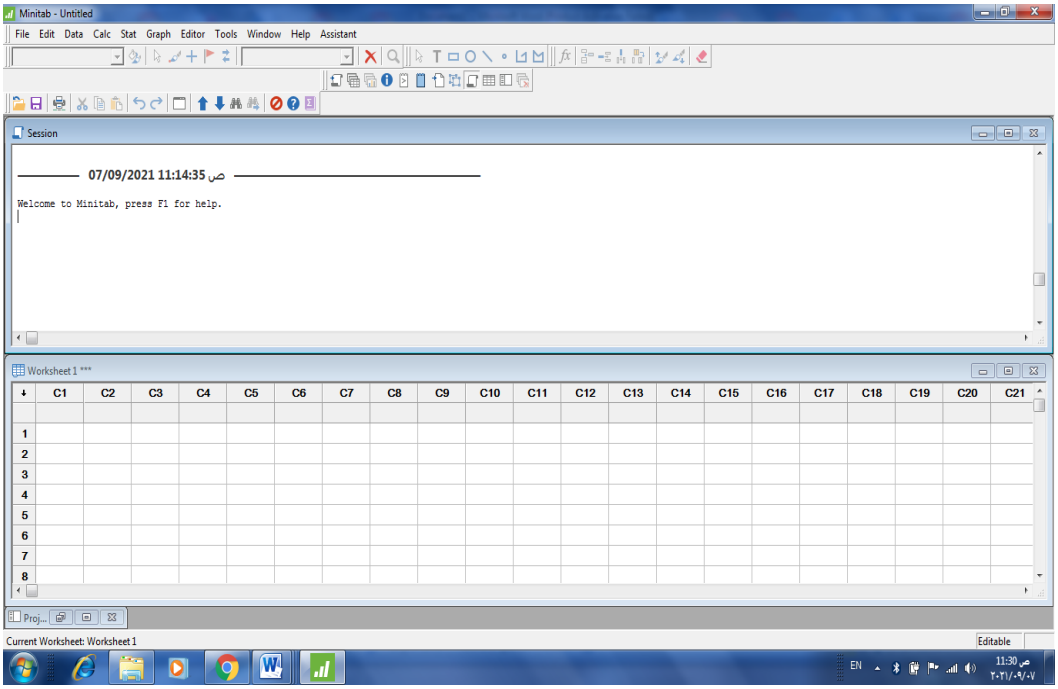

Statistical Program Interface (MINITAB)

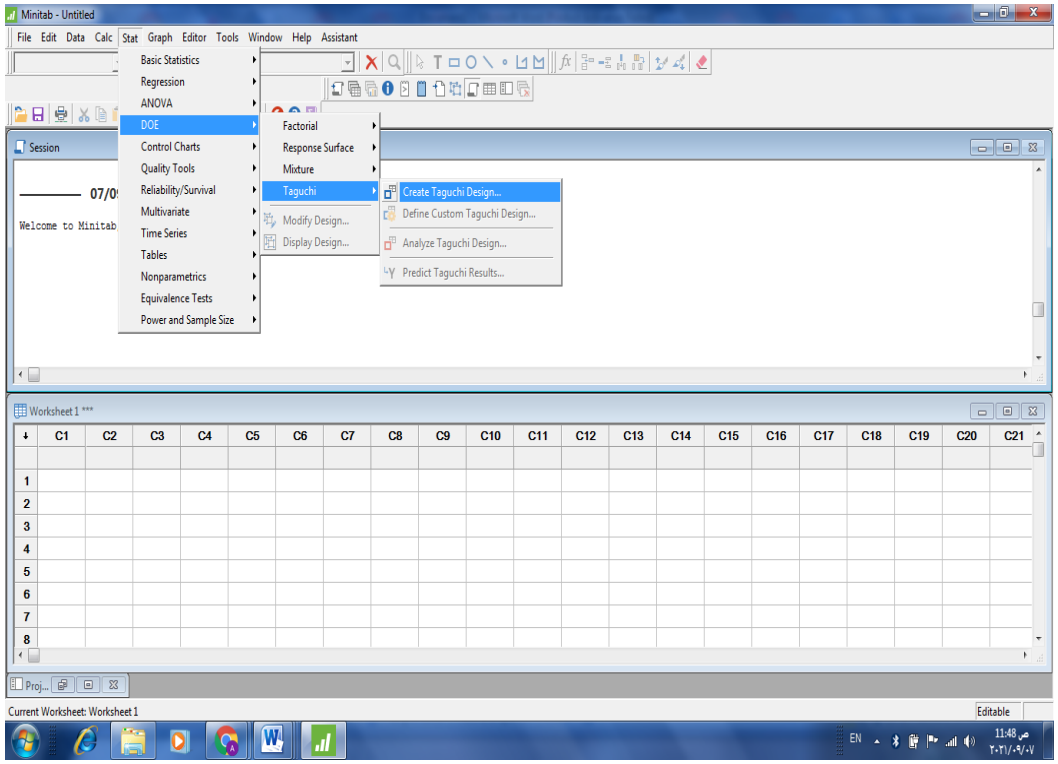

Designing statistical program experiments

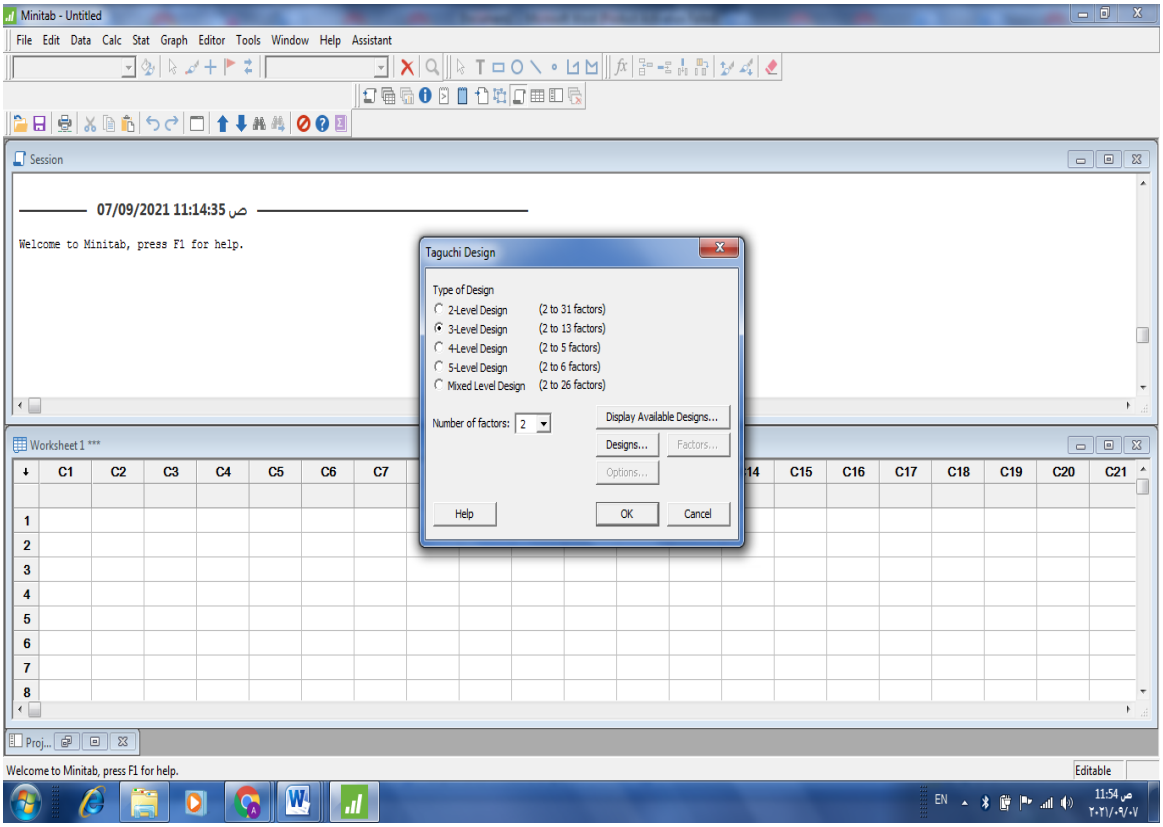

Determine the number of factors and the number of levels for experiments

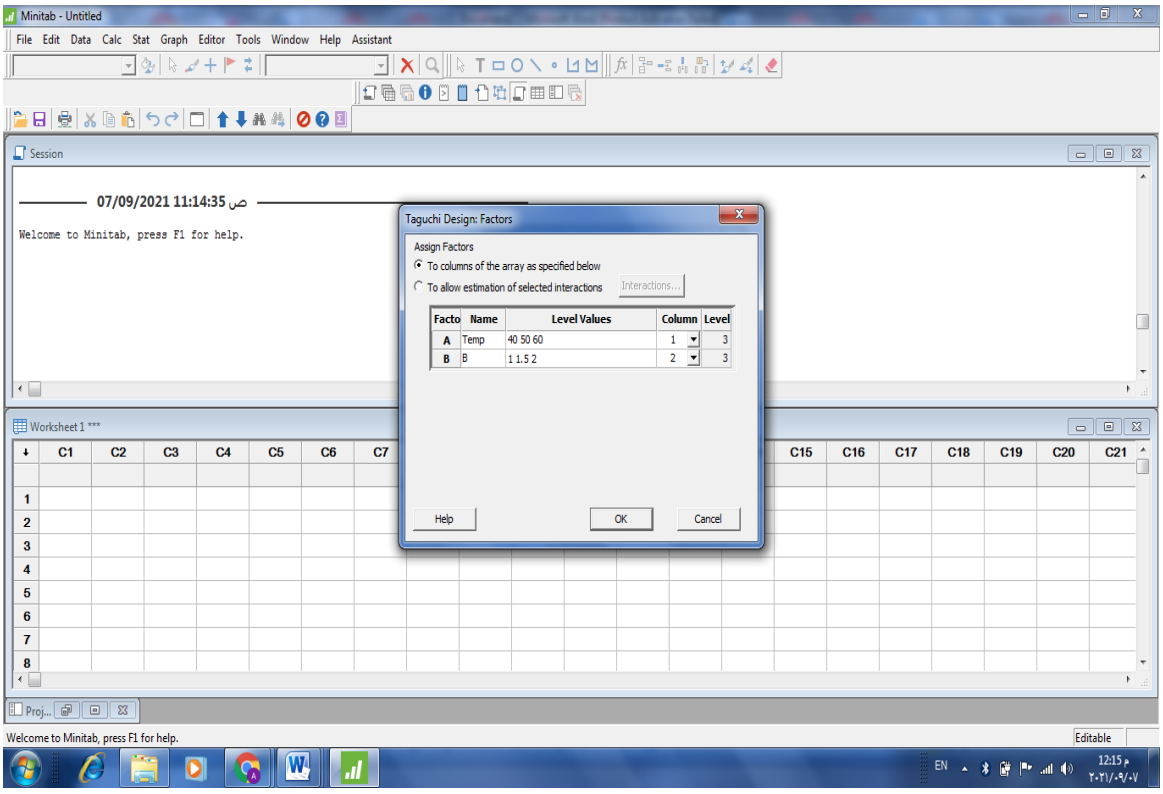

Define the names of variables and their level values

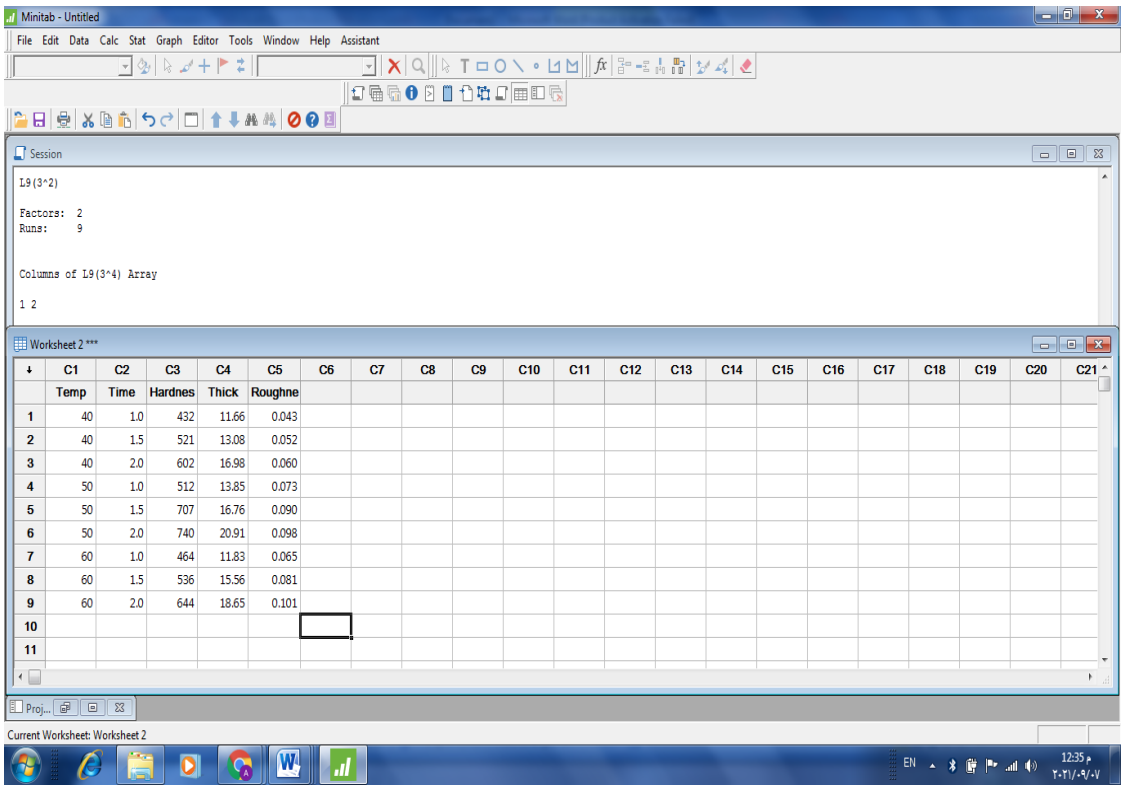

	C1	C2	C3	C4	C5	C6	C7	C8	C9	C10	C11	C12	C13	C14	C15	C16	C17	C18	C19	C20	C21
	Temp	Time	Hardnes	Thick	Roughne																
1	40	1.0	432	11.66	0.043																
2	40	1.5	521	13.08	0.052																
3	40	2.0	602	16.98	0.060																
4	50	1.0	512	13.85	0.073																
5	50	1.5	707	16.76	0.090																
6	50	2.0	740	20.91	0.098																
7	60	1.0	464	11.83	0.065																
8	60	1.5	536	15.56	0.081																
9	60	2.0	644	18.65	0.101																
10																					
11																					

Levels of experiment variables with their outputs

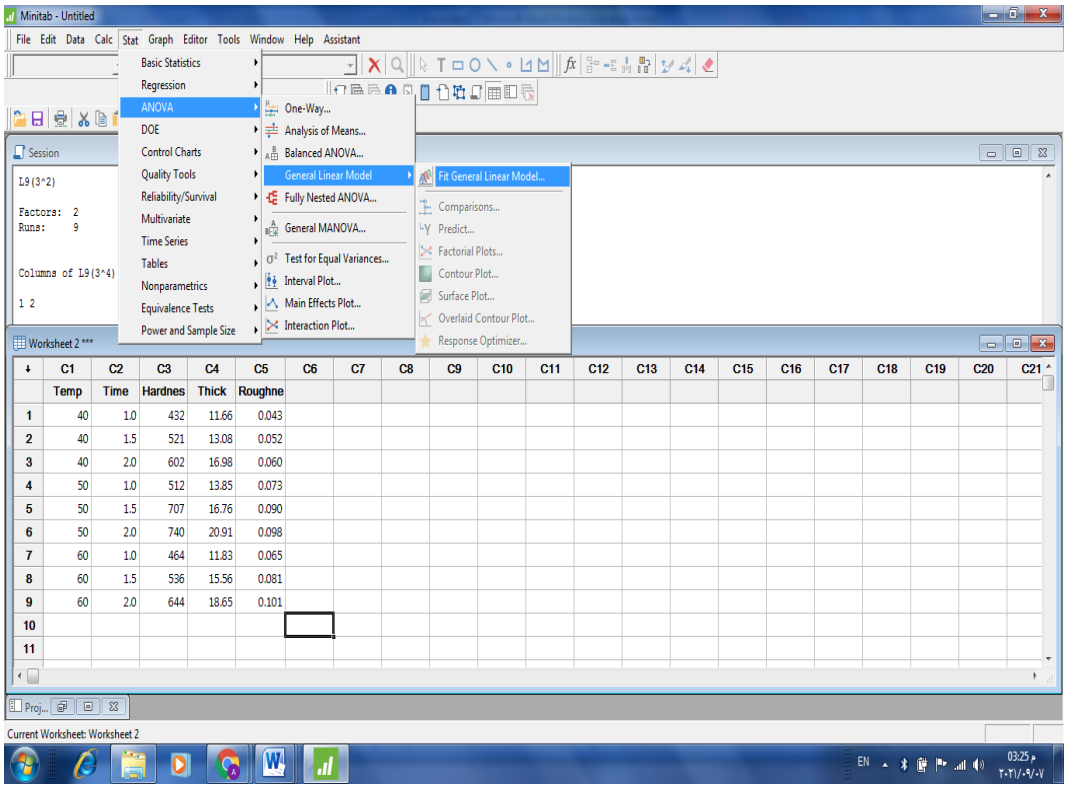

	C1	C2	C3	C4	C5	C6	C7	C8	C9	C10	C11	C12	C13	C14	C15	C16	C17	C18	C19	C20	C21
	Temp	Time	Hardnes	Thick	Roughne																
1	40	1.0	432	11.66	0.043																
2	40	1.5	521	13.08	0.052																
3	40	2.0	602	16.98	0.060																
4	50	1.0	512	13.85	0.073																
5	50	1.5	707	16.76	0.090																
6	50	2.0	740	20.91	0.098																
7	60	1.0	464	11.83	0.065																
8	60	1.5	536	15.56	0.081																
9	60	2.0	644	18.65	0.101																
10																					
11																					

Access interface for analysis of variance for variables

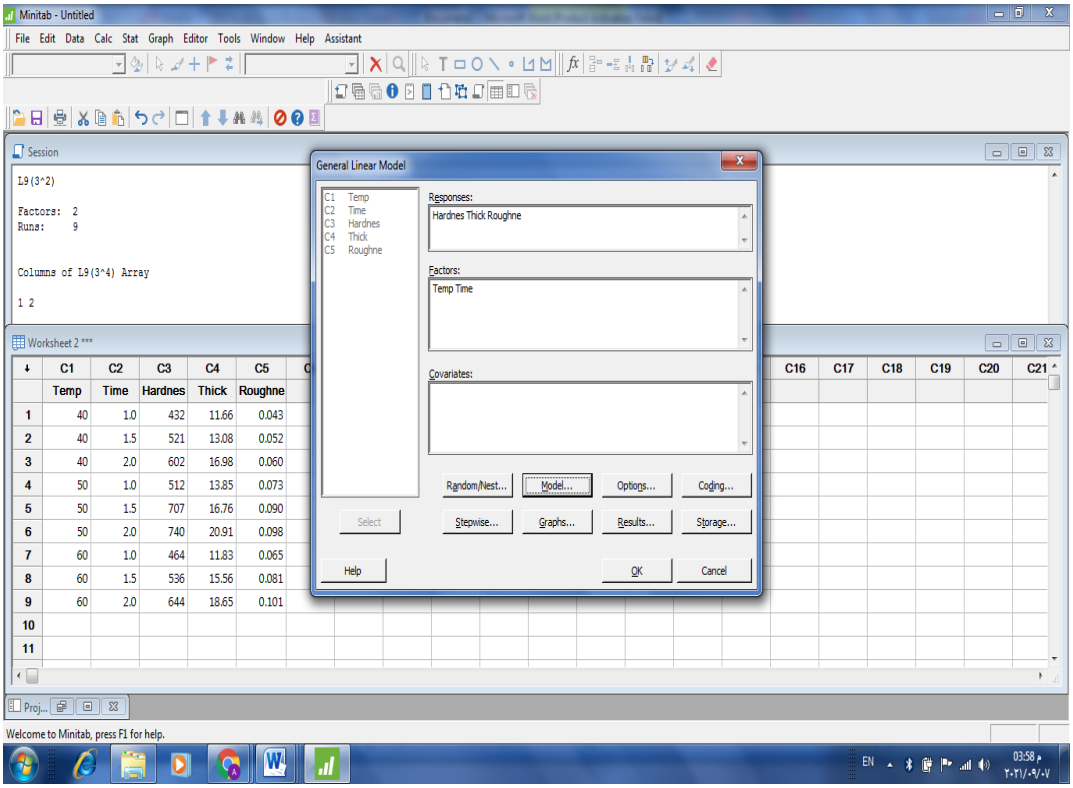

Variance control options

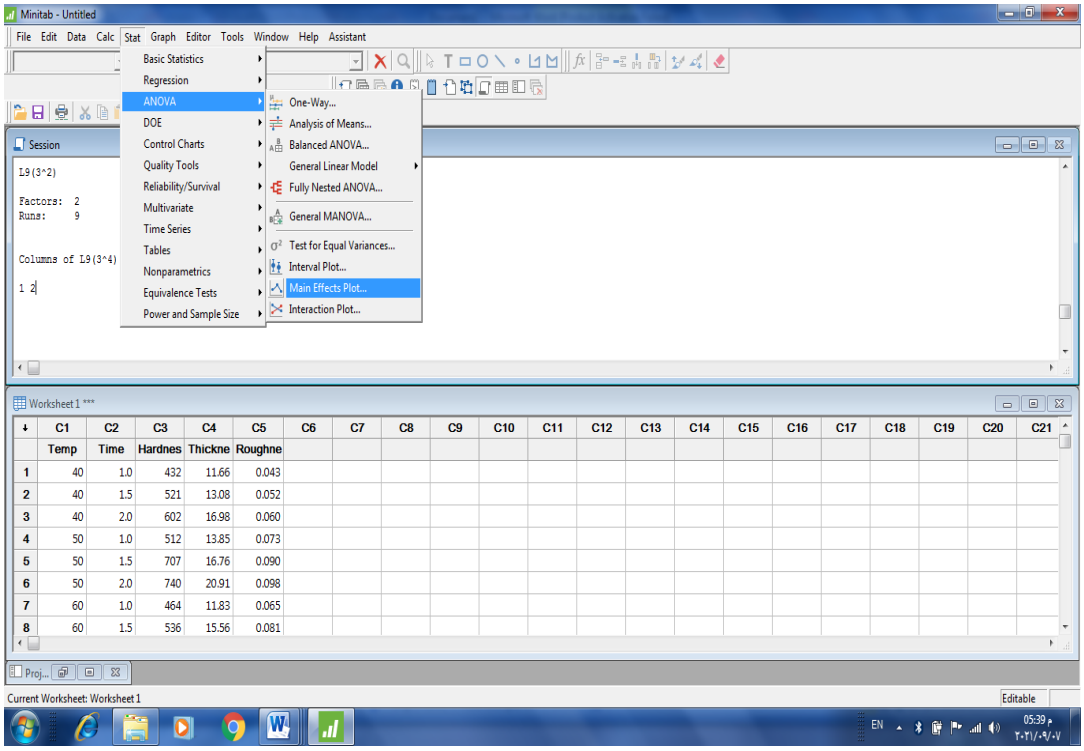

Plotting the effect of variables on outputs (Main effects)

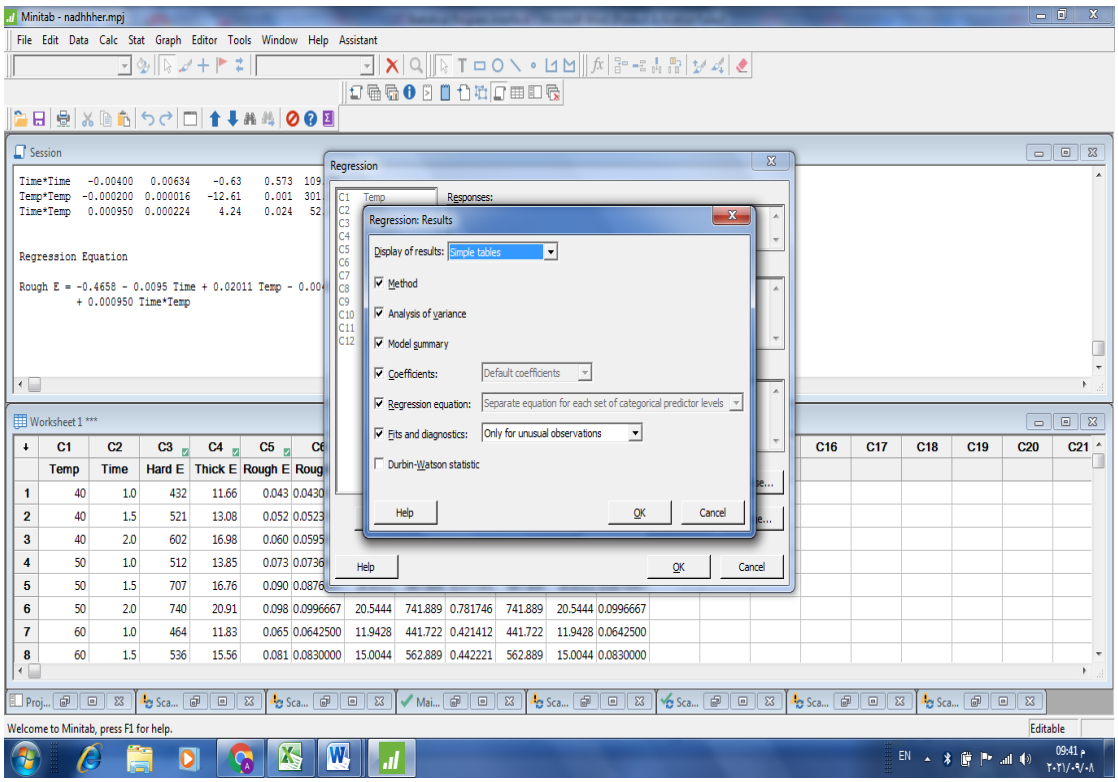

Estimated regression model

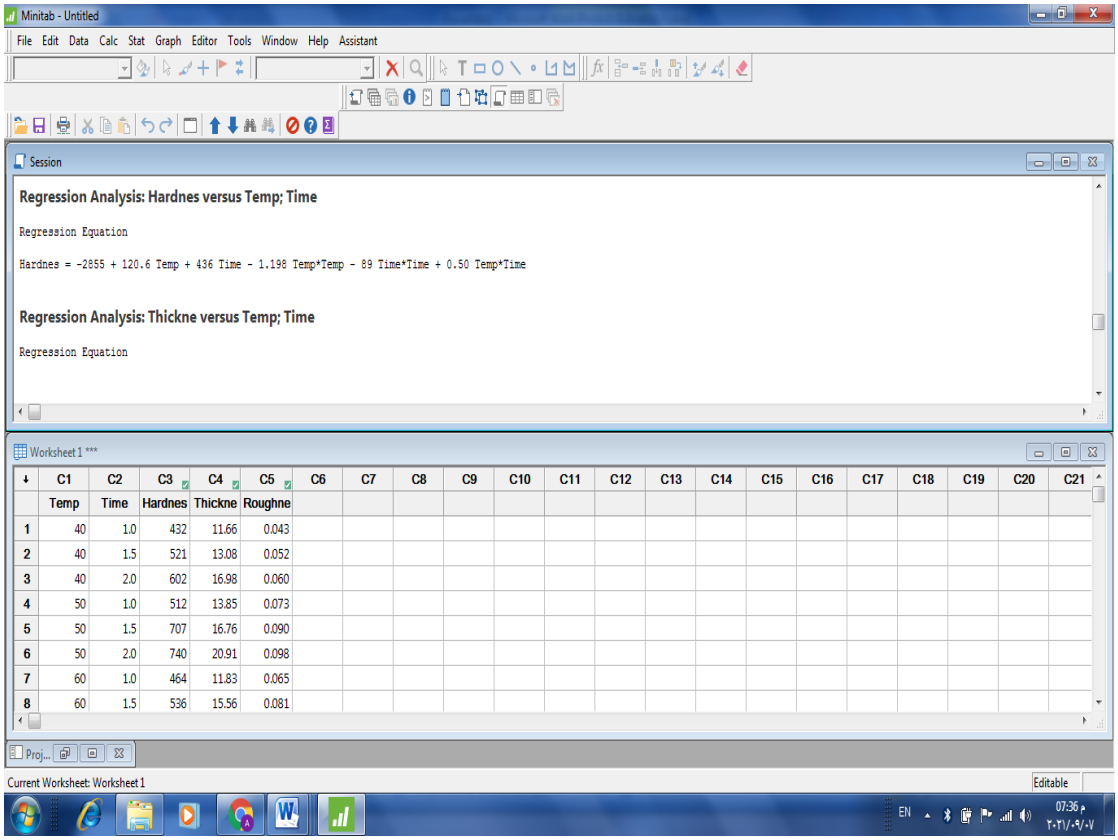

Obtaining regression equation for responses

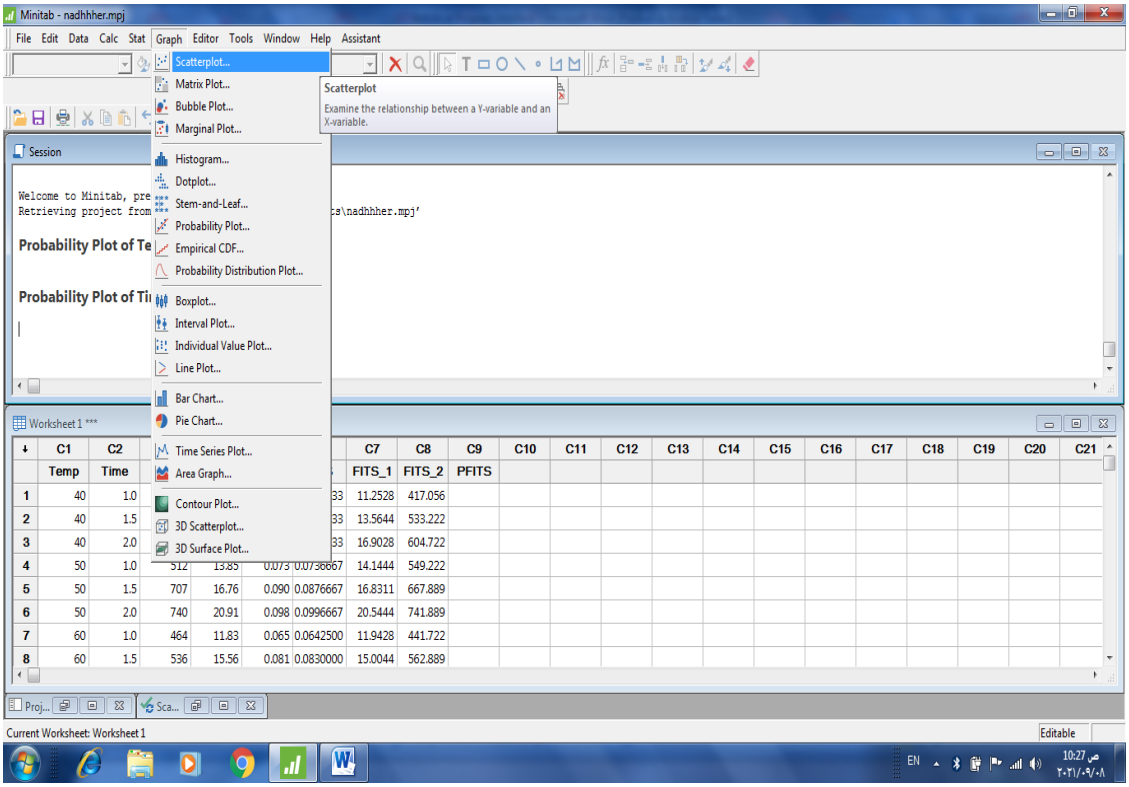

Scatter plot interface

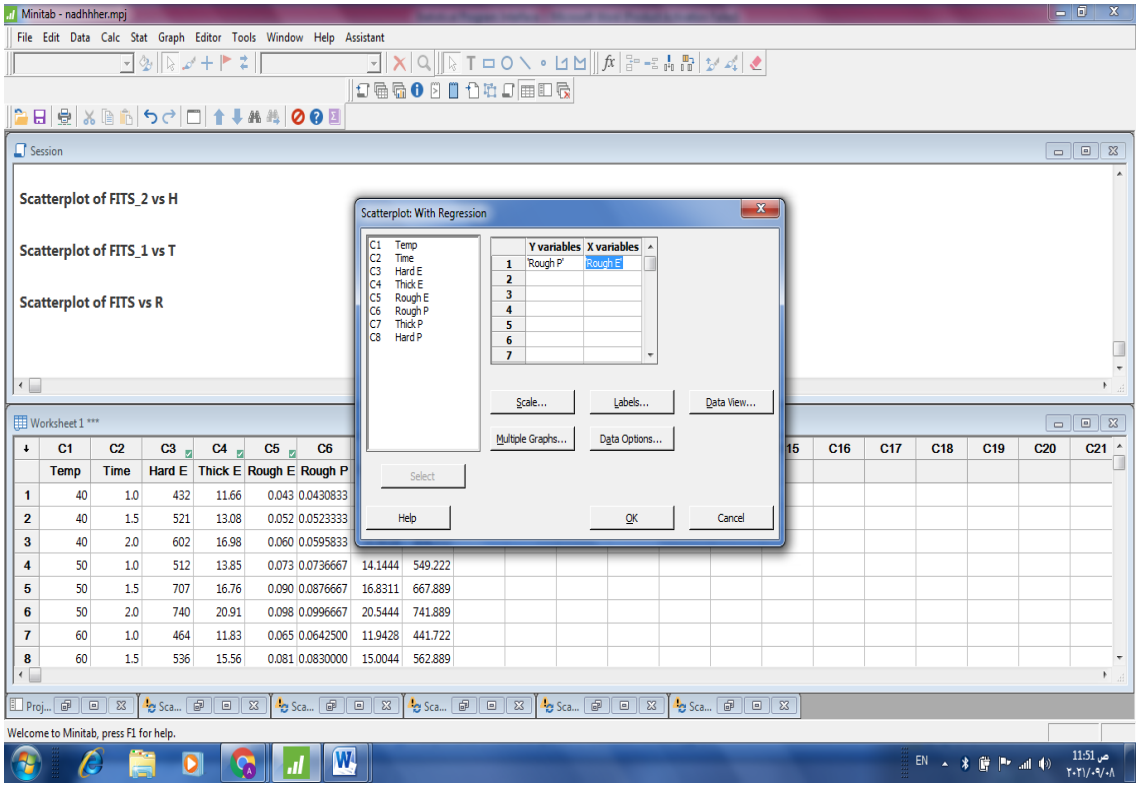

Enter the calculated and predicted values for the output

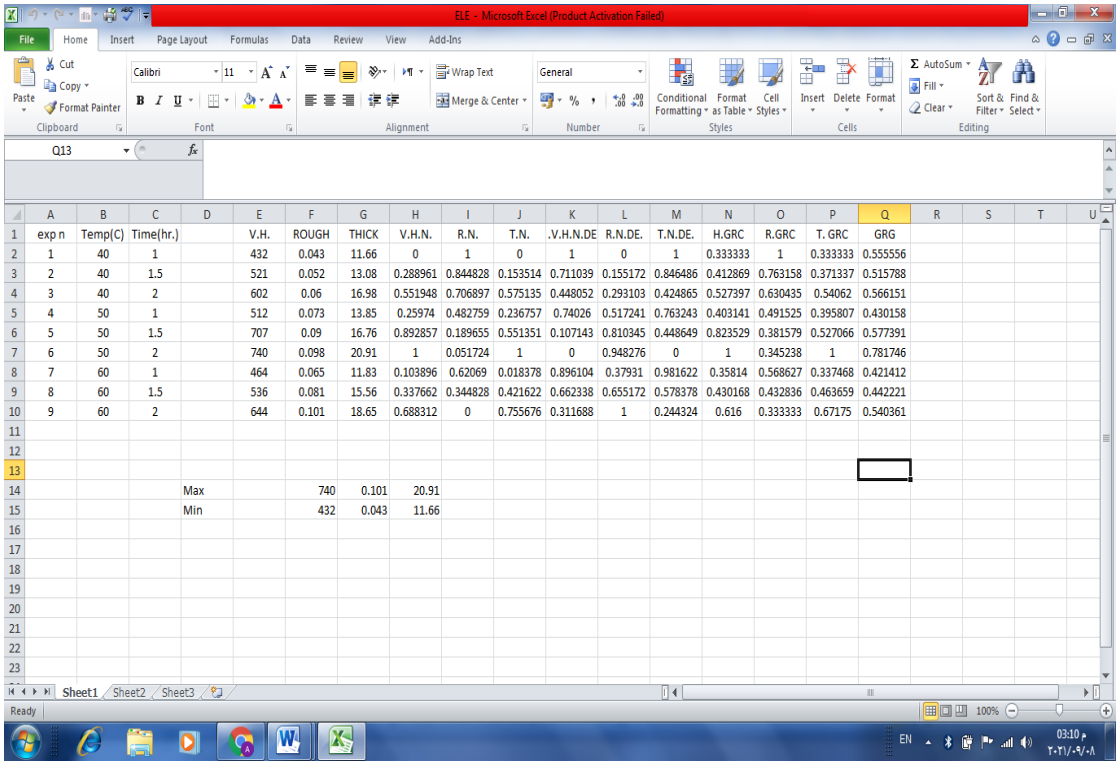

exp n	Temp(C)	Time(hr.)	V.H.	ROUGH	THICK	V.H.N.	R.N.	T.N.	.V.H.N.DE	R.N.DE.	T.N.DE.	H.GRC	R.GRC	T. GRC	GRG
1	40	1	432	0.043	11.66	0	1	0	1	0	1	0.333333	1	0.333333	0.555556
2	40	1.5	521	0.052	13.08	0.288961	0.844828	0.153514	0.711039	0.155172	0.846486	0.412869	0.763158	0.371337	0.515788
3	40	2	602	0.06	16.98	0.551948	0.706897	0.575135	0.448052	0.293103	0.424865	0.527397	0.630435	0.54062	0.566151
4	50	1	512	0.073	13.85	0.25974	0.482759	0.236757	0.74026	0.517241	0.763243	0.403141	0.491525	0.395807	0.430158
5	50	1.5	707	0.09	16.76	0.892857	0.189655	0.551351	0.107143	0.810345	0.448649	0.823529	0.381579	0.527066	0.577391
6	50	2	740	0.098	20.91	1	0.051724	1	0	0.948276	0	1	0.345238	1	0.781746
7	60	1	464	0.065	11.83	0.103896	0.62069	0.018378	0.896104	0.37931	0.981622	0.35814	0.568627	0.337468	0.421412
8	60	1.5	536	0.081	15.56	0.337662	0.344828	0.421622	0.662338	0.655172	0.578378	0.430168	0.432836	0.463659	0.442221
9	60	2	644	0.101	18.65	0.688312	0	0.755676	0.311688	1	0.244324	0.616	0.333333	0.67175	0.540361
			Max		740	0.101	20.91								
			Min		432	0.043	11.66								

Calculation of the GRG value for the experiments

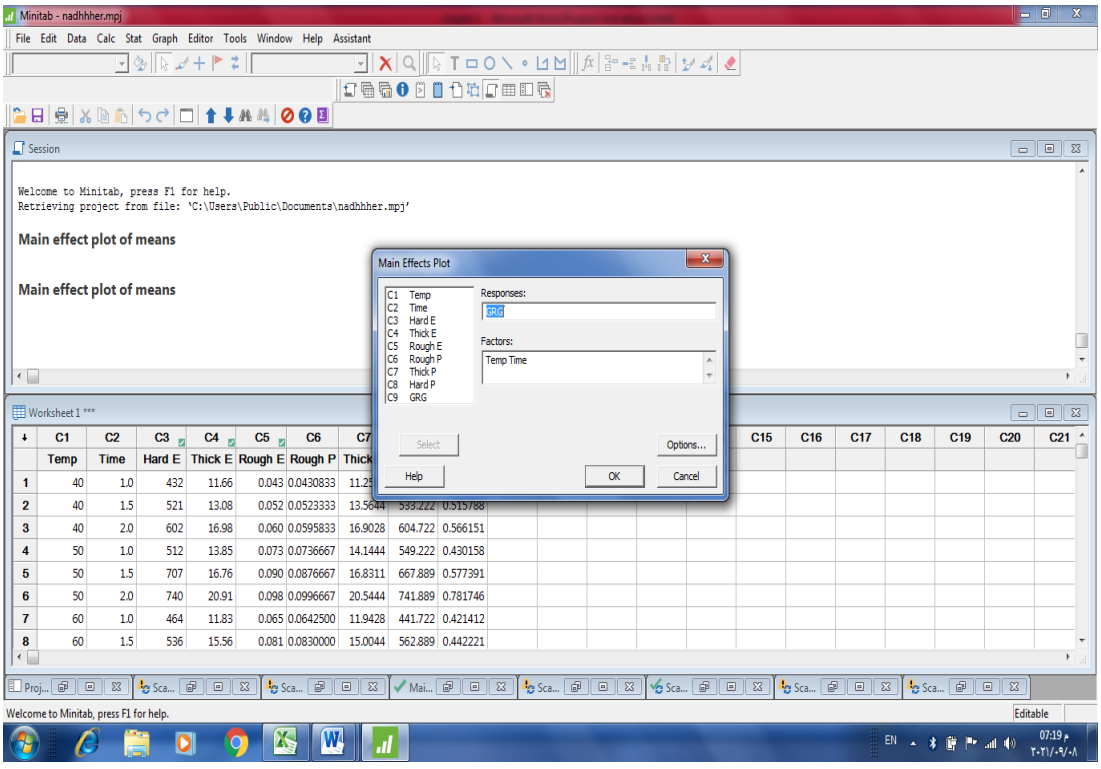

	Temp	Time	Hard E	Thick E	Rough E	Rough P	Thick P	GRG
1	40	1.0	432	11.66	0.043	0.0430833	11.25	
2	40	1.5	521	13.08	0.052	0.0523333	13.5644	0.515788
3	40	2.0	602	16.98	0.060	0.0595833	16.9028	0.566151
4	50	1.0	512	13.85	0.073	0.0736667	14.1444	0.430158
5	50	1.5	707	16.76	0.090	0.0876667	16.8311	0.577391
6	50	2.0	740	20.91	0.098	0.0996667	20.5444	0.781746
7	60	1.0	464	11.83	0.065	0.0642500	11.9428	0.421412
8	60	1.5	536	15.56	0.081	0.0830000	15.0044	0.442221

Plotting the effect of variables on GRG (Main effects)

Appendix B
(XRD Peak List for Samples)

Report | X'Pert HighScore

Peak List: (Bookmark 3) **for carbon steel**

Pos. [°2Th.]	Height [cts]	FWHM Left [°2Th.]	d-spacing [?]	Rel. Int. [%]	Tip Width	Matched by
44/7138	1314/55	0/2755	2/02678	100/00	0/3306	00-006-0696
65/0691	71/23	0/4723	1/43348	5/42	0/5668	00-006-0696
82/3369	122/21	0/4723	1/17115	9/30	0/5668	00-006-0696

Report | X'Pert HighScore

Peak List: (Bookmark 3) **for (Cr –10 g/l SiC)**

Pos. [°2Th.]	Height [cts]	FWHM Left [°2Th.]	d-spacing [?]	Rel. Int. [%]	Tip Width	Matched by
44/4568	639/53	0/1574	2/03790	100/00	0/1889	00-048-1816
44/7886	571/03	0/1968	2/02357	89/29	0/2362	00-048-1816
65/0026	40/83	0/9446	1/43479	6/38	1/1336	00-048-1816
82/3875	72/05	0/3936	1/17056	11/27	0/4723	00-048-1816

Report | X'Pert HighScore

Peak List: (Bookmark 3) **for (Cr- 20 g/l SiC)**

Pos. [°2Th.]	Height [cts]	FWHM Left [°2Th.]	d-spacing [?]	Rel. Int. [%]	Tip Width	Matched by
44/6192	386/20	0/3149	2/03086	100/00	0/3779	00-049-1727; 00-044-1433
64/9277	18/22	0/7872	1/43626	4/72	0/9446	00-049-1727; 00-044-1433
81/9358	48/01	0/9446	1/17586	12/43	1/1336	00-049-1727

Report | X'Pert HighScore

Peak List: (Bookmark 3) **for (Cr-30 g/l SiC)**

Pos. [°2Th.]	Height [cts]	FWHM Left [°2Th.]	d-spacing [?]	Rel. Int. [%]	Tip Width	Matched by
44/4909	934/28	0/2362	2/03642	100/00	0/2834	00-034-0396
64/7417	37/14	0/9446	1/43993	3/98	1/1336	00-034-0396
81/7757	122/36	0/3149	1/17776	13/10	0/3779	00-034-0396

Appendix C

(EDS Data)

EDS data for carbon steel

Element	Line Type	Apparent Concentration	k Ratio	Wt%	Wt% Sigma	Atomic %	Standard Label	Factory Standard	Standard Calibration Date
C	K series	0.42	0.00421	5.50	0.25	20.96	C Vit	Yes	
O	K series	0.40	0.00135	0.68	0.10	1.95	SiO2	Yes	
Si	K series	0.12	0.00098	0.34	0.04	0.55	SiO2	Yes	
Mn	K series	0.36	0.00360	0.90	0.11	0.75	Mn	Yes	
Fe	K series	37.70	0.37702	92.57	0.28	75.80	Fe	Yes	
Total:				100.00		100.00			

EDS data for Chromium coating

Element	Line Type	Apparent Concentration	k Ratio	Wt%	Wt% Sigma	Atomic %	Standard Label	Factory Standard	Standard Calibration Date
C	K series	0.33	0.00331	3.73	0.20	13.86	C Vit	Yes	
O	K series	1.14	0.00384	1.82	0.17	5.08	SiO2	Yes	
Cr	K series	34.59	0.34587	94.45	0.25	81.06	Cr	Yes	
Total:				100.00		100.00			

EDS data for (Cr-10 g/l SiC)

Element	Line Type	Apparent Concentration	k Ratio	Wt%	Wt% Sigma	Atomic %	Standard Label	Factory Standard	Standard Calibration Date
C	K series	0.38	0.00381	4.29	0.20	15.61	C Vit	Yes	
O	K series	1.48	0.00499	2.36	0.16	6.45	SiO2	Yes	
Si	K series	0.06	0.00050	0.17	0.04	0.26	SiO2	Yes	
Cr	K series	33.21	0.33213	88.00	0.32	73.93	Cr	Yes	
Fe	K series	0.68	0.00683	1.96	0.13	1.53	Fe	Yes	
Cu	L series	0.35	0.00346	3.22	0.19	2.22	Cu	Yes	
Total:				100.00		100.00			

EDS data for (Cr-20 g/l SiC)

Element	Line Type	Apparent Concentration	k Ratio	Wt%	Wt% Sigma	Atomic %	Standard Label	Factory Standard	Standard Calibration Date
C	K series	0.65	0.00650	7.13	0.23	23.51	C Vit	Yes	
O	K series	1.79	0.00602	3.06	0.16	7.57	SiO2	Yes	
Na	K series	0.09	0.00037	0.30	0.06	0.52	Albite	Yes	
Si	K series	0.10	0.00077	0.27	0.04	0.38	SiO2	Yes	
Ca	K series	0.15	0.00138	0.33	0.05	0.33	Wollastonite	Yes	
Cr	K series	32.18	0.32181	88.31	0.29	67.27	Cr	Yes	
Fe	K series	0.20	0.00201	0.59	0.11	0.42	Fe	Yes	
Total:				100.00		100.00			

EDS data for (Cr-30g/l SiC)

Element	Line Type	Apparent Concentration	k Ratio	Wt%	Wt% Sigma	Atomic %	Standard Label	Factory Standard	Standard Calibration Date
C	K series	7.60	0.07602	40.39	0.24	72.66	C Vit	Yes	
O	K series	1.37	0.00462	2.52	0.15	3.40	SiO2	Yes	
Na	K series	0.13	0.00054	0.23	0.04	0.22	Albite	Yes	
Al	K series	0.05	0.00037	0.09	0.03	0.07	Al2O3	Yes	
Si	K series	0.06	0.00048	0.10	0.02	0.08	SiO2	Yes	
S	K series	0.06	0.00052	0.10	0.03	0.07	FeS2	Yes	
Cr	K series	29.98	0.29977	56.57	0.24	23.51	Cr	Yes	
Total:				100.00		100.00			

Appendix D

Chemical composition results

ISO 9001:2015
ISO 14001:2015

REPUBLIC OF IRAQ
Ministry of Industry & Minerals
State Company for Inspection and Engineering Rehabilitation (SIER)

جمهورية العراق
وزارة الصناعة والمعادن
الشركة العامة للفحص والتأهيل الهندسي

القسم: التخطيط والمتابعة

العدد: ٢٠٢٠
التاريخ ٢٥/١١/٢٠٢٠

الى / وزارة التعليم العالي والبحث العلمي – جامعة بابل – كلية الدراسات العليا

م/ نتائج فحص

تهديكم تحياتنا ....
إشارة الى كتابكم المرقم (٤٤٣٥) في ٢٥/١١/٢٠٢٠....
نرفق لكم طيا نتائج الفحوصات المطلوبة بموجب كتابكم أعلاه .
... مع التقدير

المهندس
سيف الدين علي احمد
م. المدير العام
رئيس مجلس الإدارة

. للاستفسار الاتصال بالرقم (٠٧٨١٦٧٢٠٥٠١) لطفاً
. يحفظ حق المطالبة بالنموذج المفحوص بعد شهر واحد من انجاز العمل وتسلام النتائج

نسخة منه الى/
- قسم التخطيط والمتابعة - شعبة المتابعة / للحفظ مع اوليات امر العمل (٢٠٢٠/٩٩١) لطفاً .

D.G.Office: 07901779983
E-mail : siei.mahed@gmail.com , siei_mahed@yahoo.com
Website: www.siei.gov.iq
IP: 91.106.34.21 – SIER@engineering Comp.

نسخة مسيطر عليها

مكتب المدير العام ٠٧٩١٧٧٩٩٨٦٣
البريد الالكتروني : siei.mahed@gmail.com , siei_mahed@yahoo.com
الموقع الالكتروني : www.siei.gov.iq
مكتب بريد الدورة / ص.ب (١٩٠٨١) – مكتب بريد الانصار ص.ب (٩١٠٦٩)
موقع الشركة : بغداد – السيدية – طريق المرور السريع بغداد – الحلة

S.I.E R/HR/01	Issue No: 09	Date: Nov. 2020

S.I.E.R الهيئة العامة للفحص والتأهيل الهندسي
Lab. & E.I. Dep. المختبرات والتفتيش الهندسي

مختبر المعادن
Test Report

جهة المستفيدة : وزارة التعليم العالي و البحث العلمي / جامعة بابل – كلية الدراسات العليا
ر العمل : 991 / 2020
تاريخ : 25 / 11 / 2020
سم النموذج : نماذج معدنية
ع الفحص : تحليل كيميائي
جهاز المستخدم : Spectro Max
لمواصفة القياسية : ----------

Sample	C%	Si%	Mn%	P%	S%	Cr%	Mo%	Ni%	Al%	Co%	Cu%	Fe%
Sample A	0.416	0.379	0.828	0.0132	0.0110	0.0804	0.0182	0.138	0.0381	0.0121	0.199	Bal.
Sample B	0.0923	0.471	10.40	0.0503	0.0011	14.24	< 0.0020	0.890	0.0037	0.112	0.858	Bal.
Sample C	2.52	2.67	0.537	0.201	0.147	0.0623	0.0087	0.0680	0.0050	0.0155	0.115	Bal.

الملاحظات:
- النتيجة تخص النموذج المفحوص فقط.
- تم الفحص بدرجة حرارة (26°C) ونسبة الرطوبة(% 39).

مدير قسم المختبرات والتفتيش الهندسي
المهندس
احمد ناصر هاشم
١١/ ٢٥

المراجعة

الفاحص

نسخة مسيطر عليها

Doc. No: S.I.E.R/QW/9/27/01 | Issue No.02 | Date: Dec 2018

D-2

الشركة العامة للفحص والتأهيل الهندسي S.I.E.R
قسم المختبرات والتفتيش الهندسي Lab. & E.I. Dep.

مختبر المعادن

Test Report

الجهة المستفيدة : وزارة التعليم العالي و البحث العلمي / جامعة بابل – كلية الدراسات العليا
امر العمـــــل : 2020 / 991
التـــاريـــخ : 2020 / 11 / 25
اسم النمـــوذج : نماذج معدنية
نوع الفحـــص : تحليل كيميائي
الجهاز المستخدم : Spectro Max
المواصفة القياسية : ----------

Sample	C%	Si%	Mn%	P%	S%	Cr%	Mo%	Ni%	Al%	Co%	Cu%	Fe%
Sample A	0.416	0.379	0.828	0.0132	0.0110	0.0804	0.0182	0.138	0.0381	0.0121	0.199	Bal.
Sample B	0.0923	0.471	10.40	0.0503	0.0011	14.24	< 0.0020	0.890	0.0037	0.112	0.858	Bal.
Sample C	2.52	2.67	0.537	0.201	0.147	0.0623	0.0087	0.0680	0.0050	0.0155	0.115	Bal.
Sample D	0.0580	0.0062	0.364	0.0138	0.0239	0.0200	0.0020	0.0145	0.0589	< 0.0015	0.0171	Bal.
Sample E	0.403	0.382	0.826	0.0119	0.0108	0.0783	0.0160	0.139	0.0329	0.0129	0.193	Bal.

الملاحظات:
- النتيجة تخص النموذج المفحوص فقط.
- تم الفحص بدرجة حرارة (26°C) ونسبة الرطوبة(% 39).

مدير قسم المختبرات والتفتيش الهندسي
المهندس
احمد ناصر هاشم
١١/ ٢٥

المراجعة

الفاحص

نسخة مسيطر عليها

Doc. No: S.I.E.R/QWI/27/01	Issue No.02	Date: Dec 2018

TÜV AUSTRIA
EN ISO 9001:2015
EN ISO 14001:2015

Ministry of Industry and Minerals
State Company for Inspection and Engineering Rehabilitation (SIER)
Engineering Insp. & lab Department

Client: التعليم العالي و البحث العلمي – جامعة بابل – كلية الدراسات العليا – العلوم الهندسية و التكنولوجية
Order No: 240 / 2021
Tested Item: نماذج معدنية
Address: Babylon - Iraq
Date of Test: 16 / 3 / 2021
Type of Test: Chemical Composition

Test Report

Sample	C%	Si%	Mn%	P%	S%	Cr%	Mo%	Ni%	Al%	Cu%	Fe%
Sample A	0.200	0.307	0.526	0.0169	0.0123	0.0251	0.0032	0.0360	0.0051	0.0457	Bal.
Sample B	0.385	0.240	0.917	0.0151	0.0289	0.148	0.0411	0.117	< 0.0005	0.273	Bal.
Sample C	0.433	0.357	0.758	0.0070	0.0184	0.0577	0.0190	0.0658	0.0387	0.140	Bal.
Sample D	0.382	0.283	0.423	0.0080	0.0176	1.50	0.207	1.38	0.227	0.0471	Bal.

الملاحظات:
- النتيجة تخص النموذج المفحوص فقط.
- تم الفحص بدرجة حرارة (24°C) ونسبة الرطوبة(20 %).

مدير قسم الفحص الهندسي و المختبرات

المراجعة

الفاحص

Appendix E

(Address book facilitating the task)

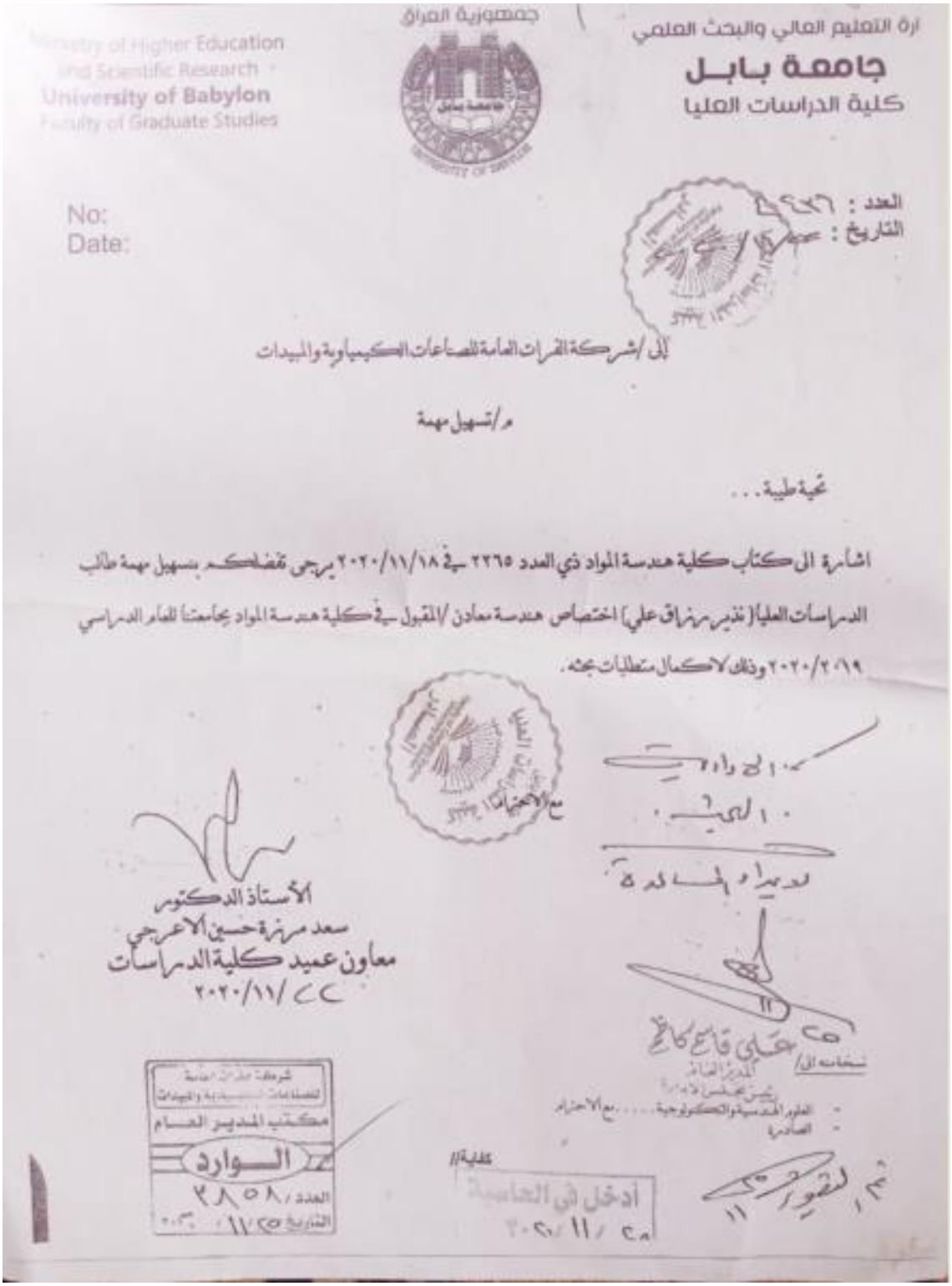

جمهورية العراق
وزارة التعليم العالي والبحث العلمي
جامعة بابل
كلية الدراسات العليا

Ministry of Higher Education and Scientific Research
University of Babylon
Faculty of Graduate Studies

No:
Date:

العدد :
التاريخ :

إلى /شركة الفرات العامة للصناعات الكيمياوية والمبيدات

م/تسهيل مهمة

تحية طيبة...

اشارة الى كتاب كلية هندسة المواد ذي العدد ٢٢٦٥ في ٢٠٢٠/١١/١٨ يرجى تفضلكم بتسهيل مهمة طالب الدراسات العليا (نذير مزهر اق علي) اختصاص هندسة معادن /المقبول في كلية هندسة المواد بجامعتنا للعام الدراسي ٢٠١٩/٢٠٢٠ وذلك لاكمال متطلبات بحثه.

مع الاحترام

الأستاذ الدكتور
سعد مزهر حسين الاعرجي
معاون عميد كلية الدراسات
٢٠٢٠/١١/ ٢٢

شركة الفرات العامة للصناعات الكيمياوية والمبيدات
مكتب المدير العام
الوارد
العدد ٢٨٥٨
التاريخ ٢٢/١١/٢٠٢٠

نسخة الى/
المدير العام
- العلوم الهندسية والتكنولوجية ... مع الاحترام
- الصادرة

ادخل في الحاسبة
٢٠٢٠/١١/ ٢٢

E-1

ISO 9001:2015

VEXIL BPS MS

شركة الفرات العامة
للصناعات الكيمياوية
والمبيدات

وزارة الصناعة
والمعادن

MINISTRY OF INDUSTRY & MINERALS *AL-FURAT STATE COMPANY FOR CHEMICAL AND PESTICIDES INDUSTRIES

القسم : البحث والتطوير

العـدد :١٤/ ٥٠٥٧

التاريخ : ٢٠٢١/ ١٠ / ٢٥

إلى / جامعة بابل / كلية هندسة المواد

م / تأييـــــد

تحية طيبة ...

إشارة إلى التعاون العلمي المشترك بين شركتنا وكليتكم الموقرة . نؤيد إكمال متطلبات انجاز الجانب العملي لرسالة الماجستير الموسومة ب

[Implementation the optimum protection from oxidation (concentrated sulphuric acid plant / Al Furat state company)]

للطالب (نذير رزاق علي صالح) وكذلك نود إعلامكم بإمكانية الاستفادة منها في شركتنا .

تفضلكم بالإطلاع . مع التقدير ..

المهندس علي قاسم كاظم
المدير العام ورئيس مجلس الإدارة
٢٠٢١ / ١٠ / ٢٥

نسخه منه إلى :-

- مكتب السيد المدير العام المحترم / تفضلكم بالإطلاع ... مع التقدير .
- قسم البحث والتطوير /مع الأوليات ..

رقم الإصدار	تاريخ الإصدار	رمز الوثيقة
01	28/6/2018	HR/01

Website :www.furattco.gov.iq P BOX 11230
E-Mail:furattco1@gmail.com,furattco@furattco.gov.iq

جمهورية العراق / بابل – سدة الهندية
ص.ب : ١١٢٣٠

E-2

Appendix F

(Published Research)

KALAHARI JOURNALS

INTERNATIONAL JOURNAL OF MECHANICAL ENGINEERING

ISSN: 0974-5823

ACCEPTANCE LETTER

Date: 16-01-2022

PAPER TITLE: The effect of adding Silicon Carbide microparticles to the optimum chromium plating on improving the corrosion resistance of carbon steel in concentrated sulfuric acid medium (98%)

PAPER ID: KLIJU5823/12-03084

AUTHOR'S NAME: **Nadheer Razzaq Ali[1], Dr. Haydar A.H. Al –juboori[2], Dr. Ekhal M. S. Salih[3]**

[1]University of Babylon - College of Materials Engineering, Babylon, Iraq.
[2]University of Babylon - College of Materials Engineering, Babylon, Iraq.
[3]University of Babylon - College of Materials Engineering, Babylon, Iraq.

Congratulations!

We are pleased to inform you that, after the peer review, your article entitled "The effect of adding Silicon Carbide microparticles to the optimum chromium plating on improving the corrosion resistance of carbon steel in concentrated sulfuric acid medium (98%)" has been accepted for publication in INTERNATIONAL JOURNAL OF MECHANICAL ENGINEERING ISSN: 0974-5823 in the upcoming issue January, 2022.

Notification of publication of your article will be sent to you once your article is online.

Thanking You

Regards,

Editor

INTERNATIONAL JOURNAL OF MECHANICAL ENGINEERING
ISSN: 0974-5823
KALAHARI JOURNALS

International Journal of Mechanical Engineering, ISSN: 0974-5823 KALAHARI JOURNALS

Scopus

Date: May 25. 2021
Paper ID:IICESAT 143

LETTER OF ACCEPTANCE

Dear Authors,

On behalf of the IICESAT-21 Committee, and based on the reviewers' evaluation after double blind peer review and Guest editors' approval we are pleased to inform you that your paper entitled:

Surface modification of carbon steel by electrodeposit composite coating for improving erosion-corrosion resistance: a review

Written By

" Dr. Ekbal M. S. Salih , Dr. Haydar A.H. Al –juboori and Nadheer R. A. Al-Hamdani "

Has been accepted and will be processed to be publish in IOP Journal of Physics (Online ISSN: 1742-6596, Print ISSN: 1742-6588, ICPAS-2021). It is our pleasure to invite you to attend the 3rd International Scientific Conference of Engineering Sciences and Advances Technologies (IICESAT), College of Material Engineering, University of Babylon, Iraq in 4-5 June, 2021., to present your paper. We congratulate you for your achievement, the technical details about the publication will be informed later. The publication of the accepted paper will be provided by September 2021

We Will encourage more quality submissions from you and your colleagues in future

Regards.

Prof. Dr. Shubham Sharma
Guest Editor of IICESAT Issue – JPCS Journal

JOURNAL OF PHYSICS: CONFERENCE SERIES
IOP Publishing

Caution: This Acceptance Letter Made by IICESAT Conference Main Guest Editors, All Approval Inquiries Should Made to Editorial Board Members of IICESAT Conference, as all Accepted Papers will Process for publication in **IOP Journal of Physics: Conference Series**

الخلاصة

تعتبر الطلاءات المعدنية والمركبة أحد تقنيات التعديل السطحي لسطوح المعادن والسبائك لغرض أكسابها خواص جديدة بالاضافة الى خواصها الاصلية أو تحسين خواصها الاصلية.

مشكلة البحث هي إنخفاض مقاومة التأكل للفولاذ المستخدم في تصنيع الانابيب الناقلة لحامض الكبريتيك المركز(98%) في مصنع حامض الكبريتيك في شركة الفرات العامة.

تم إجراء الطلاء الكهربائي بالكروم والطلاء المركب بالكروم مع مسحوق كاربيد السيليكون على (المعدن الاساس) الفولاذ الكاربوني لتحسين مقاومة التأكل .

تم إجراء عملية الطلاء على الفولاذ الكاربوني بمعدن الكروم بأستخدام تيار مستمرمقداره($20A/dcm^2$),فولتية مقدارها (4.5)فولت ,مسافة بين الاقطاب مقدارها (5)سم ,سرعة خلط(300)دورة في الدقيقة ,كانت دالة الحامضة لمحلول الطلاء تساوي(2) وكانت عملية الطلاء تتضمن تسعة تجارب بموجب مصفوفة بالاعتماد على تصميم تاكوشي (الطريقة الرمادية) وقد أعتمدت درجة حرارة محلول الطلاء و زمن عملية الطلاء كعوامل طلاء متغيرة للتجارب حيث كان مدى درجة الحرارة(40,50,60) درجة سيليزية وزمن عملية الطلاء(1,1.5,2) ساعة , إجراء الفحوصات الميكانية لطبقة طلاء الكروم المتضمنه(صلادة فيكرز,السمك,الخشونة), أجراء تحليل التباين وحساب أعلى قيمة للدرجة العلائقية الرمادية وكانت في التجربة رقم (6) والتي تمثل عينة طلاء الكروم المثلى وبدرجة حرارة (50) درجة سيليزية للمحلول و زمن طلاء (2) ساعة.

تم أجراء عملية ترسيب الطلاءات المركبة من جسيمات كاربيد السيليكون المايكروية المنغرزه في معدن الكروم على الفولاذ الكاربوني بالاعتماد على عوامل طلاء الكروم المثلى وثلاث مقاديروزنية لجسيمات كاربيد السيليكون المايكروية لكل لتر من محلول طلاء الكروم وهي (10,20,30) غرام مضافة لمحلول طلاء الكروم,تم دراسة وتحليل تأثيرمحتوي جسيمات كاربيد السيليكون المايكروية على خواص طبقة الطلاءات المركبة على الفولاذ الكاربوني .

تم أجراء فحص مطياف مشتت الطاقة و فحص حيود الاشعة السينية لاثبات العناصروالاطوار المكونة للمعدن الاساس (الفولاذ الكاربوني) وعينة طلاء الكروم المعدني المثلى وثلاث عينات من الطلاءات المركبة لجسيمات كاربيد السيليكون المايكروية(10,20,30)غرام\لتر المنغرزة في معدن

الكروم بالاضافة الى فحوصات المجهر الالكتروني الماسح ومجهر القوة الماسح لسطح العينات الخمسة .

تم إجراء نوعين من أختبارات معدل التأكل بطريقة فقدان الوزن في موقع مصنع حامض الكبريتيك المركز(98%).الاختبار الاول هو أختبار الغمرالبسيط في الحامض الساكن وبدرجة حرارة الاجواء الطبيعية والاختبار الثاني هو أختبار (التأكل- تعرية) والذي يتضمن تعرض سطح العينات الى تأثير جريان حامض الكبريتيك المركز(98%) في ظروف تماثل ظروف جريان الحامض في الانابيب الناقلة للحامض الى خزان الانتاج اليومي ثم الى خزانات خزن الحامض لتحقيق نفس الظروف التأكلية للحامض على العينات الخاضعة للأختبار.كانت نسبة التحسن التي طرأت على الفولاذ الكاربوني المحمي بالطلاءات المعدنية للكروم والطلاءات المركبة من الكروم كاربيد السيليكون قياسا الى معدل تأكل الفولاذ الكاربوني الغير محمي في أختبار الغمر البسيط على النحو الاتي :طلاء الكروم(56.73%),طلاءالكروم-10غرام\التر(67.3%), طلاءالكروم-20غرام\التر(76.95%), طلاءالكروم-30غرام\التر(53.2%). كانت نسبة التحسن التي طرأت على الفولاذ الكاربوني المحمي بالطلاءات المعدنية للكروم والطلاءات المركبة من الكروم كاربيد السيليكون قياسا الى معدل تأكل الفولاذ الكاربوني الغير محمي في أختبار (التأكل-تعرية) على النحو الاتي :طلاء الكروم(24.53%),طلاءالكروم-10غرام\التر(72.56%), طلاءالكروم-20غرام\التر(80.26%), طلاءالكروم-30غرام\التر(59.86%).

تم إجراء إختبار الاستقطاب للعينات في حامض الكبريتيك المركز(98%) و كانت نسبة التحسن التي طرأت على الفولاذ الكاربوني المحمي بالطلاءات المعدنية للكروم والطلاءات المركبة من الكروم كاربيد السيليكون قياسا الى معدل تأكل الفولاذ الكاربوني الغير محمي على النحو الاتي :طلاء الكروم(97.8%),طلاءالكروم-10غرام\التر(98.4%), طلاءالكروم-20غرام\التر(99.5%), طلاءالكروم-30غرام\التر(88.5%).

أن الطلاءات المركبة بالكروم-20غرام\التر كاربيد السيليكون تقاوم التأكل في ظروف جريان الحامض المركز(98%) حيث ينخفض مقدار التأكل بمقدار خمس مرات قياسا بتأكل الفولاذ الكاربوني بدون طبقة حماية فهو مناسب جدا للاستخدام في الانابيب الناقلة لحامض الكبريتيك المركز(98%).

وزارة التعليم العالي والبحث العلمي
جامعة بابل
كلية هندسة المواد
قسم هندسة المعادن

التأكل تعرية للفولاذ الكربوني الواطىء المستخدم في حامض الكبريتيك المركز

رسالة

مقدمة الى قسم هندسة المعادن في كلية هندسة المواد/جامعة بابل

وهي جزء من متطلبات نيل درجة الماجستير في

هندسة المواد/ المعادن

من قبل

نذير رزاق علي صالح

بإشراف

أ.د. حيدر عبد حسن الجبوري

أ.د. إقبال محمد سعيد صالح

2022م **1443 هـ**